Ernst, R.E., Pease, V., Puchkov, V.N., Kozlov, V.I., Sergeeva, N.D., Hamilton, M.

GEOCHEMICAL CHARACTERIZATION OF PRECAMBRIAN MAGMATIC SUITES OF THE SOUTHEASTERN MARGIN OF THE EAST EUROPEAN CRATON, SOUTHERN URALS, RUSSIA

ABSTRACT

The Bashkirian anticlinorium in the western slope of the southern Ural Mountains, Russia, exposes the poorly understood magmatic units of the southeastern margin of the East European craton. Volcanic and intrusive rocks were analyzed for major and trace elements (91 samples), and the data used to correlate volcanic suites and to correlate poorly-dated intrusive suites with the volcanic suites, and also assess geodynamic setting. Five distinct geochemical suites were identified although their ages are not always well-constrained 1) Early Mesoproterozoic (lower Riphean, type section) Ai formation volcanics (ca. 1650 Ma) situ, and compositionally similar sills cutting the Early Mesoproterozoic (Lower Riphean) Satka formation 2) Late Mesoproterozoic (Middle Riphean) units including the Mashak volcanics, dykes of the Bakal quarries cutting the Mesoproterozoic (uppermost Lower Riphean), the Berdyaush rapakivi pluton and crosscutting dykes (grouped as the Mashak Igneous Event) 3) Dykes and sills cutting basement of the Taratash complex as exposed in the Radashni quarry and a high Mg dyke in the Bakal quarry. 4) dykes cutting Neoproterozoic (Upper Riphean) units and finally 5) Late Neoproterozoic (Vendian) units consisting of basalts, andesite and dacite lavas and tuffs of the Arsha formation.. A precise U–Pb age of 1385,3±1,4 Ma for the Bakal dyke represents the most precise estimate available for the Mashak Igneous event. The Mashak event may represent the Mesoproterozoic breakup of the East European craton, and can be correlated with the Midsommerso sills — Zig-Zag Dal volcanics in northern Greenland.

INTRODUCTION

The southeastern part of the East European Craton preserves a Mesoproterozoic (Early-Middle Riphean) through Neoproterozoic (Late Riphean and Vendian) volcano-sedimentary history, interpreted to represent a deep (up to 15 km) intracontinental rift basin and/or a long-lived Precambrian passive margin, affected by collision in the Late Vendian (Keller and Chumakov, 1983; Puchkov, 2000).

These Precambrian units are exposed along the western slope of the Urals in the region of the Bashkirian anticlinorium (Fig. 1), where magmatic rocks have a relatively restricted geographic, chronological and volumetric occurrence. Volcanic and volcano-sedimentary rocks include the Lower Riphean (ca. 1650 Ma) Ai formation, Middle Riphean (ca. 1370 Ma) Mashak formation, and the Lower Vendian (ca. 650–600 Ma) Arsha formation. Underlying Archean-Paleoproterozoic and the Riphean complexes are intruded by dike swarms and sills.

Determining the age of clastic sediments is difficult because they generally lack fossils, however, the presence of igneous rocks provides the opportunity for radiometric dating. Combining cross-cutting relationships with radiometric dating, it is possible to constrain the relative timing and tectonic evolution of this margin. We have collected samples from the various suites of igneous rocks (Figs. 1, 2) along the southeastern margin of the East European craton, to perform modern, high-resolution geochemical analyses in order to:

1) Identify a geochemical 'fingerprint' (mainly based on incompatible trace elements) for each volcanic and intrusive suite.
2) Use these geochemical fingerprints to suggest magmatic age correlations between intrusive and extrusive sequences.
3) Use geochemistry to determine the tectonic setting and mantle sources types for the various magmatic suites.

In addition, we provide a new U–Pb age for middle Riphean dyke.

REGIONAL SETTING

The stratigraphy of the Meso- and Neoproterozoic sedimentary and volcanic formations of the region of the Bashkirian anticlinorium represents a type section for the Riphean (ca. 1650 to 650 Ma) (Keller & Chumakov, 1983). The Riphean overlies unconformably the Archean-Paleoproterozoic Taratash crystalline basement complex and is represented by mostly terrigenous and carbonate formations (Fig. 1). The Lower Riphean (Burzyanian), with a lower age limit ca. 1650 Ma consists of Ai, Satka and Bakal formations (and age-equivalent Bolsheinzer, Suran and Jusha formations in the southern Bashkirian antinclinorium). The Middle Riphean (Yurmatinian), with a lower limit ca. 1350 Ma comprises the Mashak, Zigalga, Zigazino-Komarov, and Avzyan formations. The Upper Riphean (Karatavian), with a lower limit of ca. 1000 Ma comprises the Zilmerdak, Katav, Inzer, Minyar, Uk and (locally developed) Krivoluk formations. The Riphean is overlain by the Vendian (Asha series) with a time span ca. 650–540 Ma, and which is divided into the Lower and Upper subseries and a number of formations. The Lower and Middle Riphean correspond approximately to the Mesoproterozoic, the Upper Riphean and Vendian to the Neoproterozoic,

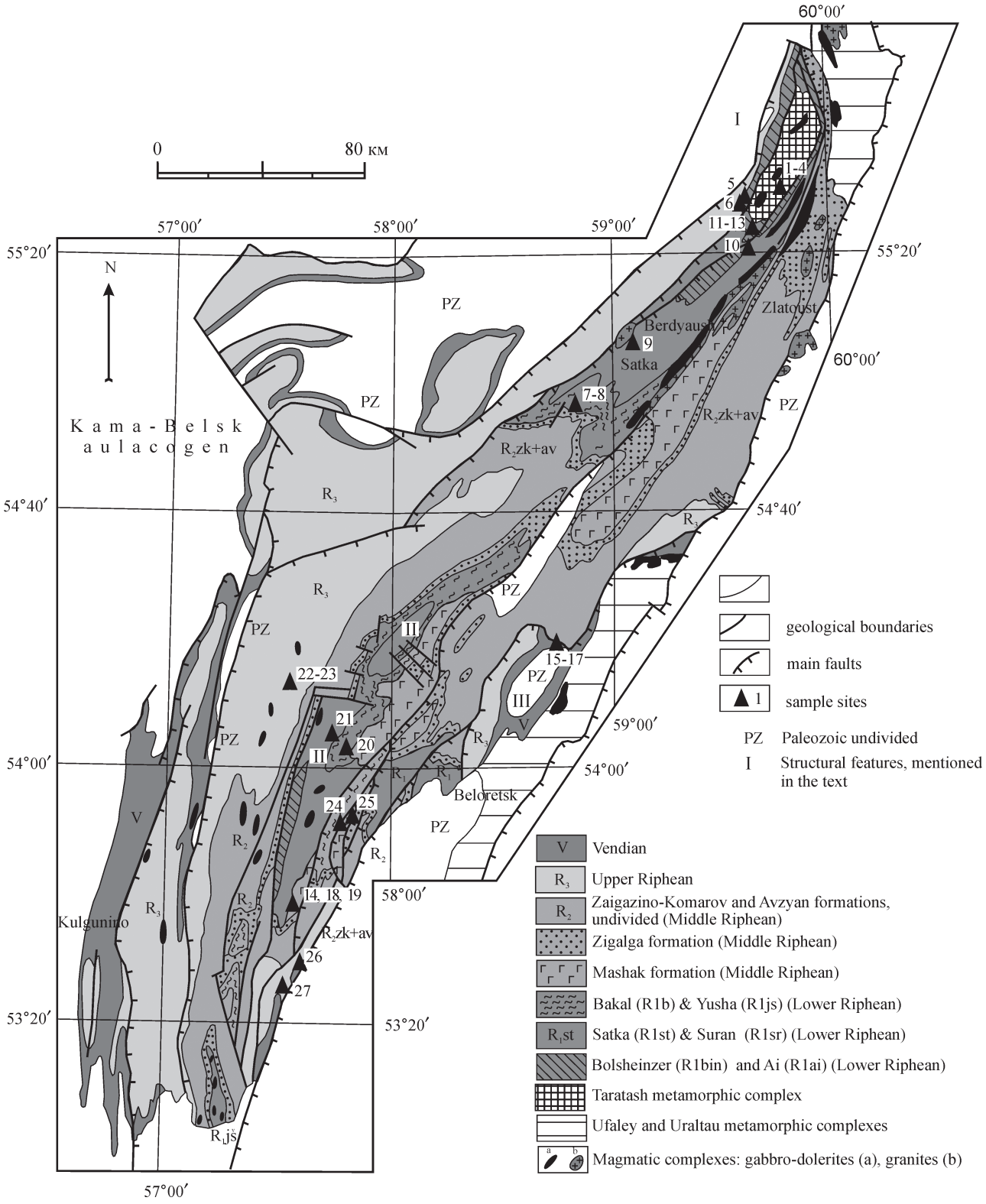

Figure 1. Schematic geological map of the Bashkirian meganticlinorium (Southern Urals, Russia). Modified from Kozlov (2002)

Sampling sites: Radashny quarry (sites 1–4), Bolshoi Miass mtn. (site 5), quarry at the southern slope of Maly Miass mtn. (site 6), main dike Bakal quarry (site 7), Irkuskan quarry (site 8), cutting Berdyaush pluton (site 9), along road to Zlatoust on southeastern outskirts of Kusa town (site 10), right banks of Kusa and Ai rivers (sites 11–13), Matveev Zalavok tract, Bolshoi Shatak range (site 14), Krutaya mtn, to the north of Tirlyan village (sites 15–17), Kapkatash mtn, Bolshoi Shatak range (site 18), Bolshoi Kliuch Creek, Bolshoi Shatak range (site 19), along road 2 km to the west from Mezhgorye town (site 20), along road 0.8 km to north-west from Berdagulovo village (site 21), along road 1.2 km to the west from the highway bridge over Maly Inzer River ("Otkop" location) (site 22), in roadcut of a abandoned railroad line, 1.5 km to the S–E of Inzer railroad station at the left bank of Maly Inzer river (site 23). 10 km to the south of Ishlya village, Karagas range, Karagas #3 drill hole (site 24), Bolyshoy Kliuch (site 25), central Bainazarova along road between Beloretsk and Byrzyan (site 26), Belaya river, 10 km downstream of Nizhni Avzyan village (site 27). Structures mentioned in the text: I – Taratash anticline, II – Yamantau anticlinorium, III – Tirlyan syncline

and the Vendian is almost coeval with Ediacarian of the International Time Scale (Gradstein et al., 2004).

Volcanic episodes are associated with the Ai (Lower Riphean), Mashak (Middle Riphean) and Arsha (Lower

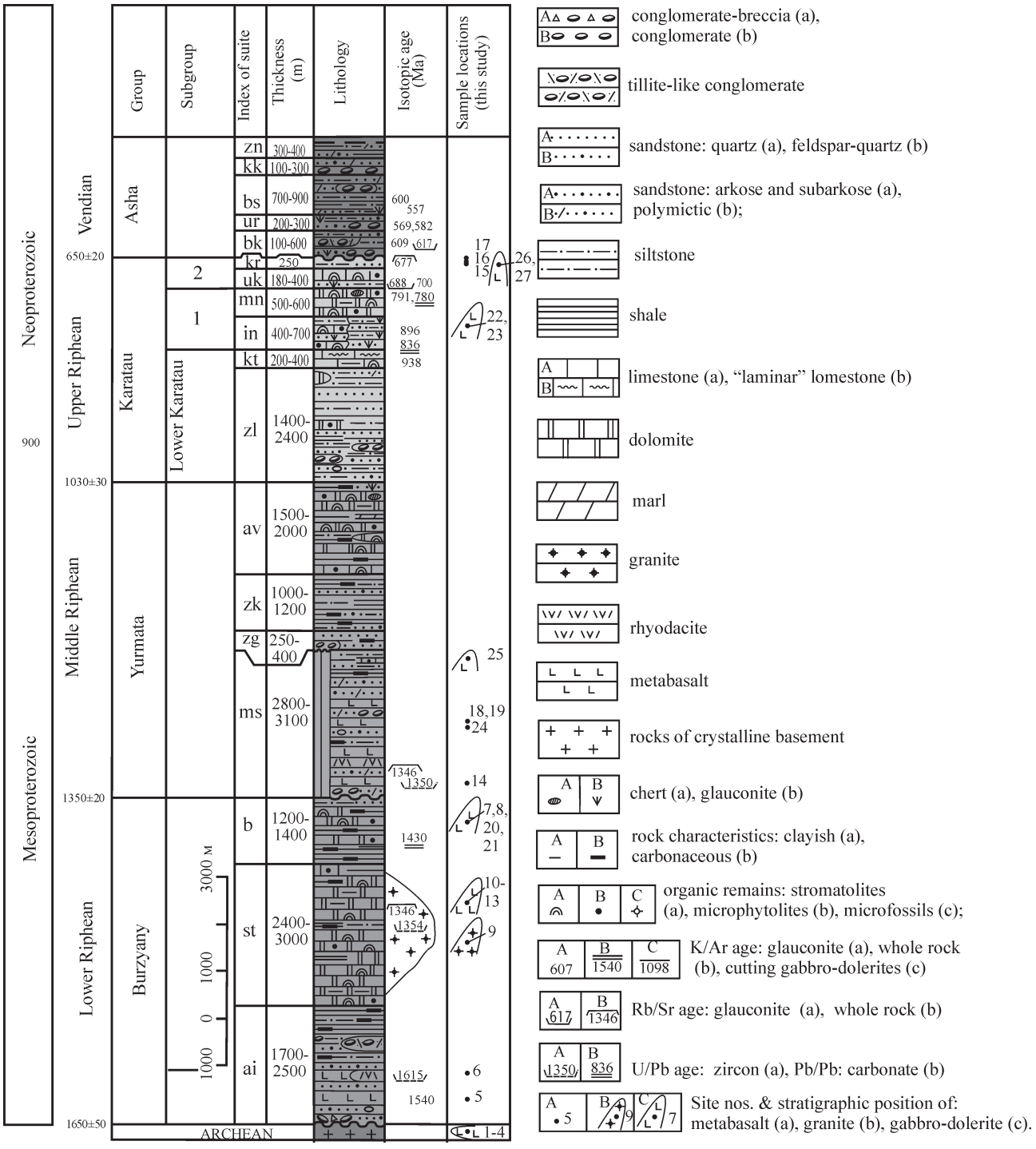

Figure 2. The general scale of the Upper Precambrian of Russia (after Semikhatov et al., 1991) and generalized stratigraphic column of the Upper Precambrian of the axial part and western limb of the Bashkirian meganticlinorium: Site numbers located in Fig. 1

Formations of the Upper Precambrian of the Southern Urals: ai – Ai, st – Satka, b – Bakal,, ms – Mashak, zg – Zigalga, zk – Zigazino-Komarovsk, av – Avzyan, zl – Zilmerdak,, kt – Ratav, in – Inzer, mn – Minyar, uk – Uk, kr – Krivoluk, bk – Bakeevo, ur – Uryuk, bs – Basinsk, kk – Kukkarauk, zn – Zigan. The Arsha formation is probably coeval with Bakeevo and Uriuk formations of this section. The age boundaries between the stratigraphic units of the Riphean and Vendian as are those approved by the All-Union Stratigraphic Meeting in Ufa, 1990 (Semikhatov et al., 1991). Since then, in early 2006, new versions of the base of Karatavian (1030 Ma) and base of the Vendian (600 Ma) were suggested in the 3rd Edition of the Stratigraphic Code of Russia. In the first case the change of the boundary is within the indicated error (±30 Ma). As for the second case, the age of the base of the Vendian is still very weakly constrained by the geological and geochronological data. It is also possible that this boundary is diachronous, getting older toward the open sea basin (i.e. in the direction of the Urals). Therefore, for the time being, we continue to use the earlier version of the boundary, which is not decreed, but generally accepted by the geological community

Vendian) formations. In addition, diabase dikes and sills of probable Riphean age(s) intrude the Archean-Paleoproterozoic Taratash crystalline complex, and the Riphean Satka, Bakal, Inzer or Krivoluk formations, and the middle Riphean rapakivi Berdyaush granite.

Lower Riphean Ai formation

Lower Riphean volcanic and volcano-sedimentary rocks are known from the northern part of the Bashkirian meganticlinorium, in limbs of the Taratash anticline (Fig. 1) which have the typical northeast trending strike of the modern Urals (e.g. Puchkov, 2002). The sedimentary component of the Ai formation consists of coarse terrigenous deposits, with conglomerates near the bottom, close to the contact with the crystalline basement. Conglomerate pebbles and boulders consist of quartzites, amphibolites, gneisses and other basement rocks (Kozlov et al., 1989). The volcanic rocks are situated in the upper unit of the Navysh subformation of Ai formation, and consist predominantly of effusive rocks (lavas, lava breccias), but also include subvolcanic bodies and dikes (dolerite, and more rare dacite porphyry) and volcanosedimentary rocks (tuff and tuffaceous units of different grain size). The Navysh lavas are predominantly metabasalt, and the Navysh dacite porphyries have a U–Pb zircon date of 1615±45 Ma (Krasnobaev, 1986; Krasnobaev et al., 1992), interpreted as the time of crystallization, which constrains the age of the lower part of the Riphean deposits in their type section. Previous K–Ar data from Navysh diabases range in age from 419–671 Ma and imply metamorphic resetting (Lennykh et al., 1978). Parnachev (1981) regards the Navysh formation as volcano-sedimentary graben facies formed in a marginal part of the Kama-Belsk (Mashak) paleorift which has a northwestern strike, oblique to the modern structure of the Urals (Puchkov, 2002).

The Ai formation is overlain by terrigenous-carbonate deposits of the Satka and Bakal formations. Further south, along the rest of the Bashkirian mega-anticlinorium the terrigenous-volcanogenic Ai formation is replaced by the age equivalent carbonate-terrigenous Bolsheinzer formation. Although the analogues of the Lower Riphean are exposed in the axial part of the Yamantau anticlinorium (Fig. 1) volcanogenic material is absent there.

Middle Riphean (Mashak Fm and correlatives)

The Middle Riphean volcanic and volcano-sedimentary rocks of the Mashak formation, form a northeast trending belt (parallel to the typical Uralian strike (20°–30° NE), more than 100 km long and 1–12 km wide. In the northern part of the Bashkirian anticlinorium the analogues of Mashak formation are metamorphosed to zonal greenschist and amphibolite facies and are known as Kuvash formation. Mashak formation volcanic rocks include effusives and subvolcanic intrusions of basaltic to rhyolitic compositon. The most comprehensive section of Mashak formation is found in the No 3 Karagas borehole (Fig. 1, point 15). The borehole penetrates basic metavolcanics of effusive and volcanoclastic facies. Volcano-sedimentary and sedimentary rocks are observed to alternate in an irregular way.

Brecciated lavas (Dungan-Sungan mtn.) and some subvolcanic bodies are identified as the necks of ancient volcanoes (Yamaev and Shvetsov, 1973). Parnachev (1981) concluded that Mashak volcanism and sedimentation occurred in graben-like (rift) structures (with NNE strike).

Acid volcanic rocks are recorded only in the lower parts of the formation and comprise 10–15% of the total thickness of volcanic rocks. They are represented by rhyolites, trachy-rhyolites and dacites. The rhyolites were dated by the conventional multi-grain U–Pb (zircon, 1350±30 Ma) and Rb–Sr (whole rock, 1346±41 Ma) methods (Krasnobaev, 1986), which constrains the age of the lower part of the Yurmatinian series. In addition, a Rb–Sr age of 1360±35 Ma was obtained for a dyke in the Bakal quarry (Ellmies et al., 2000), and a Pb–Pb single zircon age of ca. 1350 Ma was obtained for an eclogite facies mafic dyke in the Beloretzk metamorphic complex (Glasmacher et al., 2001). A comprehensive listing of previous geochronology is provided in Fig. 2.

Recently more accurate ages have been obtained from Berdyaush intrusive suite rocks, cutting Satka formation, mainly by SIMS (Secondary Ion Mass Spectrometry) method (Ronkin et al., 2005). Specifically, 1395±20 Ma was obtained from a gabbro (probably a xenolith, and perhaps representing an inclusion from a co-genetic intrusion), 1372±12 Ma from a quartz syenite-diorite, 1369±13 Ma from a rapakivi granite and 1373±21 and 1368.4±6.2 Ma from a nepheline syenite. Therefore, the age of the Berdyaush suite is ca. 1370.

Lower Vendian (Arsha Formation)

Lower Vendian volcanogenic rocks in the Southern Urals occur locally in the northern part of the Tirlyan syncline (Fig. 1), (eastern limb of the Bashkirian meganticlinorium, 40–50 km to the north from town of Beloretsk). These volcanic rocks are situated in the middle part of the Arsha formation in association with terrigenous rocks, tillites among them. The Arsha volcanics include effusive, explosive and volcano-sedimentary facies. Andesitic and rare dacite-andesitic lavas and brecciated lavas predominate (Parnachev and Kozlov, 1979, Alekseyev, 1984, Parnachev, 1981). Andesites of Krutaya mtn. were dated by the Rb–Sr method as 677±31 Ma (Gorozhanin, 1995). According to Parnachev (1981), the Arsha complex belongs to the NNW-trending Kama-Belsk paleorift structure.

PREVIOUS GEOCHEMISTRY

According to Parnachev (1981), the least altered trachybasalts of the Early Riphean Ai formation (23 chemical analyses) have high TiO_2 (2.74%), total alkalis (6.69%) and P_2O_5 (0.79%), while Ni/Co ratios and the distribution of REEs are comparable to trachybasalts of the East African rift zone.

Metabasalts of the Middle Riphean Mashak and correlative Kuvash formations correspond to olivine tholeiites with low contents of Cr (70 ppm), Ni (70 ppm), Ba (210 ppm), Sr (100 ppm), and REE (90 ppm), and high contents of V (285 ppm) (Parnachev, 1981; Parnachev et al., 1986). These metabasalts are part of a bi-modal association characteristic of continental rift complexes (Grachev, 1977). A more recent trace element study by Karsten et al. (1997) interpreted metabasalts of the Mashak formation as tholeiites of rather complex character. Concentrations of Zr, Y, Nb, Ti, are lower than typical basalts of continental rifts, but higher than those in the oceanic rifts (NMORB). The absence of an Eu-anomaly suggests mantle genesis of primary magmas and no fractionation of plagioclase. According to Karsten et al. (1997), metabasalts and metarhyodacites of Mashak formation have differing geochemical characteristics and therefore do not belong to a single bi-modal magmatic association; the metabasalts are linked to active rifting while metarhyolites situated closer to the lower part of the volcanic section could be formed in an intraplate setting prior to, or at an early stage of rifting.

Lower Vendian (see the comments to the Fig. 2) Arsha metabasalts (Parnachev and Kozlov, 1979; Parnachev, 1981 his table 1, 29 chemical analyses) have high TiO_2 (up to 3%), Fe oxides (up to 18.5%), P_2O_5 (up to 1.53%), REE concentrations, Ni/Co ratios (0.15). These chemical features combined with a trachytoid type of matrix texture classify them as trachybasalts.

Lennykh and Petrov (1978) studied dykes cutting the Archaean-Paleoproterozoic metamorphic rocks of the Taratash complex at the Radashny quarry. Based on geochemistry (34 analyses) and geochronology (mostly K–Ar), they identified three groups of diabases. The oldest group (ca. 1650 Ma) represents tholeiitic diabase of composition similar to "traps" (flood basalts) of ancient platforms. Tholeiitic diabase of the second group has ages of 1250–1150 Ma, and based on alkali and titanium content and alkali/alumina ratio correspond to "traps" (flood basalts) of young platforms. The third group comprises intrusions of essexite-diabase with ages of 670–420 Ma. Taking into account the widespread regional alteration affecting all suites (discussed earlier), it is unlikely that these K–Ar dates are reliable.

To summarize, previous geochemical studies have established that three ages of volcanic rocks are present (lower Riphean, middle Riphean and lower Vendian) and that each has geochemical similarities with extensional volcanism. There are also several intrusive suites recognized. However, a strong link between the intrusive and extrusive is difficult to make based on the available K–Ar and trace element data. Apart from the recent study by Karsten et al. (1997) on the Mashak and related Kuvash formation, the available trace element data is very old. Therefore, it is important to reevaluate the geochemical setting of all the magmatic suites in the Bashkirian anticlinorium using a modern trace element dataset.

SAMPLING SUMMARY AND METHODOLOGY

Samples were collected from various magmatic suites through sections of the Lower Riphean Ai and Satka formations, the Middle Riphean Mashak formation, and the Vendian Arsha formation (Fig. 2). In addition samples were collected from dykes and sills intruding the Archean-Paleoproterozoic and Lower Riphean Taratash, Bakal, and Satka formations, as well as Upper Riphean Inzer and Krivoluk formations. Site information is summarized in Table 1 and 2 and details of locations are given Figs. 1 & 2.

Table 1

Location and descriptions of extrusive samples (more details are given in Figs. 1 & 2)

Site No.	Site Label	Location (N. lat)	Location (E. long)	No. of samples	Unit
LOWER RIPHEAN					
5	EQ03–05	55.4963	059.6610	8	Traverse through section of Ai formation
6	EQ03–06	55.4085	059.6397	2	Ai formation
MIDDLE RIPHEAN					
14	EQ03–14	53.6617	057.5840	11	Traverse through sills and volcanics of Mashak formation
18	EQ03–18	53.6605	057.6173	4	Traverse through Mashak fm
19	EQ03–19	53.6790	057.6363	6	Traverse though Mashak fm
24	EQ03–24	53.14	057.31	16	500 m of drill core in Mashak fm
VENDIAN					
15	EQ03–15	54.3020	058.6778	1	Volcanic breccia in Arsha fm
16	EQ03–16	54.3032	058.6760	7	Traverse through Arsha fm
17	EQ03–17	54.3018	058.6812	1	Dacite in Arsha fm

Table 2

Location and descriptions of intrusive samples (more details are given in Figs. 1 & 2)

Site No.	Site Label	Location (N. lat)	Location (E. long)	No. of samples	Unit
CUTTING PRE-RIPHEAN BASEMENT					
1	EQ03–01	55.5265	059.7923	1	Diabase sheet (strike 178, dip 54 E, thickness 2 m)
2	EQ03–02	~55.526	~059.794	3	Diabase dyke (strike ~25 , dip 75 SW, two pulses)
3	EQ03–03	55.5267	059.7947	2	Diabase sill (changes from 3–20 m thick west to east)
4	EQ03–04	55.5265	059.7958	3	Diabase dyke (strike 166, dip 85 E)
CUTTING SATKA FORMATION (LOWER RIPHEAN)					
10	EQ03–10	55.3218	059.4437	6	Diabase sill
11	EQ03–11	55.3465	059.4128	2	Diabase sill (strike 220, dip 50 SE, thickness > 4 m), following bedding in Satka fm.
12	EQ03–12	55.3463	059.4087	1	Diabase sill (strike 220, dip 50 SE, thickness 1.5 m)
13	EQ03–13	55.3460	059.4035	1	Diabase sill (strike 145, dip 35 NE)
CUTTING SURAN FORMATION (LOWER RIPHEAN)					
20	EQ03–20	54.0867	057.8058	1	Diabase sheet (strike 210, dip 70 SE, thickness 15 m)
21	EQ03–21	54.1658	057.7677	1	Diabase dyke (strike 160, dip 70 E, thickness >13 m)
CUTTING BAKAL FORMATION (LOWER RIPHEAN)					
7	EQ03–07	54.9190	058.7873	1	Diabase dyke (strike 40–50, dip 60–70 E, thickness 100 m)
8	EQ03–08	54.9168	058.8463	4	Vertical, to subhorizontal sheet (sill)
CUTTING MIDDLE RIPHEAN					
25	EQ03–25 (552–107, 552–108)	53.51	057.11	2	Gabbro-dolerite ($\leq R_2$)
CUTTING BERDYAUSH PLUTON (MIDDLE RIPHEAN)					
9	EQ03–09	55.1568	059.1273	2	Diabase dike (strike 75, dip 60 N, thickness 4 m)
CUTTING INZER FORMATION (UPPER RIPHEAN)					
22	EQ03–22	54.2097	057.5872	1	Diabase dyke (trend 160, dip 80 E, thickness >4 m)
23	EQ03–23	54.2182	057.5902	2	Diabase dyke (trend ~200, thickness 60 m)
CUTTING KRIVOLUK FORMATION (UPPER RIPHEAN)					
26	EQ03–26 (644–4)	53.28	056.50	1	Diabase dyke/strike 20, dip 60–70 E
27	EQ03–27 (646–1)	53.48	057.48	1	Diabase (sill?)

All geochemistry samples were cleaned of surface alteration by hydraulic splitting followed with sandblasting. Geochemistry samples were submitted to Activation Laboratories, Canada for milling and analysis. All samples were milled in "mild steel" (RX2 procedure) which produces only minor iron contamination (<0.2%). Major and trace elements were analyzed using the "4Litho" package. Major element oxides were determined by lithium metaborate fusion using 0.2 g of whole rock powder and the ICP–ES technique (results reported in weight percent). Trace elements (including REE) were analyzed by ICP–MS and are reported in parts per million (ppm). Calibrations were made using reference samples and international standards. Relative standard deviations are ~1% for SiO_2 and ~2% for the other major elements, except MnO and P_2O_5 (±0.01%) and K_2O (±0.005%). Relative standard deviations are generally better than about 5% for most trace elements. Detection limits of particular interest include the high field strength elements (Hf = 0.1, Nb = 0.2, Ta = 0.01, Th = 0.05, U =

0.01, light REE = 0.05, middle and heavy REE = 0.01). The determination of structurally bound H_2O was made via loss on ignition (LOI). The analytical data are presented in Table 3. Data was normalized to 100% volatile-free before plotting.

GEOCHEMISTRY

Various major and trace element compositions can be useful for distinguishing between magmatic events and assessing the contribution of various mantle components (e.g. Condie, 2003 and references therein). This is best achieved with pristine samples representative of primitive melt compositions, i.e. — fresh samples unaffected by crystal-melt processes (crystal cumulates, crystal fractionates, etc.) which can obscure mantle processes/components. HFSE and REE are least mobile during metamorphic processes (e.g. amphibolite facies — Polat et al., 2003; blueschist facies — Mocek, 2001; eclogite facies — Becker et al., 2000). Consequently, these elements are more likely to preserve unaltered geochemical signatures and can be used to identify mantle reservoirs in altered samples. Each of these factors is evaluated and potential geochemical 'fingerprints' for the igneous suites are presented below.

Identification of altered and anomalous samples

Most of the analyzed samples have LOIs less than 3%, though some have values up to 10%. (Fig. 3). Since fresh, unaltered basalts generally have LOI≤3 wt %, those high LOI values may be evidence of subsequent alteration. However, specific suites have higher LOIs which seem to be characteristic of the units: Ai formation (lower Riphean) volcanics (units 5 and 6); Middle Riphean rocks (units 14, 18 and 24, but not unit 19), and sills; and dykes cutting the Satka formation (units 10–13). In addition, two of the four high MgO samples from the intrusive unit 8 have high LOI. The lower Riphean volcanics and intrusives cutting lower Riphean group up to just over 5% LOI. So as to avoid splitting these apparent natural groups, we take the high LOI cutoff as 5.5%.

Many Middle Riphean samples have very low K (Figs. 4a and 7). This may be partly characteristic of the suite, but may represent systematic removal of K (and Ba and Rb) during the low grade metamorphism that affected the suites. In most cases the alteration has not significantly affected the patterns of high field strength trace elements (e.g. REE on Fig. 5), and those data can be used to define groupings with which to recognize anomalous samples**.** The data from sites 5 and 6 are well grouped. Site 14 has two groups, samples 2–7 representing the more mafic group and 9–11 being more felsic, and the remaining sample (no. 1) falls outside both groups and is considered anomalous. In site 16, sample 05 is set apart from the other samples. In site 18, sample 04 is anomalous. At site 19, sample 06 is anomalous. Site 24 does not show a simple grouping; a dominant group is represented by samples 37.5, 40, 51, 260, 280, 296, 311, 513 and 514. Samples that are clearly anomalous include sample 477, and possibly 210 and 224 Samples 394 and 399.5 match each other but have distinctly steeper LREE from the other samples (and have high LOIs of about 4.5%).

A similar complex situation is observed for the intrusive suites. Sites 1–4 in the Radashny quarry have a main group defined by samples 0201, 0202, 0203, 0401, 0402. Both samples from site 3 are anomalous to this group and to each other, and sample 0403 is also anomalous. In site 10, sample 06 is anomalous; samples 1–5 are from the main sill while sample 6 is from a thin (0.5 m) satellite sill located nearby but above the main sill. The rest of the intrusive data is relatively consistent within a site.

Consequently, we eliminate those samples with very high LOI (>5.5%): 24–477, 24–257.5, 24–513, 1803, 1605, 0801, and 0802, and anomalous samples (identified above), 14–01, 14–08, 16–05, 18–04, 19–06, 24–210, 24–224 and 24–477, from subsequent analysis.

Geochemical Diagrams

The samples are mainly mafic, but with some felsic components (sites 6, 16, 17, 24–185, and selected samples from site 14: samples 1, 9, 10 and 11) (Fig. 4). To distinguish felsic samples in subsequent figures, we enclose their symbols with an open circle. The extrusive and intrusive suites are considered separately and are each assessed using a variety of diagrams: standard classification diagrams, trace element setting diagrams and mantle source diagrams (e.g. LeBas, 1986; Condie, 1997, 2001; Tomlinson and Condie, 2001; Rudnick, 1995; Herzberg, 1995; Rollinson, 1993; Pearce, 1996). We first provide an overview using the TAS diagram (Fig. 4), REE diagrams (Fig. 5), multi-element diagrams (Fig. 6), AFM diagram (Fig. 7), TiO_2 vs Mg# (Fig. 8), and Zr/TiO_2 vs Nb/Y (Fig. 9). Among these (as discussed above) the trace element diagrams are least susceptible to the effects of alteration. Additional diagrams that are useful for tectonic setting include Zr vs Ti vs Y (Fig. 10), MnO_2 vs TiO_2 vs P_2O_5 (Fig. 11), La vs Y vs Nb (Fig. 12), and Ti vs V (Fig. 13). These diagrams can basically distinguish mid-ocean ridge basalts (MORB), from volcanic arc (VAB), from within plate basalts (WPB), and there are subcategories: thus MORB and WPB can divide into tholeiites and alkali basalt groups, VAB can divide into tholeiites, calc-alkaline basalts and shoshonitic, and both VAB and WPB can also divide into oceanic and continental types (Pearce, 1996). These diagrams as well as Figs. 14–18 are useful for developing geochemical 'fingerprints' for the various magmatic suites, and Figs. 16–18 can also be used to assess mantle source reservoirs (after Condie, 2003).

Activation Laboratories Ltd. Work Order No. A04-2169 Report No. A04-2169

Table 3

Geochemical data from Precambrian magmatic units of the southeastern margin of the East European Craton, southern Urals, Russia

Notes:
1) analyzed by ACTLABS (www.actlabs.com, Ancaster Ontario laboratory)
2) negative values indicate less than the reporting limit
3) details on sample locations in caption to Figure 1, and in Tables 1 and 2. Analytical details discussed in text.

Site No.	SAMPLE	SiO2	Al2O3	Fe2O3	MnO	MgO	CaO	Na2O	K2O	TiO2	P2O5	LOI	TOTAL	V	Cr	Co	Ni	Cu	Zn	Ga
1	EQ03-01-01	54,41	10,50	14,91	0,118	3,12	7,20	1,04	0,93	0,629	0,15	3,06	96,08	171	53	26	-20	>10,000	57	14
2	EQ03-02-01	52,83	13,19	12,36	0,188	5,59	8,34	3,09	1,13	0,870	0,12	1,34	99,04	271	39	41	29	164	76	18
2	EQ03-02-02	53,35	14,01	11,54	0,168	5,95	9,69	2,33	0,99	0,878	0,11	0,75	99,75	213	108	37	31	56	66	18
2	EQ03-02-03	53,48	13,84	11,63	0,173	5,87	9,28	2,39	1,12	0,905	0,11	0,90	99,70	226	130	39	-20	37	87	19
3	EQ03-03-01	48,93	13,50	14,06	0,151	4,77	7,55	3,67	1,27	3,146	0,40	1,69	99,13	316	45	41	93	45	125	26
3	EQ03-03-02	50,78	12,50	12,47	0,201	8,00	10,10	2,00	1,72	0,822	0,08	1,29	99,97	268	97	45	66	96	77	16
4	EQ03-04-01	48,48	14,38	13,59	0,218	6,73	9,11	1,97	1,88	1,007	0,27	2,13	99,78	254	95	48	81	79	115	18
4	EQ03-04-02	48,81	14,01	13,24	0,176	6,96	8,76	2,36	0,96	1,064	0,29	2,44	99,06	264	99	46	69	79	84	18
4	EQ03-04-03	54,22	12,91	14,35	0,156	2,44	6,52	2,96	0,87	2,549	0,52	2,58	100,06	276	-20	27	-20	23	118	25
5	EQ03-05-01	47,20	14,25	14,87	0,093	8,70	1,46	0,19	4,95	2,773	0,84	4,76	100,08	244	43	40	48	-10	107	23
5	EQ03-05-02	46,12	13,93	15,54	0,088	8,24	2,59	0,29	5,27	2,658	0,79	4,35	99,86	243	42	38	56	19	109	23
5	EQ03-05-03	48,06	13,66	14,04	0,092	7,54	2,87	0,35	4,96	2,666	0,80	4,11	99,14	235	44	37	46	-10	101	22
5	EQ03-05-04	46,84	14,22	14,81	0,120	8,52	1,41	0,31	5,70	2,576	0,73	4,41	99,64	220	46	38	59	-10	97	21
5	EQ03-05-05	47,55	14,89	14,71	0,140	4,77	6,29	3,29	0,85	2,587	0,72	3,13	98,92	231	58	41	62	27	134	23
5	EQ03-05-06	45,96	15,18	14,50	0,120	7,33	2,35	1,69	3,90	2,705	0,75	4,54	99,01	242	59	52	55	11	125	25
5	EQ03-05-07	49,66	13,44	14,77	0,173	4,06	6,21	2,52	2,55	2,564	0,80	2,96	99,70	228	51	42	39	38	145	24
5	EQ03-05-08	49,92	13,82	14,79	0,195	4,59	3,04	3,86	2,49	2,532	0,79	2,60	98,64	241	40	38	35	30	159	24
6	EQ03-06-01	66,79	11,90	7,76	0,014	4,81	0,35	0,91	4,36	0,747	0,24	2,97	100,85	-5	33	5	-20	22	66	24
6	EQ03-06-02	60,71	13,67	10,71	0,139	1,68	2,66	2,43	3,80	1,570	0,52	1,84	99,73	137	-20	19	29	14	149	27
7	EQ03-07-01	46,62	17,29	12,50	0,180	4,35	9,43	3,34	1,03	1,624	0,18	2,68	99,20	273	67	47	58	178	69	27
8	EQ03-08-01	46,48	14,25	8,63	0,083	16,81	2,68	1,63	1,59	0,840	0,12	6,64	99,76	235	424	37	103	40	65	17
8	EQ03-08-02	45,37	8,52	10,75	0,168	18,45	8,72	0,88	0,46	0,471	0,08	5,86	99,73	152	592	81	623	41	77	11
8	EQ03-08-03	48,73	12,54	10,03	0,164	10,02	11,39	1,07	2,65	0,690	0,10	2,18	99,56	209	404	48	204	74	67	16
8	EQ03-08-04	49,17	12,54	9,63	0,167	10,44	10,44	1,20	2,58	0,685	0,09	2,28	99,21	207	430	40	178	68	-30	14
9	EQ03-09-01	42,34	14,42	16,72	0,220	6,95	9,76	1,86	2,33	1,930	0,22	2,32	99,06	359	-20	65	77	80	111	23
9	EQ03-09-02	42,48	14,81	16,58	0,214	7,26	9,83	1,70	2,39	1,895	0,21	1,95	99,31	359	25	67	90	78	105	24
10	EQ03-10-01	48,08	16,21	11,32	0,139	8,02	6,34	3,32	1,19	1,436	0,29	2,96	99,30	234	35	42	47	35	89	22
10	EQ03-10-02	48,89	16,07	10,99	0,128	7,02	7,42	3,20	1,22	1,437	0,30	3,34	100,01	239	49	38	43	28	107	22
10	EQ03-10-03	47,97	15,59	11,10	0,154	5,58	8,70	3,29	1,19	1,385	0,28	4,33	99,55	221	36	38	51	58	74	21
10	EQ03-10-04	48,80	15,31	12,50	0,167	6,26	6,95	3,20	1,34	1,622	0,32	2,89	99,35	266	57	41	52	29	77	23
10	EQ03-10-05	46,94	16,03	11,27	0,160	6,12	7,77	3,17	1,70	1,325	0,25	4,79	99,52	213	33	38	44	29	109	21
10	EQ03-10-06	61,92	15,78	5,07	0,008	4,74	0,19	0,09	7,16	0,615	0,13	3,01	98,72	94	86	16	39	20	-30	21
11	EQ03-11-01	47,79	14,21	10,73	0,152	7,70	8,68	3,36	1,53	1,243	0,22	4,47	100,09	230	473	36	164	79	83	19
11	EQ03-11-02	48,59	15,37	11,27	0,155	6,53	8,96	2,77	1,64	1,301	0,23	3,29	100,08	234	228	40	87	48	97	20
12	EQ03-12-01	46,86	13,30	13,27	0,161	6,09	7,43	2,98	2,35	2,164	0,34	5,11	100,04	262	55	47	100	115	100	20
13	EQ03-13-01	48,20	13,87	12,37	0,129	6,35	6,02	3,57	1,75	2,229	0,34	5,21	100,03	270	59	38	55	76	90	22
14	EQ03-14-01	71,48	11,14	8,39	0,111	1,91	0,71	0,31	1,71	0,706	0,10	2,61	99,17	96	103	15	57	11	139	16
14	EQ03-14-02	49,38	12,60	15,04	0,287	5,57	10,24	0,04	-0,01	2,076	0,30	3,46	98,98	403	72	41	52	136	138	20
14	EQ03-14-03	49,58	12,52	15,91	0,311	6,36	7,94	-0,01	0,03	2,043	0,29	3,99	98,95	408	66	53	55	74	169	19
14	EQ03-14-04	48,41	12,92	14,91	0,276	5,59	8,50	1,22	-0,01	2,162	0,29	4,74	98,98	402	157	43	76	20	224	21
14	EQ03-14-05	48,02	13,23	15,52	0,251	6,56	7,59	2,45	-0,01	2,110	0,29	3,13	99,12	390	155	40	81	44	121	20
14	EQ03-14-06	43,33	13,65	18,07	0,233	6,09	11,20	0,08	-0,01	2,118	0,30	3,68	98,73	411	168	45	110	14	138	24
14	EQ03-14-07	49,29	13,90	15,49	0,127	7,98	2,30	2,18	0,02	2,329	0,31	4,87	98,78	410	169	31	71	-10	87	23
14	EQ03-14-08	29,29	19,19	27,13	0,188	11,99	0,75	-0,01	0,77	0,699	0,19	7,77	97,97	61	-20	37	82	-10	131	46

Negative values indicate less than the reporting limit
LOI values less than -0.01% represent a Gain on Ignition

Activation Laboratories Ltd. Work Order No. A04-2169 Report No. A04-2169

Site No.	SAMPLE	SiO2	Al2O3	Fe2O3	MnO	MgO	CaO	Na2O	K2O	TiO2	P2O5	LOI	TOTAL	V	Cr	Co	Ni	Cu	Zn	Ga
14	EQ03-14-09	75,56	12,05	2,66	0,014	1,20	0,45	2,85	2,54	0,517	0,13	1,69	99,66	10	-20	2	-20	-10	-30	20
14	EQ03-14-10	73,55	11,32	5,26	0,035	1,44	0,20	3,64	1,61	0,542	0,11	1,48	99,19	11	26	5	-20	-10	-30	18
14	EQ03-14-11	72,40	12,40	5,12	0,019	1,00	0,24	3,96	2,54	0,575	0,12	1,11	99,48	9	-20	3	-20	-10	-30	22
15	EQ03-15-01	55,06	17,00	8,95	0,143	2,82	6,87	3,69	0,96	1,167	0,18	2,56	99,40	121	23	19	-20	12	97	26
16	EQ03-16-01	59,64	15,93	7,15	0,112	2,48	5,85	4,90	0,05	1,115	0,20	2,03	99,46	125	46	16	-20	20	99	27
16	EQ03-16-02	60,36	15,38	7,82	0,130	2,07	6,71	3,98	0,14	1,093	0,20	2,05	99,92	129	29	19	-20	-10	60	25
16	EQ03-16-03	63,41	13,88	8,04	0,132	3,12	4,15	3,39	0,40	0,987	0,17	2,42	100,10	114	41	25	-20	20	105	21
16	EQ03-16-04	50,55	15,95	16,39	0,107	0,94	3,30	5,57	1,73	3,040	0,46	1,62	99,64	107	-20	35	-20	20	125	21
16	EQ03-16-05	62,15	6,47	7,94	0,609	0,77	10,14	2,67	0,21	1,125	0,33	7,80	100,21	38	22	19	-20	-10	52	7
16	EQ03-16-06	56,22	13,39	14,11	0,201	1,19	3,92	5,44	0,59	2,396	0,58	1,40	99,44	78	-20	28	-20	31	74	15
16	EQ03-16-07	49,35	15,23	12,25	0,269	3,13	10,24	2,27	0,12	2,730	0,53	2,73	98,84	109	-20	26	-20	23	88	23
17	EQ03-17-01	73,23	9,51	5,10	0,108	1,75	3,39	2,91	0,33	0,674	0,13	1,82	98,94	61	25	16	-20	22	42	14
18	EQ03-18-01	49,13	12,20	15,62	0,234	5,59	8,94	2,71	0,27	1,900	0,19	2,12	98,89	411	67	54	66	130	134	22
18	EQ03-18-02	51,52	12,57	15,35	0,130	6,14	5,65	3,20	0,60	2,087	0,21	2,70	100,16	426	62	41	57	30	89	21
18	EQ03-18-03	42,78	12,79	18,66	0,088	10,15	4,20	1,15	0,04	2,072	0,20	7,18	99,33	435	67	85	73	45	141	24
18	EQ03-18-04	58,21	13,87	11,79	0,032	3,34	1,77	4,96	0,92	2,209	0,22	2,09	99,41	402	69	32	120	14	64	20
19	EQ03-19-01	48,59	13,34	14,69	0,249	6,52	7,77	3,70	0,03	1,502	0,15	2,48	99,03	358	147	58	94	141	168	20
19	EQ03-19-02	48,87	13,06	15,14	0,248	6,74	7,74	3,35	0,07	1,482	0,15	2,56	99,40	336	132	60	93	55	165	21
19	EQ03-19-03	48,56	13,14	14,44	0,249	6,97	8,09	3,61	0,02	1,388	0,15	2,43	99,03	355	137	61	84	228	161	22
19	EQ03-19-04	49,35	13,80	14,56	0,245	7,19	5,32	4,71	0,17	1,392	0,15	2,59	99,47	342	131	65	77	54	164	21
19	EQ03-19-05	49,35	13,31	14,56	0,218	6,83	7,01	4,37	0,26	1,438	0,15	2,22	99,73	365	123	52	72	31	154	21
19	EQ03-19-06	55,48	11,50	16,95	0,071	2,03	3,17	5,52	0,08	2,043	0,87	0,94	98,66	187	20	35	30	238	55	16
20	EQ03-20-01	49,01	13,41	13,07	0,203	6,05	9,04	3,02	1,10	2,309	0,24	1,81	99,27	308	90	39	54	85	61	20
21	EQ03-21-02	49,03	13,97	12,71	0,188	6,81	9,94	2,20	1,51	1,405	0,17	2,30	100,23	308	233	42	80	152	87	17
22	EQ03-22-01	48,78	13,77	13,00	0,231	6,07	11,62	2,45	0,11	1,635	0,16	1,50	99,31	316	150	46	88	144	102	20
23	EQ03-23-01	49,79	13,82	13,44	0,194	6,60	10,69	2,23	0,22	1,690	0,16	0,66	99,50	316	173	45	92	155	100	20
23	EQ03-23-02	49,58	12,46	14,80	0,185	5,67	8,41	2,36	0,73	2,079	0,20	2,68	99,16	328	98	46	72	158	121	22
24	EQ03-24-(C-3K-37.5)	48,78	14,37	14,31	0,246	8,24	5,19	3,87	0,04	1,508	0,15	3,42	100,12	332	98	61	72	44	154	18
24	EQ03-24-(C-3K-40)	49,71	13,69	13,83	0,245	6,65	8,21	3,42	0,02	1,419	0,14	2,50	99,84	337	92	46	65	126	107	19
24	EQ03-24-(C-3K-51)	50,12	13,47	13,43	0,201	5,95	8,45	2,98	-0,01	1,417	0,14	3,18	99,33	327	95	38	56	165	106	18
24	EQ03-24-(C-3K-185)	61,95	13,91	11,59	0,070	2,67	1,16	3,69	1,82	1,043	0,11	2,02	100,02	303	87	30	47	-10	45	19
24	EQ03-24-(C-3K-210)	56,76	16,45	11,35	0,075	3,11	1,71	5,29	1,56	1,360	0,15	2,19	100,02	280	128	29	54	-10	51	21
24	EQ03-24-(C-3K-224)	58,30	13,89	13,10	0,099	4,38	1,37	4,36	0,45	1,180	0,11	2,69	99,93	236	82	41	55	-10	66	19
24	EQ03-24-(C-3K-257.5)	42,23	15,62	14,78	0,184	9,23	4,85	3,24	0,01	1,554	0,16	7,49	99,33	358	105	62	73	62	161	26
24	EQ03-24-(C-3K-260)	50,22	12,90	13,78	0,178	6,09	7,77	3,31	-0,01	1,317	0,14	3,15	98,83	315	82	42	59	179	95	18
24	EQ03-24-(C-3K-280)	49,62	13,38	13,89	0,226	6,22	9,81	2,73	-0,01	1,414	0,14	2,31	99,74	321	90	42	57	80	96	19
24	EQ03-24-(C-3K-296)	49,66	13,58	14,09	0,255	6,92	7,14	3,82	0,05	1,433	0,14	2,57	99,66	328	86	49	63	125	110	18
24	EQ03-24-(C-3K-311)	48,21	13,98	14,30	0,275	8,38	5,94	4,18	0,02	1,326	0,13	3,03	99,75	319	111	63	95	-10	132	18
24	EQ03-24-(C-3K-394)	48,19	14,67	13,56	0,176	7,31	6,40	1,62	-0,01	2,565	0,42	4,82	99,74	314	34	42	50	-10	111	22
24	EQ03-24-(C-3K-399.5)	48,60	14,98	14,45	0,158	7,93	3,35	2,67	-0,01	2,599	0,45	4,60	99,77	310	35	36	41	11	135	22
24	EQ03-24-(C-3K-477)	41,91	15,76	10,84	0,200	11,18	5,94	2,62	-0,01	0,591	0,05	10,23	99,34	215	85	53	157	-10	87	15
24	EQ03-24-(C-3K-513)	47,79	13,02	16,88	0,280	7,25	4,87	2,54	-0,01	1,836	0,17	5,47	100,06	477	40	61	57	229	204	23
24	EQ03-24-(C-3K-514)	49,70	12,39	16,24	0,272	5,80	5,52	3,84	-0,01	1,712	0,16	3,48	99,12	423	31	51	64	94	129	20
25	EQ03-25-(552-107)	43,57	15,25	17,60	0,163	5,21	8,58	3,23	0,15	2,619	0,25	2,76	99,38	250	76	41	37	29	110	18
25	EQ03-25-(552-108)	44,33	13,18	19,25	0,217	6,03	7,90	3,02	0,33	2,861	0,28	2,39	99,78	263	80	47	52	11	125	17
26	EQ03-26-(644-4)	45,18	16,16	12,93	0,172	8,10	7,76	3,29	0,40	1,666	0,17	4,03	99,86	277	77	47	72	56	129	18
27	EQ03-27-(646-1)	44,14	16,35	12,79	0,167	8,74	8,24	3,29	0,38	1,584	0,15	3,70	99,53	240	70	45	73	54	80	16

Negative values indicate less than the reporting limit
LOI values less than -0.01% represent a Gain on Ignition

Site No.	SAMPLE	Ge	As	Rb	Sr	Y	Zr	Nb	Mo	Ag	In	Sn	Sb	Cs	Ba	La	Ce	Pr	Nd
1	EQ03-01-01	-1	-5	31	266	19	61	5	6	-0,5	-0,2	1	-0,5	1,0	330	17,3	34,1	3,76	14,5
2	EQ03-02-01	1	-5	38	215	20	74	4	-2	-0,5	-0,2	1	-0,5	-0,5	304	12,0	26,1	3,01	12,4
2	EQ03-02-02	-1	-5	27	172	19	96	4	-2	-0,5	-0,2	-1	-0,5	-0,5	284	15,4	32,3	3,58	14,4
2	EQ03-02-03	1	-5	34	178	20	104	5	-2	-0,5	-0,2	2	-0,5	-0,5	335	16,5	34,7	3,86	15,5
3	EQ03-03-01	1	-5	34	475	29	258	20	-2	-0,5	-0,2	2	-0,5	0,5	510	45,3	99,1	11,5	46,6
3	EQ03-03-02	2	-5	59	152	18	48	3	-2	-0,5	-0,2	-1	-0,5	-0,5	265	4,8	11,4	1,47	6,8
4	EQ03-04-01	1	-5	67	240	22	87	4	-2	-0,5	-0,2	-1	-0,5	-0,5	691	18,0	38,8	4,55	19,0
4	EQ03-04-02	1	-5	31	211	23	91	4	-2	-0,5	-0,2	-1	-0,5	-0,5	438	19,9	42,9	5,04	20,8
4	EQ03-04-03	1	-5	28	340	36	300	16	-2	-0,5	-0,2	2	-0,5	0,6	621	56,3	116	13,0	50,7
5	EQ03-05-01	-1	-5	36	28	31	215	16	-2	-0,5	-0,2	1	-0,5	-0,5	436	41,3	94,0	11,5	47,2
5	EQ03-05-02	1	-5	37	39	32	208	15	-2	-0,5	-0,2	1	-0,5	-0,5	565	45,3	98,7	11,8	47,6
5	EQ03-05-03	-1	-5	37	32	31	207	16	-2	-0,5	-0,2	1	-0,5	-0,5	663	44,9	96,0	11,2	45,9
5	EQ03-05-04	-1	-5	31	31	31	187	15	-2	-0,5	-0,2	1	-0,5	-0,5	827	41,9	87,2	10,8	46,2
5	EQ03-05-05	2	-5	14	597	30	182	16	-2	-0,5	-0,2	1	-0,5	-0,5	959	36,7	82,0	9,98	42,0
5	EQ03-05-06	2	-5	51	90	28	186	17	-2	-0,5	-0,2	-1	-0,5	-0,5	683	40,6	92,2	10,5	45,0
5	EQ03-05-07	2	-5	46	682	30	205	17	-2	-0,5	-0,2	-1	-0,5	-0,5	1 550	48,5	105	12,1	51,7
5	EQ03-05-08	1	-5	26	130	27	180	15	-2	-0,5	-0,2	-1	-0,5	-0,5	854	37,8	86,0	10,1	43,9
6	EQ03-06-01	1	-5	50	49	56	679	28	3	-0,5	-0,2	-1	-0,5	-0,5	1 050	118	235	24,8	92,3
6	EQ03-06-02	2	-5	77	338	51	532	28	2	-0,5	-0,2	-1	-0,5	0,9	2 420	127	268	27,7	104
7	EQ03-07-01	1	-5	23	273	19	125	11	-2	-0,5	-0,2	-1	-0,5	0,6	264	13,5	31,9	3,86	17,7
8	EQ03-08-01	2	-5	39	49	18	100	7	-2	-0,5	-0,2	-1	-0,5	3,8	288	16,1	34,4	3,65	14,5
8	EQ03-08-02	1	-5	17	71	11	52	4	-2	-0,5	-0,2	-1	-0,5	3,7	127	10,0	21,0	2,27	9,1
8	EQ03-08-03	2	-5	36	279	16	72	5	-2	-0,5	-0,2	-1	-0,5	1,5	1 080	14,3	29,5	3,13	12,7
8	EQ03-08-04	1	-5	38	248	15	71	5	-2	-0,5	-0,2	-1	-0,5	1,6	919	14,2	30,1	3,26	13,0
9	EQ03-09-01	1	-5	109	391	21	110	8	-2	-0,5	-0,2	-1	-0,5	4,0	919	12,9	31,7	4,06	19,1
9	EQ03-09-02	1	-5	90	370	19	102	7	-2	-0,5	-0,2	-1	-0,5	2,8	899	11,4	28,9	3,71	17,4
10	EQ03-10-01	1	-5	22	477	20	125	10	-2	-0,5	-0,2	-1	-0,5	0,8	774	29,4	62,5	6,97	28,9
10	EQ03-10-02	1	-5	21	560	20	128	11	-2	-0,5	-0,2	1	-0,5	0,7	749	28,4	60,9	6,81	28,3
10	EQ03-10-03	1	-5	25	509	18	120	10	-2	-0,5	-0,2	-1	-0,5	1,3	602	27,1	58,0	6,53	27,0
10	EQ03-10-04	1	-5	22	517	22	139	12	-2	-0,5	-0,2	-1	-0,5	0,8	782	29,7	64,8	7,33	30,2
10	EQ03-10-05	1	-5	24	556	17	104	9	-2	-0,5	-0,2	-1	-0,5	0,9	656	23,4	51,1	5,79	24,1
10	EQ03-10-06	2	-5	159	32	16	112	9	-2	-0,5	-0,2	-1	-0,5	3,6	585	40,8	79,3	8,46	31,0
11	EQ03-11-01	1	-5	33	291	17	96	8	-2	-0,5	-0,2	1	-0,5	-0,5	753	18,8	40,8	4,75	20,2
11	EQ03-11-02	1	-5	42	532	18	107	9	-2	-0,5	-0,2	-1	-0,5	0,9	555	20,4	43,9	5,13	22,1
12	EQ03-12-01	1	-5	85	334	21	161	14	-2	-0,5	-0,2	-1	-0,5	7,0	620	32,4	72,3	8,42	35,8
13	EQ03-13-01	1	-5	40	365	22	166	16	-2	-0,5	-0,2	-1	-0,5	2,9	662	32,7	73,8	8,67	36,5
14	EQ03-14-01	-1	-5	80	28	15	157	11	-2	-0,5	-0,2	-1	-0,5	2,0	526	28,7	60,7	6,47	23,7
14	EQ03-14-02	2	-5	-2	505	32	157	14	-2	-0,5	-0,2	-1	-0,5	-0,5	13	20,7	48,4	5,81	24,8
14	EQ03-14-03	1	-5	-2	405	30	155	14	-2	-0,5	-0,2	-1	-0,5	-0,5	8	18,9	43,8	5,26	22,9
14	EQ03-14-04	2	-5	-2	340	33	165	15	-2	-0,5	-0,2	-1	-0,5	-0,5	19	19,2	46,4	5,66	25,0
14	EQ03-14-05	1	-5	-2	241	31	149	14	-2	-0,5	-0,2	-1	-0,5	-0,5	19	18,9	44,6	5,27	23,9
14	EQ03-14-06	2	-5	-2	484	32	155	14	-2	-0,5	-0,2	-1	-0,5	-0,5	10	16,9	41,0	5,05	21,9
14	EQ03-14-07	2	-5	-2	9	35	181	16	-2	-0,5	-0,2	-1	-0,5	-0,5	13	31,2	70,1	8,01	33,0
14	EQ03-14-08	3	-5	29	3	89	657	58	-2	-0,5	-0,2	2	-0,5	0,5	89	29,1	73,0	8,49	36,4

Negative values indicate less than the reporting limit
LOI values less than -0.01% represent a Gain on Ignition

Activation Laboratories Ltd. Work Order No. A04-2169 Report No. A04-2169

Site No.	SAMPLE	Ge	As	Rb	Sr	Y	Zr	Nb	Mo	Ag	In	Sn	Sb	Cs	Ba	La	Ce	Pr	Nd
14	EQ03-14-09	1	-5	97	12	59	494	60	-2	-0,5	-0,2	4	-0,5	1,7	320	26,5	65,6	7,37	28,2
14	EQ03-14-10	1	-5	48	22	64	531	60	-2	-0,5	-0,2	8	-0,5	0,9	400	54,3	110	11,9	46,3
14	EQ03-14-11	1	-5	65	26	65	566	62	-2	-0,5	-0,2	6	-0,5	1,7	427	93,5	180	21,1	78,0
15	EQ03-15-01	2	-5	43	382	41	409	56	-2	-0,5	-0,2	4	-0,5	1,0	290	65,8	132	13,7	49,8
16	EQ03-16-01	2	-5	3	523	39	367	55	-2	-0,5	-0,2	3	-0,5	-0,5	37	52,6	106	11,3	41,7
16	EQ03-16-02	2	-5	4	1 260	38	343	51	-2	-0,5	-0,2	3	-0,5	-0,5	36	54,1	111	12,0	43,0
16	EQ03-16-03	2	-5	14	968	35	303	46	-2	-0,5	-0,2	2	-0,5	-0,5	113	63,9	115	11,9	42,4
16	EQ03-16-04	2	-5	62	172	31	265	78	-2	-0,5	-0,2	-1	-0,5	1,7	390	59,3	115	13,0	50,4
16	EQ03-16-05	-1	-5	9	212	13	110	36	-2	-0,5	-0,2	-1	-0,5	-0,5	80	34,1	62,1	6,48	24,7
16	EQ03-16-06	1	-5	21	282	26	194	61	-2	-0,5	-0,2	-1	-0,5	0,6	282	58,2	105	11,1	43,2
16	EQ03-16-07	2	-5	6	936	30	237	75	-2	-0,5	-0,2	-1	-0,5	-0,5	87	51,6	104	11,5	45,2
17	EQ03-17-01	-1	-5	19	196	22	202	36	-2	-0,5	-0,2	1	-0,5	0,5	313	56,3	88,4	8,86	30,6
18	EQ03-18-01	2	-5	9	157	33	137	16	-2	-0,5	-0,2	-1	-0,5	1,0	64	14,3	33,0	4,25	19,2
18	EQ03-18-02	1	-5	11	88	38	142	15	-2	-0,5	-0,2	-1	-0,5	-0,5	236	15,1	36,0	4,76	21,6
18	EQ03-18-03	2	-5	-2	31	33	144	13	-2	-0,5	-0,2	-1	-0,5	-0,5	12	13,4	33,1	4,36	19,9
18	EQ03-18-04	1	-5	26	49	24	154	14	-2	-0,5	-0,2	1	-0,5	0,7	183	7,5	19,4	2,53	11,7
19	EQ03-19-01	2	-5	-2	128	26	116	11	-2	-0,5	-0,2	-1	-0,5	-0,5	43	14,9	32,8	4,05	17,7
19	EQ03-19-02	2	-5	3	140	27	114	10	-2	-0,5	-0,2	-1	-0,5	-0,5	39	12,9	29,9	3,84	17,4
19	EQ03-19-03	2	-5	2	165	28	108	10	-2	-0,5	-0,2	-1	-0,5	-0,5	61	14,3	32,0	4,00	17,7
19	EQ03-19-04	1	-5	3	85	25	105	10	-2	-0,5	-0,2	-1	-0,5	-0,5	97	10,7	25,1	3,25	14,7
19	EQ03-19-05	2	-5	6	157	29	112	10	-2	-0,5	-0,2	-1	-0,5	-0,5	140	13,1	28,8	3,68	16,1
19	EQ03-19-06	2	-5	-2	19	62	262	21	-2	-0,5	-0,2	1	-0,5	-0,5	43	21,6	55,2	7,98	38,0
20	EQ03-20-01	1	-5	22	282	30	159	15	-2	-0,5	-0,2	-1	-0,5	-0,5	144	12,6	31,6	4,28	20,2
21	EQ03-21-02	2	-5	86	177	22	88	9	-2	-0,5	-0,2	-1	-0,5	3,6	214	9,8	22,1	2,81	12,9
22	EQ03-22-01	2	-5	2	174	24	96	7	-2	-0,5	-0,2	-1	-0,5	-0,5	65	7,2	18,2	2,55	12,6
23	EQ03-23-01	1	-5	9	168	25	95	6	-2	-0,5	-0,2	-1	-0,5	0,5	91	7,1	18,6	2,58	13,1
23	EQ03-23-02	1	-5	21	183	29	125	8	-2	-0,5	-0,2	-1	-0,5	0,9	209	13,7	32,1	4,08	18,2
24	EQ03-24-(C-3K-37.5)	1	-5	-2	67	26	105	10	-2	-0,5	-0,2	-1	-0,5	-0,5	12	12,9	29,9	3,74	16,3
24	EQ03-24-(C-3K-40)	1	-5	-2	149	25	93	9	-2	-0,5	-0,2	-1	-0,5	-0,5	11	11,1	26,4	3,35	14,8
24	EQ03-24-(C-3K-51)	2	-5	-2	184	25	92	9	-2	-0,5	-0,2	-1	-0,5	-0,5	9	11,9	26,8	3,34	14,8
24	EQ03-24-(C-3K-185)	2	-5	59	20	22	136	11	-2	-0,5	-0,2	-1	-0,5	1,3	384	21,2	44,5	5,17	21,6
24	EQ03-24-(C-3K-210)	2	-5	50	31	27	151	14	-2	-0,5	-0,2	3	-0,5	1,2	433	36,0	70,8	7,78	28,8
24	EQ03-24-(C-3K-224)	2	-5	15	14	18	133	12	-2	-0,5	-0,2	1	-0,5	-0,5	143	8,4	19,5	2,36	10,0
24	EQ03-24-(C-3K-257.5)	2	-5	-2	17	32	109	11	-2	-0,5	-0,2	1	-0,5	-0,5	9	14,8	39,2	5,28	23,1
24	EQ03-24-(C-3K-260)	2	-5	-2	117	23	94	9	-2	-0,5	-0,2	-1	-0,5	-0,5	8	12,4	26,7	3,28	14,6
24	EQ03-24-(C-3K-280)	2	-5	-2	177	25	96	10	-2	-0,5	-0,2	-1	-0,5	-0,5	11	11,6	26,7	3,33	15,0
24	EQ03-24-(C-3K-296)	1	-5	-2	114	25	96	10	-2	-0,5	-0,2	2	-0,5	-0,5	11	12,4	28,6	3,52	15,7
24	EQ03-24-(C-3K-311)	1	-5	-2	81	22	93	9	-2	-0,5	-0,2	-1	-0,5	-0,5	7	10,5	25,1	3,14	14,3
24	EQ03-24-(C-3K-394)	2	-5	-2	383	32	208	41	-2	-0,5	-0,2	-1	-0,5	-0,5	9	37,5	78,0	9,00	37,3
24	EQ03-24-(C-3K-399.5)	1	-5	-2	207	31	221	48	2	-0,5	-0,2	2	-0,5	-0,5	9	38,6	81,3	9,35	38,5
24	EQ03-24-(C-3K-477)	1	-5	-2	34	12	23	7	-2	-0,5	-0,2	-1	-0,5	-0,5	-3	2,8	6,5	0,88	4,3
24	EQ03-24-(C-3K-513)	2	-5	-2	68	38	114	10	-2	-0,5	-0,2	-1	-0,5	-0,5	11	11,8	27,0	3,45	16,7
24	EQ03-24-(C-3K-514)	2	-5	-2	69	32	105	9	-2	-0,5	-0,2	-1	-0,5	-0,5	13	9,8	22,0	2,88	14,1
25	EQ03-25-(552-107)	2	-5	2	233	37	149	12	-2	-0,5	-0,2	1	-0,5	-0,5	30	13,7	32,9	4,51	19,5
25	EQ03-25-(552-108)	2	-5	4	159	40	162	13	-2	-0,5	-0,2	1	-0,5	-0,5	72	16,2	40,2	5,29	22,3
26	EQ03-26-(644-4)	2	6	5	277	28	86	8	3	-0,5	-0,2	1	0,6	0,7	91	9,5	22,2	2,94	12,4
27	EQ03-27-(646-1)	2	-5	4	221	25	74	8	-2	-0,5	-0,2	-1	-0,5	-0,5	123	7,9	18,2	2,46	10,9

Negative values indicate less than the reporting limit
LOI values less than -0.01% represent a Gain on Ignition

Site No.	SAMPLE	Sm	Eu	Gd	Tb	Dy	Ho	Er	Tm	Yb	Lu	Hf	Ta	W	Tl	Pb	Bi	Th	U
1	EQ03-01-01	2,9	1,06	2,8	0,5	3,0	0,7	2,2	0,33	2,2	0,33	1,6	0,3	1	0,3	8	4,8	1,4	0,3
2	EQ03-02-01	3,0	1,07	3,4	0,6	3,7	0,8	2,4	0,36	2,3	0,33	2,1	0,2	-1	0,3	-5	-0,4	1,9	0,3
2	EQ03-02-02	3,4	1,05	3,4	0,6	3,6	0,7	2,2	0,32	2,0	0,31	2,7	0,2	-1	0,2	-5	-0,4	3,6	0,4
2	EQ03-02-03	3,7	1,11	3,8	0,7	3,8	0,8	2,4	0,35	2,2	0,33	3,0	0,2	-1	0,4	8	-0,4	3,9	0,5
3	EQ03-03-01	9,6	2,96	8,4	1,2	6,2	1,1	3,1	0,38	2,5	0,33	6,6	1,3	-1	0,4	11	0,7	5,5	0,9
3	EQ03-03-02	2,0	0,85	2,7	0,5	3,3	0,7	2,2	0,34	2,2	0,31	1,5	0,1	-1	0,5	-5	-0,4	0,5	0,1
4	EQ03-04-01	3,9	1,34	4,0	0,7	4,0	0,8	2,5	0,38	2,5	0,37	2,3	0,1	-1	0,7	5	-0,4	1,1	0,2
4	EQ03-04-02	4,3	1,40	4,3	0,7	4,3	0,9	2,8	0,42	2,6	0,40	2,4	0,2	-1	0,4	-5	-0,4	1,3	0,2
4	EQ03-04-03	9,7	3,12	9,1	1,3	7,1	1,3	4,0	0,54	3,4	0,49	7,7	0,9	-1	0,5	16	-0,4	7,8	0,7
5	EQ03-05-01	9,3	2,79	8,5	1,3	6,3	1,1	3,3	0,46	3,0	0,43	5,5	0,9	-1	0,3	-5	0,6	3,1	0,5
5	EQ03-05-02	9,4	3,23	8,7	1,3	6,5	1,2	3,4	0,48	3,0	0,43	5,3	0,9	-1	0,4	-5	-0,4	3,0	0,5
5	EQ03-05-03	8,9	2,61	8,3	1,2	6,2	1,1	3,2	0,43	2,8	0,38	5,1	0,9	-1	0,4	-5	-0,4	3,0	0,5
5	EQ03-05-04	9,2	3,06	8,4	1,3	6,7	1,2	3,4	0,48	3,0	0,43	4,9	0,9	-1	0,2	-5	-0,4	2,5	0,5
5	EQ03-05-05	8,4	2,86	7,7	1,2	5,9	1,1	3,1	0,44	2,8	0,41	4,7	0,9	-1	-0,1	10	-0,4	2,5	0,5
5	EQ03-05-06	9,0	3,12	7,9	1,2	6,4	1,2	3,4	0,47	2,9	0,40	4,9	0,9	-1	0,3	5	-0,4	2,5	0,3
5	EQ03-05-07	9,9	3,28	8,4	1,2	6,4	1,2	3,5	0,46	2,9	0,43	5,2	0,9	-1	0,4	8	0,5	3,4	0,7
5	EQ03-05-08	8,8	2,66	7,6	1,1	5,9	1,1	3,2	0,43	2,7	0,38	4,7	0,8	1	0,2	6	0,8	3,1	0,6
6	EQ03-06-01	16,4	4,58	12,8	2,1	11,5	2,2	6,8	0,98	6,0	0,88	17,4	1,5	-1	0,9	8	0,6	19,3	1,7
6	EQ03-06-02	17,6	4,49	13,9	2,1	11,0	2,1	6,3	0,89	5,6	0,80	14,3	1,3	-1	1,0	33	0,9	14,6	1,2
7	EQ03-07-01	4,5	1,69	4,6	0,8	4,2	0,8	2,3	0,31	1,9	0,26	3,6	0,4	-1	0,3	-5	-0,4	1,7	0,4
8	EQ03-08-01	3,2	0,99	3,3	0,6	3,5	0,7	2,2	0,34	2,0	0,29	2,9	0,3	-1	0,4	-5	-0,4	3,7	0,6
8	EQ03-08-02	2,0	0,64	2,1	0,4	2,2	0,4	1,3	0,20	1,2	0,17	1,5	0,1	-1	0,3	7	0,6	2,2	0,3
8	EQ03-08-03	2,8	0,88	2,9	0,5	3,0	0,6	1,9	0,28	1,7	0,25	2,0	0,3	-1	0,3	6	0,7	3,1	0,5
8	EQ03-08-04	3,0	0,91	2,9	0,5	3,2	0,6	1,9	0,28	1,8	0,26	2,0	0,2	-1	0,2	-5	-0,4	3,0	0,5
9	EQ03-09-01	5,1	1,88	5,1	0,8	4,5	0,8	2,3	0,33	2,0	0,26	3,2	0,4	1	1,7	-5	0,6	0,7	0,2
9	EQ03-09-02	4,5	1,71	4,8	0,8	4,1	0,8	2,2	0,29	1,7	0,25	3,0	0,4	-1	1,6	-5	-0,4	0,6	0,1
10	EQ03-10-01	5,9	2,06	5,2	0,8	4,1	0,8	2,3	0,30	1,9	0,27	3,4	0,5	-1	0,3	6	-0,4	1,8	0,4
10	EQ03-10-02	5,8	2,00	5,0	0,8	4,1	0,7	2,2	0,30	1,9	0,26	3,4	0,6	-1	0,3	-5	-0,4	1,7	0,4
10	EQ03-10-03	5,5	1,81	4,6	0,7	3,9	0,7	2,1	0,28	1,8	0,26	3,2	0,5	-1	0,3	6	0,8	1,7	0,4
10	EQ03-10-04	6,1	2,04	5,4	0,8	4,4	0,8	2,4	0,33	2,1	0,29	3,7	0,6	-1	0,2	-5	-0,4	1,9	0,4
10	EQ03-10-05	5,0	1,72	4,4	0,7	3,6	0,7	1,9	0,27	1,6	0,23	2,9	0,5	-1	0,2	-5	-0,4	1,4	0,3
10	EQ03-10-06	5,4	1,12	3,7	0,6	3,3	0,6	2,0	0,32	1,9	0,28	3,2	0,8	-1	1,0	-5	0,4	12,2	2,0
11	EQ03-11-01	4,4	1,37	4,0	0,7	3,5	0,6	2,0	0,28	1,7	0,23	2,7	0,5	-1	0,2	-5	-0,4	1,4	0,3
11	EQ03-11-02	4,5	1,61	4,1	0,7	3,5	0,7	1,9	0,27	1,7	0,23	2,8	0,5	-1	0,3	-5	-0,4	1,4	0,3
12	EQ03-12-01	7,4	2,44	6,2	1,0	4,6	0,8	2,3	0,29	1,8	0,24	4,4	0,9	-1	0,7	-5	9,1	2,2	0,5
13	EQ03-13-01	7,5	2,49	6,2	0,9	4,7	0,8	2,3	0,30	1,9	0,27	4,5	1,0	-1	0,8	-5	0,4	2,4	0,4
14	EQ03-14-01	4,4	1,02	3,3	0,6	2,9	0,5	1,6	0,23	1,5	0,22	4,2	0,6	-1	0,5	-5	-0,4	8,3	1,2
14	EQ03-14-02	5,9	1,90	5,9	1,1	6,1	1,2	3,8	0,56	3,3	0,50	4,4	0,8	-1	-0,1	74	-0,4	2,1	0,5
14	EQ03-14-03	5,3	1,63	5,3	0,9	5,6	1,1	3,4	0,51	3,2	0,47	4,1	0,8	-1	-0,1	603	-0,4	2,0	0,5
14	EQ03-14-04	5,9	2,01	6,2	1,1	6,2	1,3	3,9	0,56	3,4	0,50	4,3	0,8	-1	-0,1	18	2,2	1,7	0,4
14	EQ03-14-05	5,6	1,90	5,7	1,0	6,1	1,2	3,6	0,54	3,3	0,49	4,1	0,8	-1	-0,1	8	-0,4	1,6	0,4
14	EQ03-14-06	5,3	1,38	5,6	1,0	5,8	1,2	3,6	0,55	3,3	0,49	4,1	0,7	-1	-0,1	12	-0,4	1,6	0,4
14	EQ03-14-07	7,4	1,35	6,9	1,2	6,5	1,3	3,8	0,54	3,4	0,50	4,8	0,9	-1	-0,1	-5	-0,4	1,7	0,5
14	EQ03-14-08	12,4	2,45	14,6	3,2	19,0	3,7	11,9	1,90	12,5	1,93	18,0	4,6	-1	0,1	-5	-0,4	22,7	7,4

Negative values indicate less than the reporting limit
LOI values less than -0.01% represent a Gain on Ignition

Activation Laboratories Ltd. Work Order No. A04-2169 Report No. A04-2169

Site No.	SAMPLE	Sm	Eu	Gd	Tb	Dy	Ho	Er	Tm	Yb	Lu	Hf	Ta	W	Tl	Pb	Bi	Th	U
14	EQ03-14-09	6,1	1,02	6,2	1,3	8,9	2,1	7,1	1,14	7,2	1,11	13,3	3,5	1	0,6	-5	-0,4	15,0	3,0
14	EQ03-14-10	9,7	1,86	8,7	1,8	11,4	2,4	7,7	1,18	7,5	1,10	14,3	3,6	-1	0,3	-5	0,8	16,7	3,4
14	EQ03-14-11	14,9	2,71	12,7	2,1	12,3	2,5	8,0	1,25	7,8	1,16	15,5	3,9	-1	0,3	-5	9,9	17,6	3,3
15	EQ03-15-01	8,8	2,04	7,1	1,3	7,6	1,5	4,8	0,75	4,6	0,64	11,2	3,7	1	0,3	23	2,1	19,1	4,6
16	EQ03-16-01	8,0	1,80	7,1	1,3	7,2	1,4	4,2	0,68	4,1	0,58	9,9	3,3	1	-0,1	16	1,4	15,8	3,6
16	EQ03-16-02	8,1	1,84	7,8	1,3	6,9	1,4	4,2	0,66	4,1	0,58	9,6	3,3	-1	-0,1	14	1,7	15,5	3,8
16	EQ03-16-03	7,6	1,69	6,6	1,1	6,5	1,2	3,9	0,63	3,9	0,58	8,3	2,8	-1	-0,1	20	2,3	13,4	2,9
16	EQ03-16-04	8,9	3,15	8,1	1,3	6,3	1,2	3,2	0,47	2,9	0,41	6,6	4,7	1	0,3	8	2,3	6,5	0,9
16	EQ03-16-05	4,2	1,26	3,5	0,5	2,6	0,5	1,4	0,20	1,2	0,17	2,5	1,7	-1	-0,1	-5	1,4	2,4	0,6
16	EQ03-16-06	7,6	2,51	6,5	1,0	5,1	0,9	2,6	0,36	2,2	0,32	5,0	3,6	-1	-0,1	-5	0,8	5,0	0,7
16	EQ03-16-07	8,2	3,00	7,5	1,1	6,0	1,1	3,0	0,43	2,7	0,39	5,7	4,2	-1	-0,1	7	0,7	5,9	1,1
17	EQ03-17-01	5,0	1,08	4,3	0,7	4,0	0,8	2,4	0,38	2,4	0,38	5,0	1,8	2	-0,1	5	0,7	8,0	1,6
18	EQ03-18-01	5,0	1,70	5,9	1,0	6,2	1,2	3,7	0,57	3,6	0,52	4,0	0,6	-1	-0,1	-5	0,7	1,8	0,4
18	EQ03-18-02	6,0	2,08	6,7	1,2	7,1	1,4	4,1	0,60	3,9	0,55	4,2	0,6	-1	-0,1	-5	2,5	1,8	0,4
18	EQ03-18-03	5,3	1,52	5,9	1,0	6,3	1,3	3,8	0,58	3,7	0,56	4,3	0,7	-1	-0,1	-5	1,6	1,8	0,4
18	EQ03-18-04	3,1	0,59	3,6	0,7	4,5	1,0	3,2	0,54	3,5	0,52	4,5	0,7	-1	0,1	-5	3,8	1,9	0,5
19	EQ03-19-01	4,3	1,28	4,9	0,8	5,0	1,0	3,0	0,47	3,0	0,45	3,5	0,5	-1	-0,1	-5	3,0	1,5	0,3
19	EQ03-19-02	4,3	1,26	4,9	0,9	5,1	1,0	3,0	0,47	2,9	0,44	3,4	0,5	-1	-0,1	-5	0,8	1,5	0,3
19	EQ03-19-03	4,1	1,39	4,7	0,8	5,1	1,0	3,1	0,47	3,0	0,43	3,1	0,5	-1	-0,1	-5	0,4	1,3	0,3
19	EQ03-19-04	3,7	0,91	4,2	0,7	4,5	0,9	2,8	0,44	2,7	0,41	3,1	0,5	-1	-0,1	-5	1,4	1,3	0,3
19	EQ03-19-05	4,1	1,40	4,6	0,8	5,1	1,0	3,1	0,47	3,1	0,43	3,2	0,5	-1	-0,1	-5	1,1	1,3	0,3
19	EQ03-19-06	10,6	3,78	11,6	2,1	12,0	2,3	7,0	1,05	6,8	0,99	7,2	1,4	2	-0,1	-5	1,5	5,3	1,3
20	EQ03-20-01	5,5	2,01	6,2	1,1	6,2	1,2	3,3	0,48	3,0	0,42	4,5	0,9	-1	-0,1	-5	0,6	1,2	0,3
21	EQ03-21-02	3,3	1,21	4,0	0,7	4,3	0,8	2,5	0,39	2,5	0,36	2,5	0,5	-1	1,3	-5	0,5	1,1	0,3
22	EQ03-22-01	3,7	1,41	4,5	0,8	4,8	0,9	2,7	0,39	2,4	0,35	2,9	0,3	20	0,5	7	1,1	1,0	0,3
23	EQ03-23-01	3,8	1,44	4,7	0,8	4,9	1,0	2,7	0,40	2,5	0,36	2,8	0,3	-1	0,3	-5	0,7	1,1	0,3
23	EQ03-23-02	4,8	1,69	5,6	1,0	5,8	1,1	3,2	0,48	3,0	0,43	3,7	0,5	-1	0,3	6	1,3	2,6	0,5
24	EQ03-24-(C-3K-37.5)	4,1	1,37	4,7	0,9	5,1	1,0	2,9	0,46	2,9	0,42	3,1	0,6	-1	-0,1	-5	1,6	1,6	0,4
24	EQ03-24-(C-3K-40)	3,8	1,31	4,3	0,8	4,7	1,0	2,8	0,45	2,7	0,40	2,9	0,5	-1	-0,1	-5	0,5	1,4	0,4
24	EQ03-24-(C-3K-51)	3,8	1,41	4,3	0,8	4,7	0,9	2,8	0,44	2,7	0,40	2,8	0,5	-1	-0,1	7	0,7	1,4	0,3
24	EQ03-24-(C-3K-185)	4,4	1,42	4,3	0,8	4,3	0,8	2,5	0,40	2,5	0,38	4,0	0,7	-1	0,4	-5	1,0	4,9	1,2
24	EQ03-24-(C-3K-210)	4,7	1,80	4,9	0,8	4,8	1,0	3,2	0,51	3,1	0,45	4,4	0,8	-1	0,4	-5	3,4	5,5	1,2
24	EQ03-24-(C-3K-224)	2,4	0,66	2,5	0,5	3,3	0,7	2,4	0,40	2,6	0,38	3,9	0,7	-1	0,1	-5	2,6	4,6	0,8
24	EQ03-24-(C-3K-257.5)	5,4	1,33	5,5	1,0	5,9	1,2	3,6	0,53	3,3	0,49	3,2	0,6	-1	-0,1	-5	1,0	1,6	0,4
24	EQ03-24-(C-3K-260)	3,7	1,32	4,1	0,8	4,5	0,9	2,7	0,40	2,6	0,37	2,7	0,5	-1	-0,1	-5	-0,4	1,4	0,3
24	EQ03-24-(C-3K-280)	3,7	1,36	4,2	0,8	4,8	1,0	2,8	0,42	2,7	0,40	2,8	0,6	-1	-0,1	5	0,4	1,5	0,4
24	EQ03-24-(C-3K-296)	4,0	1,37	4,6	0,8	4,9	1,0	2,9	0,43	2,8	0,41	3,0	0,5	-1	-0,1	-5	-0,4	1,4	0,3
24	EQ03-24-(C-3K-311)	3,5	0,94	4,0	0,7	4,4	0,8	2,5	0,40	2,5	0,36	2,8	0,5	-1	-0,1	-5	1,4	1,3	0,2
24	EQ03-24-(C-3K-394)	7,6	2,61	7,3	1,2	6,6	1,2	3,5	0,51	3,2	0,45	5,5	2,6	-1	-0,1	9	8,5	4,7	1,2
24	EQ03-24-(C-3K-399.5)	8,1	2,48	7,4	1,2	6,5	1,2	3,4	0,51	3,2	0,46	5,6	2,9	-1	-0,1	-5	5,5	5,1	1,2
24	EQ03-24-(C-3K-477)	1,4	0,60	1,8	0,4	2,2	0,5	1,4	0,22	1,4	0,20	0,8	0,1	-1	-0,1	-5	-0,4	0,3	-0,1
24	EQ03-24-(C-3K-513)	4,7	2,10	5,9	1,1	6,7	1,3	4,1	0,66	4,2	0,61	3,3	0,5	-1	-0,1	-5	1,9	1,1	0,3
24	EQ03-24-(C-3K-514)	4,0	1,47	5,1	1,0	6,0	1,2	3,7	0,58	3,7	0,54	3,1	0,4	-1	-0,1	-5	0,6	1,0	0,2
25	EQ03-25-(552-107)	5,3	1,98	6,5	1,0	5,8	1,2	3,6	0,54	3,3	0,49	3,6	0,9	-1	0,1	-5	0,5	1,4	0,4
25	EQ03-25-(552-108)	6,0	1,82	7,2	1,1	6,4	1,3	3,9	0,57	3,5	0,53	3,9	1,0	-1	-0,1	13	-0,4	1,6	0,4
26	EQ03-26-(644-4)	3,4	1,51	4,6	0,7	4,4	0,9	2,7	0,39	2,3	0,36	2,2	0,5	-1	-0,1	-5	-0,4	0,7	0,2
27	EQ03-27-(646-1)	3,0	1,32	4,0	0,7	3,8	0,8	2,4	0,34	2,1	0,33	1,9	0,5	-1	-0,1	-5	-0,4	0,6	0,2

Negative values indicate less than the reporting limit
LOI values less than -0.01% represent a Gain on Ignition

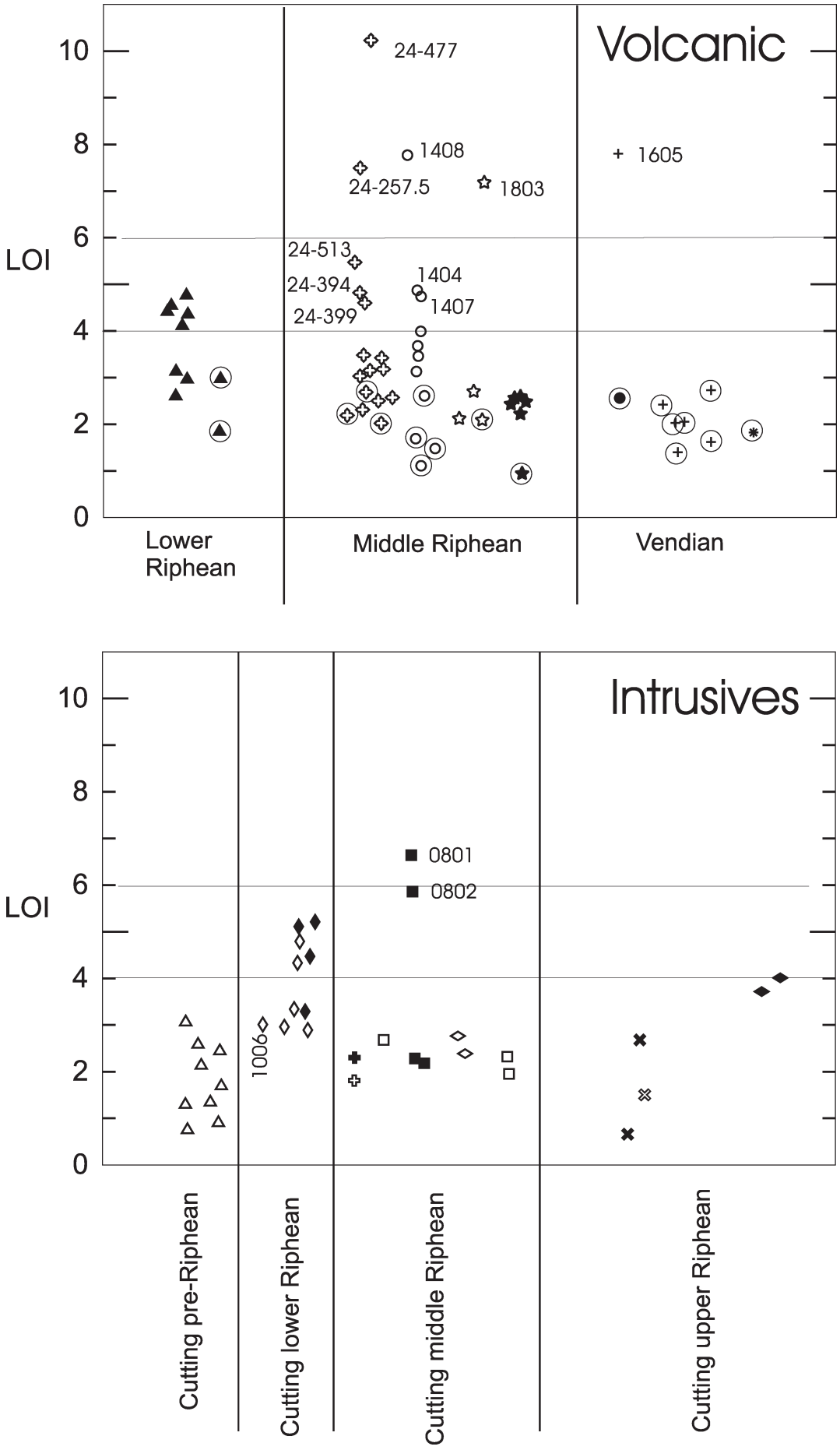
Volcanic
LOI
10
8
6
4
2
0
24-477
1408
24-257.5
1803
1605
24-513
24-394
24-399
1404
1407
Lower Riphean
Middle Riphean
Vendian
Intrusives
0801
0802
1006
Cutting pre-Riphean
Cutting lower Riphean
Cutting middle Riphean
Cutting upper Riphean

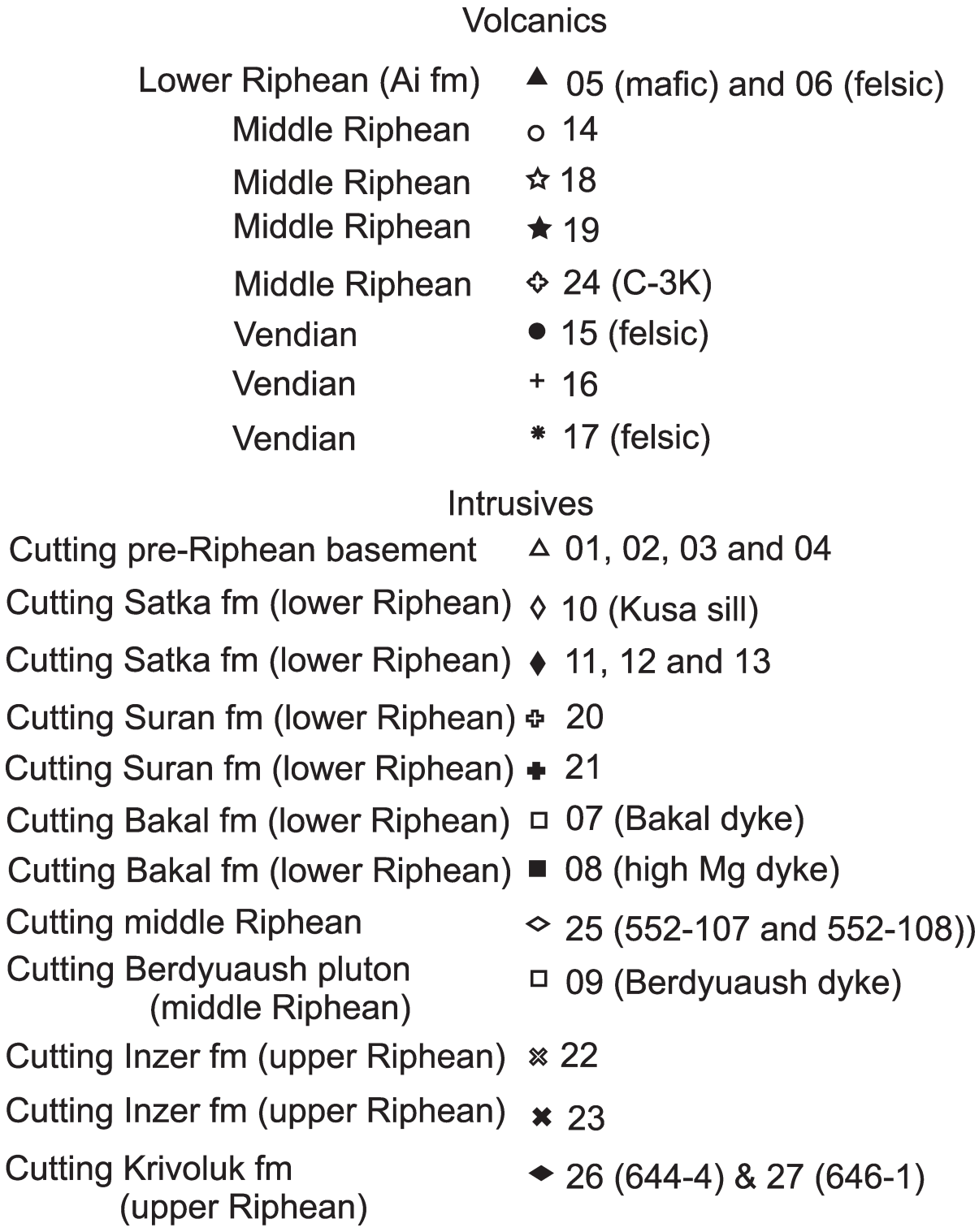

Figure 3. Loss-on-ignition (LOI). Legend for symbols used in this and other geochemical figures. Felsic samples here and on subsequent plots are shown in open circles

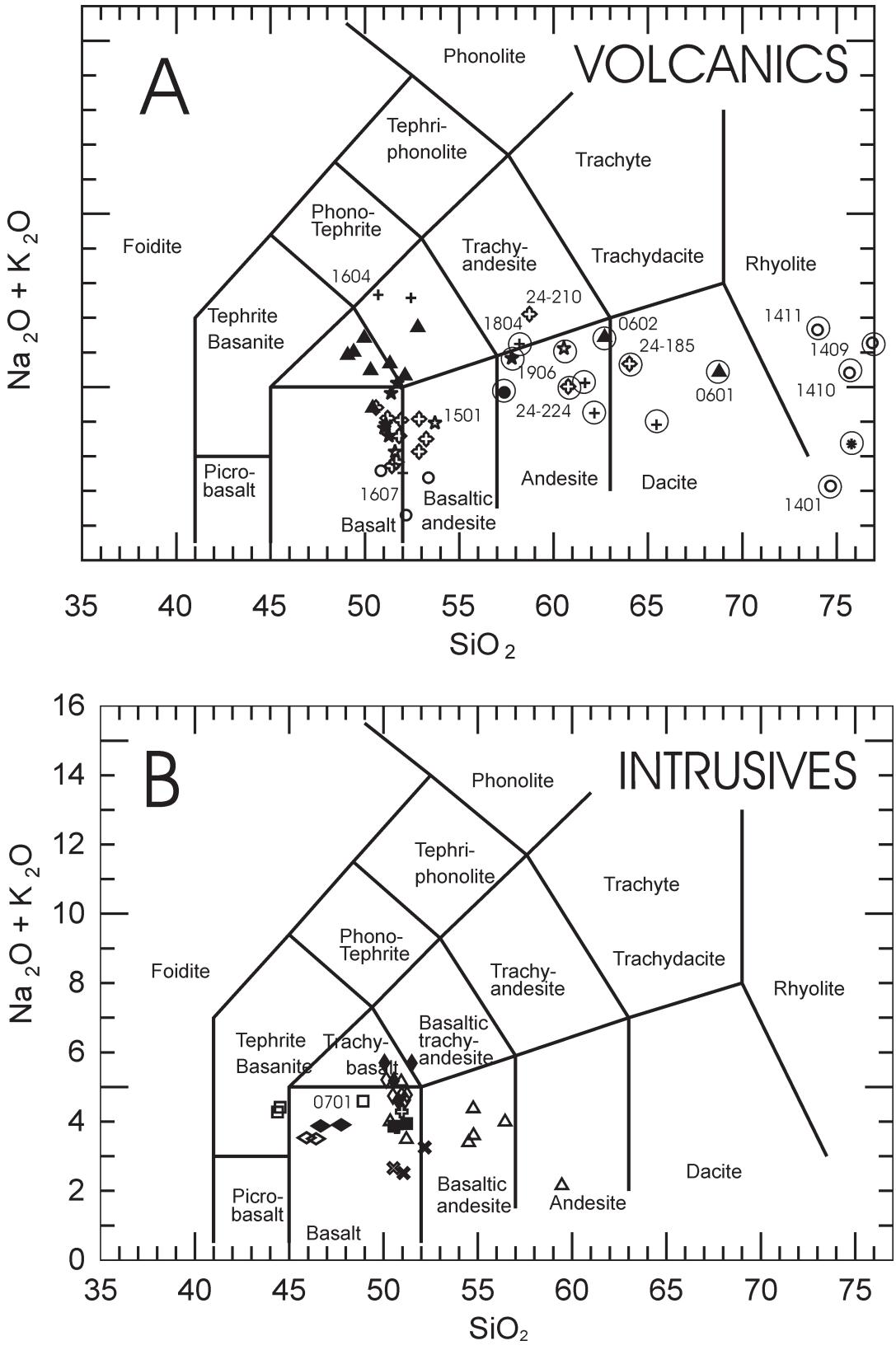

Figure 4. Total alkalis versus SiO_2 (TAS) volcanic rock classification diagram (after LeBas et al., 1986). A) Volcanic rocks. B) Intrusive rocks superimposed on TAS for comparison to possible extrusive equivalents

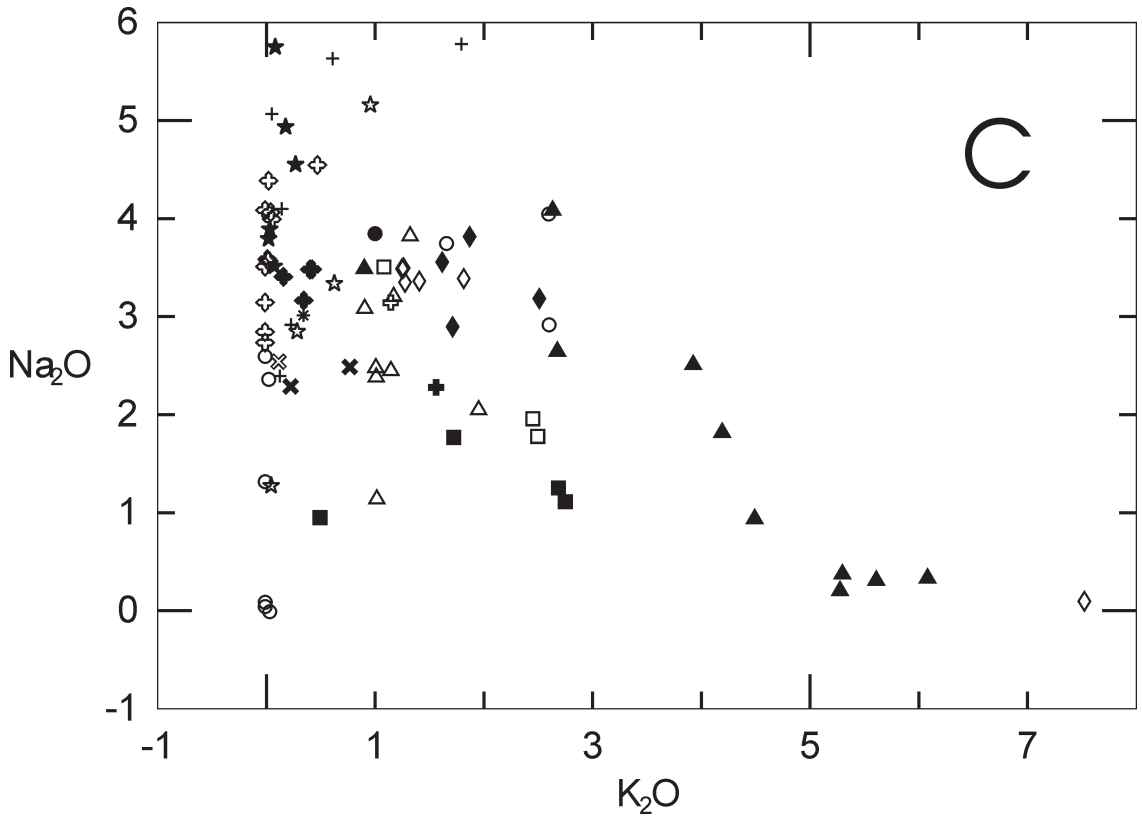

Figure 4. Total alkalis versus SiO_2 (TAS) volcanic rock classification diagram (after LeBas et al., 1986). C) Na_2O vs K_2O Symbols as in Fig. 3.

The La/Nb ratio (Fig. 14) is a key discriminant of the subduction (recycled) component in the mantle. Values for this ratio greater than 1.4 distinguish basalts erupted at ocean ridges, ocean islands and oceanic plateaus from those erupted in arc environments because Nb largely remains in the descending slab, whereas La is carried into the hydrated mantle wedge during subduction (Rudnick, 1995). The hydrated mantle wedge, which is the source of most subduction-related magmas, has high La/Nb. Basalt with ratios >1.4 can reflect an arc source, contamination of the lithosphere by arc sources, or reflect partial melting of the subcontinental lithospheric mantle. Plotting La/Nb against Hf/Sm (Fig. 14) minimizes the effects of i) partial melting because incompatible high field strength elements are insensitive to 'large' degree partial melts, as represented by most tholeiites, and ii) restite garnet because Hf is less incompatible than Sm in garnet; if garnet is present in the source, low Hf/Sm ratios will be generated during partial melting. La/Sm versus Gd/Yb (Fig. 15) compares the slopes of heavy and light REEs.

The La/Yb ratio summarizes the overall REE slope, which varies with the degree of partial melting when garnet is left in the residue. The Th/Ta ratio minimizes the effect of garnet fractionation and tends to be slightly enriched in plume related sources. Plotting these two ratios against each other (Fig. 16) can be used to discriminate mafic magmatic suites, and can also be used to recognize mantle components (Condie, 1997, 2001, 2003). Mantle components include MORB, EM1, EM2, HIMU, FOZO (Hart, 1988; Hart et al., 1992), and also potential crustal and lithospheric contamination. Originally identified using isotopes (e.g. Nd, Sr, Pb, Hf), these components can also be recognized in terms of their trace element compositions. More recently, Condie (2003) has grouped the deep mantle reservoirs into the following end members (on trace element diagrams, Figs. 16–18): DEP (a depleted source similar to MORB, but located in the deep mantle — probably equivalent to FOZO). REC is near average OIB (EM1 and EMII) and HIMU, and are assumed to represent recycled lithosphere, and EN is near continental crust and presumably reflects crustal materials carried to depth in the mantle. Figure Nb/Y vs Zr/Y (Fig. 18) can also be used to assess whether or not a plume source is involved based on a discriminant based on Icelandic data (Fitton et al., 1997).

Volcanic Suites

The volcanic formations define distinct geochemical groups, e.g. have geochemical fingerprints. The lower Riphean (ca. 1650 Ma) Ai formation is represented by med-K calcalkaline trachybasalts (site 5) and dacites (site 6). Both mafic and felsic sites have steep REE slopes, with enriched chondrite normalized LREE/HREE [(La/Yb)n = 7–13 for mafic and 13–15 for felsic samples],

a pronounced negative La–Nb anomaly), and a negative Sr anomaly. The mafic samples also have a positive K anomaly. The Ai formation defines a geochemical fingerprint (Figs. 14–16 and Table 4) with high La/Nb (2.2–3 and 4.2–4.6 for mafic / felsic samples) and low Hf/Sm ratios (0.6); moderate Th/Ta (2.5–4 and 11 for mafic / felsic samples) and high La/Yb ratios (11–19 and 20–23 for mafic / felsic samples), moderate La/Sm (4–5 and 7 for mafic / felsic samples) and high Gd/Yb ratios (2.8–3.0 and 2.2–2.6 for mafic / felsic samples). In terms of tectonic setting they plot as within-plate and alkaline affinities (Figs. 10–13) and in terms of mantle sources they plot as a mixture of Recycled and Enriched sources (Figs. 16–18), and the negative La–Nb anomaly is likely due to lithospheric contamination rather than a subduction component.

The middle Riphean (ca. 1370 Ma) Mashak events (sites 14, 18, 19, and 24) are characterized by low- to medium-K, mainly tholeiitic basalts (Fig. 3). This suite is characterized by a negative Sr anomaly, and negative K and Ba anomalies, though this is probably a consequence of the widespread low grade metamorphism. REE patterns are moderately enriched chondrite normalized LREE/HREE, (La/Yb)n = 2–4, and there is a weak Ta–Nb anomaly. With respect to geochemical fingerprinting (Figs. 14–16), the Mashak magmatic events have low La/Nb ratio ranging from 0.8–1.5, low Hf/Sm ratios (0.8), low to moderate Th/Ta (2–3) and La/Yb ratios (mainly 3.3–6), La/Sm (2–4) and low Gd/Yb ratios (1.5–1.9). In terms of tectonic setting they plot as withinplate (Figs. 10–13) and in terms of mantle sources they plot as Depleted and significant addition of Enriched and

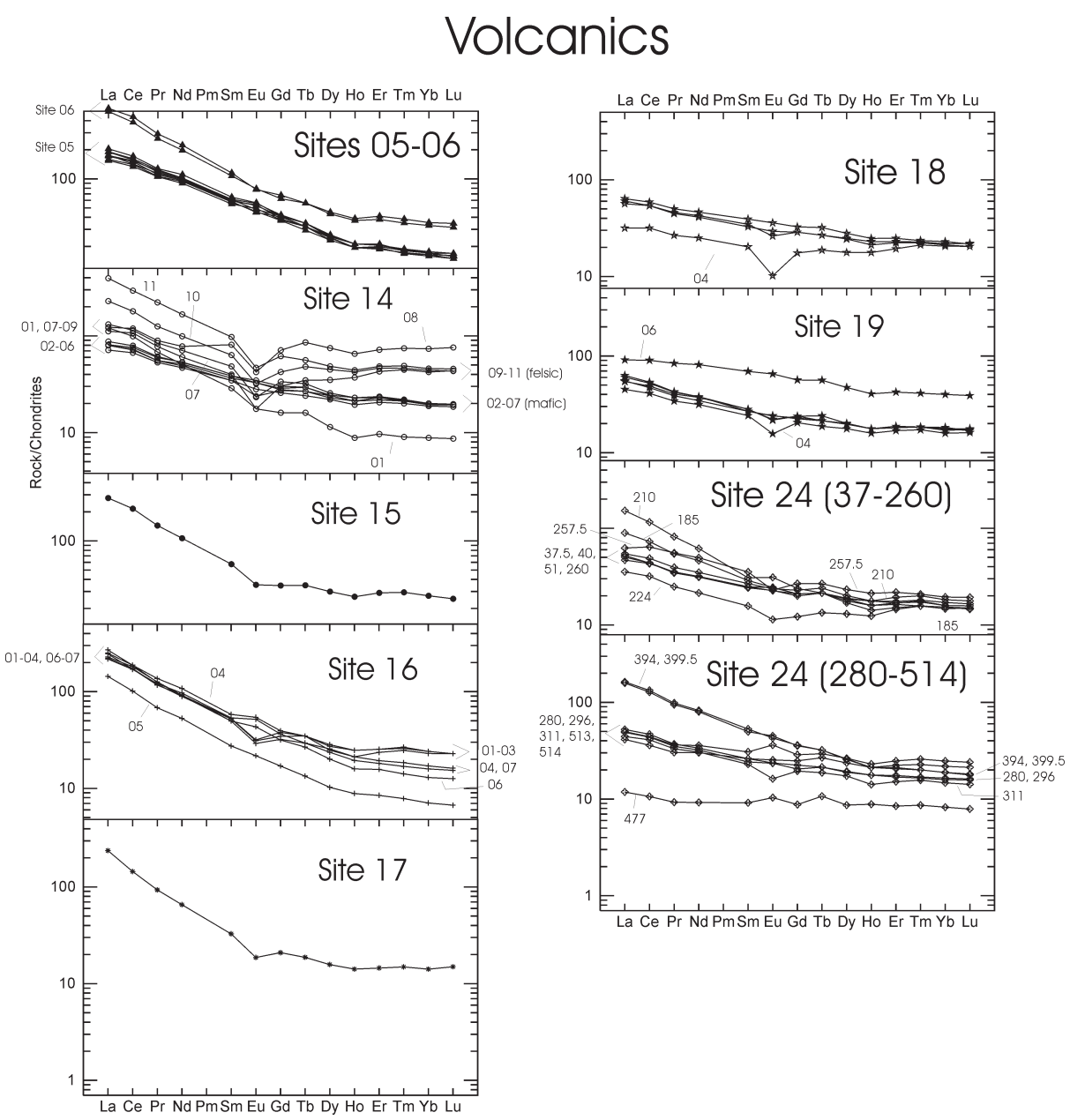

Figure 5. REE data normalized by chrondritic values

Recycled sources (Figs. 16–18). More felsic samples from site 14 have a distinctly different pattern consisting of negative K, Ba,m Rb, Sr P and Ti anomalies.

The Vendian (ca. 600 Ma) Arsha formation is distinct from the older formations in having higher SiO_2 and lower MgO. These low- to medium-K rocks are broadly andesitic, but with Na_2O+K_2O and SiO_2 negatively correlated (Fig. 4). The Arsha formation has the steepest REE slopes with very enriched chondrite normalized LREE/HREE, (La/Yb)n = 9–20. Its geochemical fingerprint (Figs. 14–16) is defined by low La/Nb (below the critical value of <1.4), scattered Hf/Sm ratios (0.4 & 1.2), variable to low Th/Ta (1.3 & 4.3) and high La/Yb ratios (13 & 20–30), high La/Sm (6.5–8.5) and moderate to high Gd/Yb ratios (1.7 & 2.9). In terms of tectonic setting they plot mostly in the within-plate field and in terms of deep mantle sources they plot near the REC source.

Intrusive Rocks

Dykes and sills also form distinct geochemical groups (Figs. 4–19). Units cutting basement in the Radashny quarry are scattered on some diagrams. Most typically, they exhibit moderate to high LOIs (1.5–5 wt%), low TiO_2, intermediate Mg# (30–50), have a variable REE slopes, (La/Yb)n 1–13, a strong subduction signature (La/Nb 2.2–5.0), and minor negative P anomalies (Fig. 6). The high Mg site 8 which cuts the Bakal formation has a similar composition to the Radashny quarry units,

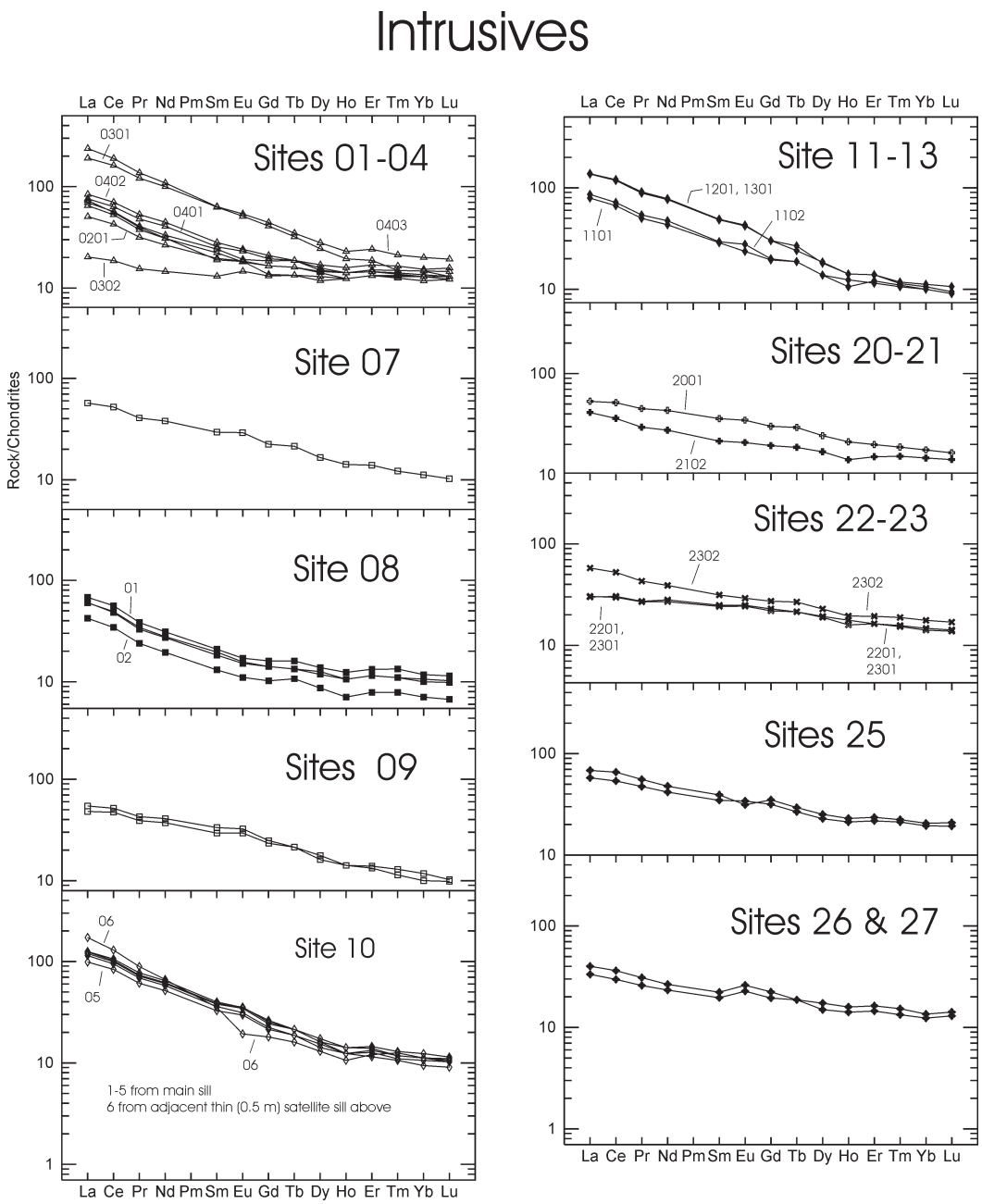

in Sun and McDonough (1989). Symbols as in Fig. 3

Table 4

Geochemical Summary of Extrusive Suites

Geochemical Plot	Ai fm (sites 5 and 6)	Mashak (sites 14, 18, 19, 24)	Vendian (sites 15–17)
LOI (Fig. 3)	Site 5 (2.6–4.8%); site 6 (1.8–3.0%)	Most 2–4%, some as high as 10%, and as low as 1%	1–4–2.7%, one 7.8%
TAS (Fig. 4)	Site 5 (mainly trachybasalts Site 6 (andesite/dacite)	Basalts to basaltic andesite, and andesite-dacite	Andesite, dacite rhyolite
Spider (Fig. 6)	Mafic Site 5: pos K, neg. Nb–Ta and Sr Felsic Site 6: neg Nb–Ta, Sr, P and Ti	Mafic: Neg K, Ba, Rb, & Sr Felsic: neg. K, Ba, Rb, Sr, P, Ti	Felsic: neg. K, Ba, Rb, Sr, P, Ti
AFM (Fig. 7)	Transitional (thol. & calc alkaline)	tholeiitic	Mainly thol.
TIO_2 vs Mg# (Fig. 8)	High TiO_2 (2.5–3%) over a range of Mg# (also one has low TiO_2 probably from site 6; the other site 6 samples must have)	Intermed TiO_2 (1.2–2.6%) over a range of Mg#	3 with low TiO_2 (1–1.2% and 1 with high TiO_2 (3%
$ZrTiO_2$ vs NbY (Fig. 9)	Basalt (site 5) Andesite-basalt to rhyolite-dacite (site 6)	Basalt & trachyte	Alkali basalt to trachy-andesite
Zr–Ti–Y (Fig. 10)	Site 5 (within plate) Site 6 (outside of fields because of intermediate-felsic composition)	Ocean floor (or calc-alkali) & within plate	Within plate
MnO_2-TiO_2-P_2O_5 (Fig. 11)	OIA	Mostly IAT to MORB	Mostly IAT and OIA
La–Y–Nb (Fig. 12)	Calc-alkali	continental	Mostly continental
Ti vs V (Fig. 13)	Alkaline	MORB / BAB MORB	Variable
La/Nb (subduction signature) (Fig. 14)	Strong subduction signature: Site 5 (2.2–3); site 6 (4.2–4.6)	No subduction signature: 0.8–1.5	No subduction signature: 0.6–1.4
Hf/Sm (Fig. 14)	~0.6	~0.8	~0.4 & 1.2
La/Sm (Fig. 15)	Site 5: 4–5 Site 6: 7	2–4	6–8
Gd/Yb (Fig. 15)	Site 5: 2.8–3.0 Site 6: 2.2–2.6	1.5–1.9	1.7 & 2.9
Th/Ta (Fig. 16)	Site 5: 2.5–4 Site 6: ~11	2–3	1.3 & 4.3
La/Yb (Fig. 16)	Site 5: 11–19 Site 6: 20–23	Mainly 3.3–6	13 & ~20–30
Zr/Nb (Fig. 17)	11	8–12	3 & 7.2
Nb/Th (Fig. 17)	5	6–10	4 & 15
Nb/Y (Fig. 18)	Site 5: 0.5 Site 6: 0.5	0.3–0.5	1.1 & 2.7
Zr/Y (Fig. 18)	Site 5: 6–7 Site 6: 11	3.2–5.2	7–10

although it is more primitive (Mg# >75). It also has low TiO_2 (0.5–1%), high La/Nb (2.9), La/Sm is 5, Gd/Yb is 1.7, high Th/Ta (10–13), high La/Yb (8), low Nb/Th (2), moderate Zr/Nb (13). Like sites 1–4 it also has a negative P anomaly. Considered as a group (sites 1–4 and site 8), they are calc-alkali (Figs. 7 & 9) and in terms of mantle sources they show a wide scatter around the deep mantle Depleted and Enriched components (Figs. 16–18).

The sills (sites 10–13) which cut lower Riphean Satka formation (including the Kusa sill) define a second group. They have moderate to high LOIs (3–5.5 wt%), plot as basalts near the trachy-basalt boundary (Figs. 4 & 9), and have intermediate TiO_2 (1.2–2.4 wt%) and Mg# (35–50) (Fig. 8), high La/Nb (2.2–3.0). In terms of tectonic setting they define a predominantly within plate setting, although the La/Nb value (>1.4) suggests a subduction component. In terms of mantle sources, they plot between the REC and EN fields (Figs. 16–18).

The remaining intrusions plot together, but based on cross-cutting relationships must represent at least two distinct ages (Middle Riphean and Upper Riphean or younger). They consist of intrusions cutting lower Riphean units: dykes (sites 20 and 21 cut the Suran formation which is considered an equivalent of the Satka formation. Dyke (site 7) also cuts the Bakal formation (and is dated at 1385,3 Ma, see below). There are several intrusions constrained to be equivalent to or younger than Middle Riphean. Site 25 cuts middle Riphean strata, and site 9 cuts the Berdyuash rapakivi pluton which is dated as ca. 1370 Ma. The second group consists of Sites 22, 23, 26 and 27 which cut upper Riphean. Broadly speaking all these sites have low LOI (2–2.7%), low La/Sm (0.8–3), a range in Gd/Yb (1.9–2), moderate to high TiO_2 (1.5–3 wt%), low-moderate La/Nb (~1), and a range in Th/Ta (1.1–5). Within this group sites 9 & 20–21 are compositionally similar to the dyke of site 7 which has known middle Riphean age. Site 25 has a distinctive decrease in the more mobile elements, a pattern which is also present to a lesser degree in upper Riphean sites 26 and 27 (Fig. 6). Upper

Table 5

Geochemical Summary of Intrusive Suites

Geochemical Plot	Cutting pre-Riphean basement (sites 1–4)	Cutting lower Riphean) (Sites 10–13	Cutting lower Riphean-group 2 (site 20 & 21)	Bakal and Berdyuaush (sites 7 and 9)	Cutting Lower Riphean: picrite intrusion (site 8)	Cutting middle Riphean (site 25)	Cutting Upper Riphean-Group 1: sites 22–23) Group 2: sites 26, 27
LOI (Fig. 3)	0.8–3.1%	2.9–5.2%	1.8–2.3%	2.0–2.7%	2.2% & 5.9–6.6%	2.4–2.8%	0.7–4.0%
TAS (Fig. 4)	Mainly basalts to basaltic andesites	Mainly trachybasalt to basalt	Basalt	Basalt-tephrite basinite	Basalt	basalt	basalt
Spider (Fig. 6)	Neg. Nb–Ta, Th, Ba	Neg. Nb–Ta, Th, (Sr)	Post. Rb, K	Neg. Nb–Ta Pos. (Rb, K)	Neg. Nb–Ta, Pos. K	Neg. Sr, K, Rb, Ba	–
AFM (Fig. 7)	tholeiites	calc alkaline	Tholeiite	tholeiitic	High Mg	tholeiite	tholeiite
TIO_2 vs Mg# (Fig. 8)	Low TiO_2; intermediate Mg# (mainly 50)	Intermediate TiO_2 (1.2–2.4%); Mg# (30–45)	Intermed TiO_2 (1.7–2.2%); Mg# (35)	Intermed. TiO_2 (1.7–2.1%)	Very low TiO_2 (<1% for a high Mg#	High TiO_2 (2.8%); low Mg# (25)	Intermed TiO_2 (1.4–2.4%)
Zr/TiO_2 vs Nb/Y (Fig. 9)	Basalt (near andesite/basalt boundary)	Basalt (near alkali basalt boundary)	Basalt	basalt	Basalt (near andesite-basalt boundary	Basalt	basalt
Zr–Ti–Y (Fig. 10)	Within plate to calc-alkali (or IAT or ocean floor)	Within plate	within plate	Within plate,	Calc-alkali	Within plate,	Ocean floor (or IAT or calc alkali)
MnO_2–TiO_2–P_2O_5 (Fig. 11)	Mostly IAT	Mostly OIA	MORB	MORB,	IAT	OIT	MORB
La–Y–Nb (Fig. 12)	Calc-alkali	Mostly calc-alkali	Continental & EMORB	continental	Calc alkali	continental	continental
Ti vs V (Fig. 13)	MORB / BAB MORB with IAT	MORB / BAB MORB	MORB / BAB MORB	MORB / BAB MORB	MORB / BAB MORB	alkaline	MORB / BAB MORB
La/Nb (subduction signature); (Fig. 14) critical value 1.4	Strong subduction: signature 2.2–5.0	Subduction signature: 2–3	No subduction signature: mainly ~1	On boundary: 1.2–1.6	Subduction signature: 2.9	No subduction signature: 1.1–1.3	Mostly no subduction signature: ~1
Hf/Sm (Fig. 14)	~0.5–0.8	~0.6	~0.8	Site 7: 0.8 Site 9: 0.6	~0.7	~0.7	0.7–0.8
La/Sm (Fig. 15)	2–6	4–5	2–3	2.5–3	5	2.5–3	0.8–3
Gd/Yb (Fig. 15)	1–3.5	2.4–3.5	1.6–2.1	2.4–2.9	~1.7	2	1.9–2
Th/Ta (Fig. 16)	4–20	2–3.5	1.1–2	Site 7: 4 Site 9: 1.7	10–13	1.4	Sites 22–23: 3–5 Site 27: 1.1–1.3
La/Yb (Fig. 16)	2–20	11–19	4	7	8	4–5	3–5
Zr/Nb (Fig. 17)	~20	~10	10	10–10.2	13	11	9–1.4
Nb/Th (Fig. 17)	~5	5–18	8–16	Site 7: 6 Site 9: 12	2	8	Sites 22–23: 3–7 Sites 26–27: 12–14
Nb/Y (Fig. 18	0.2	0.2–0.3	0.4	0.4–0.6	0.3		0.2–0.3
Zr/Y (Fig. 18)	4–5.3	3–4.2	4–5.2	Site 7: 6.6 Site 9: 5.1	4.8		Sites 22–23: 4–4.4 Sites 26–27: 3

Riphean sites 22 and 23 have the flattest REE patterns and may represent a third geochemical subgroup. In terms of tectonic setting, these define a within plate (Figs. 10–13). In terms of mantle sources, the data plot with Depleted signature with minor Recycled and Enriched contributions. In most diagrams these sites (22 & 23) are geochemically similar to the middle Riphean Mashak volcanics, though stratigraphically, it is clear that some of the dykes in this group must be Upper Riphean or younger. Therefore, this group must define a second event which is indistinguishable geochemically from the Middle Riphean group.

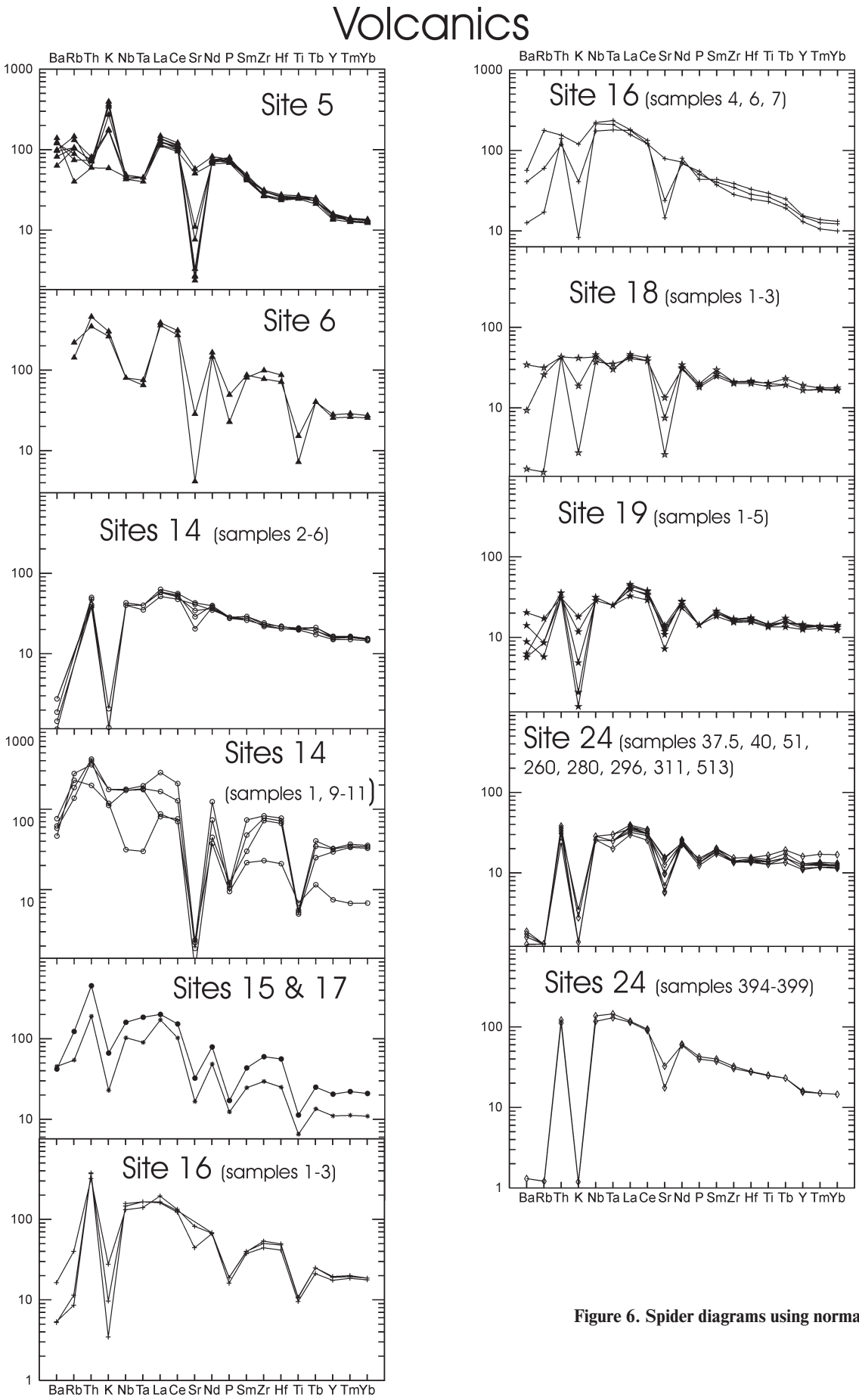

Figure 6. Spider diagrams using normalization

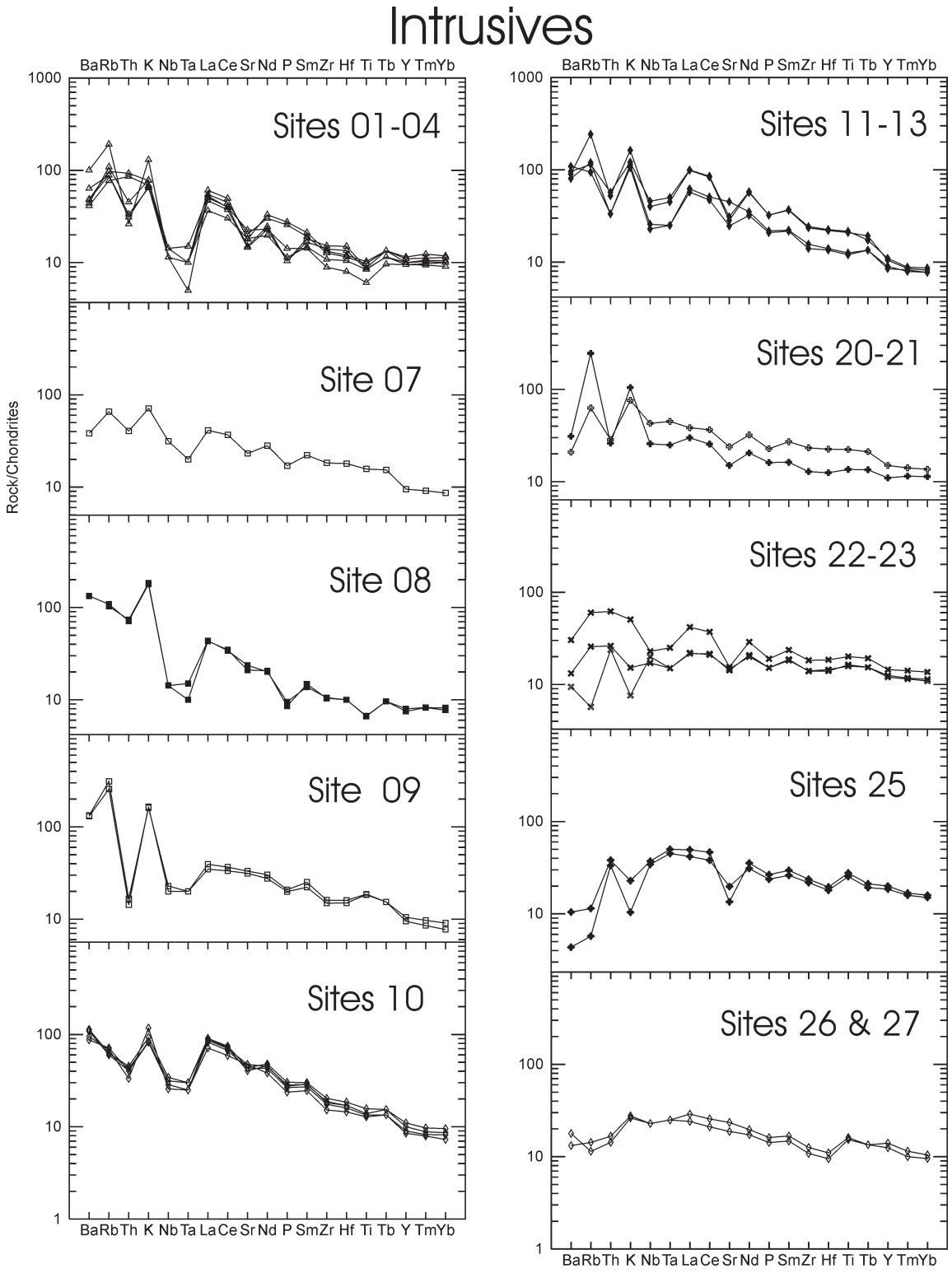

values in Thompson et al. (1983). Symbols as in Fig. 3

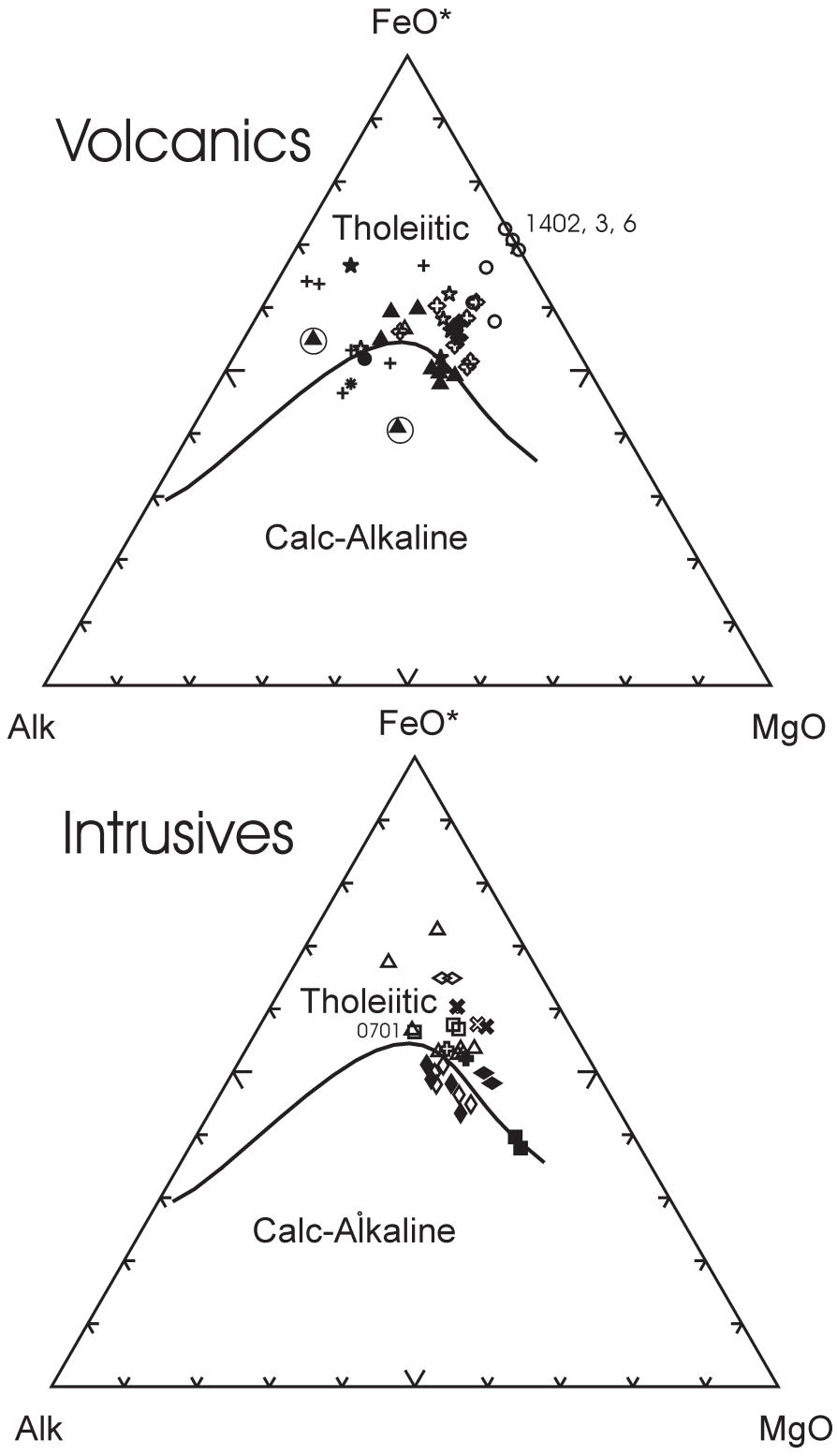

Figure 7. AFM classification diagram after Irvine and Baragar (1971). Symbols as in Fig. 3

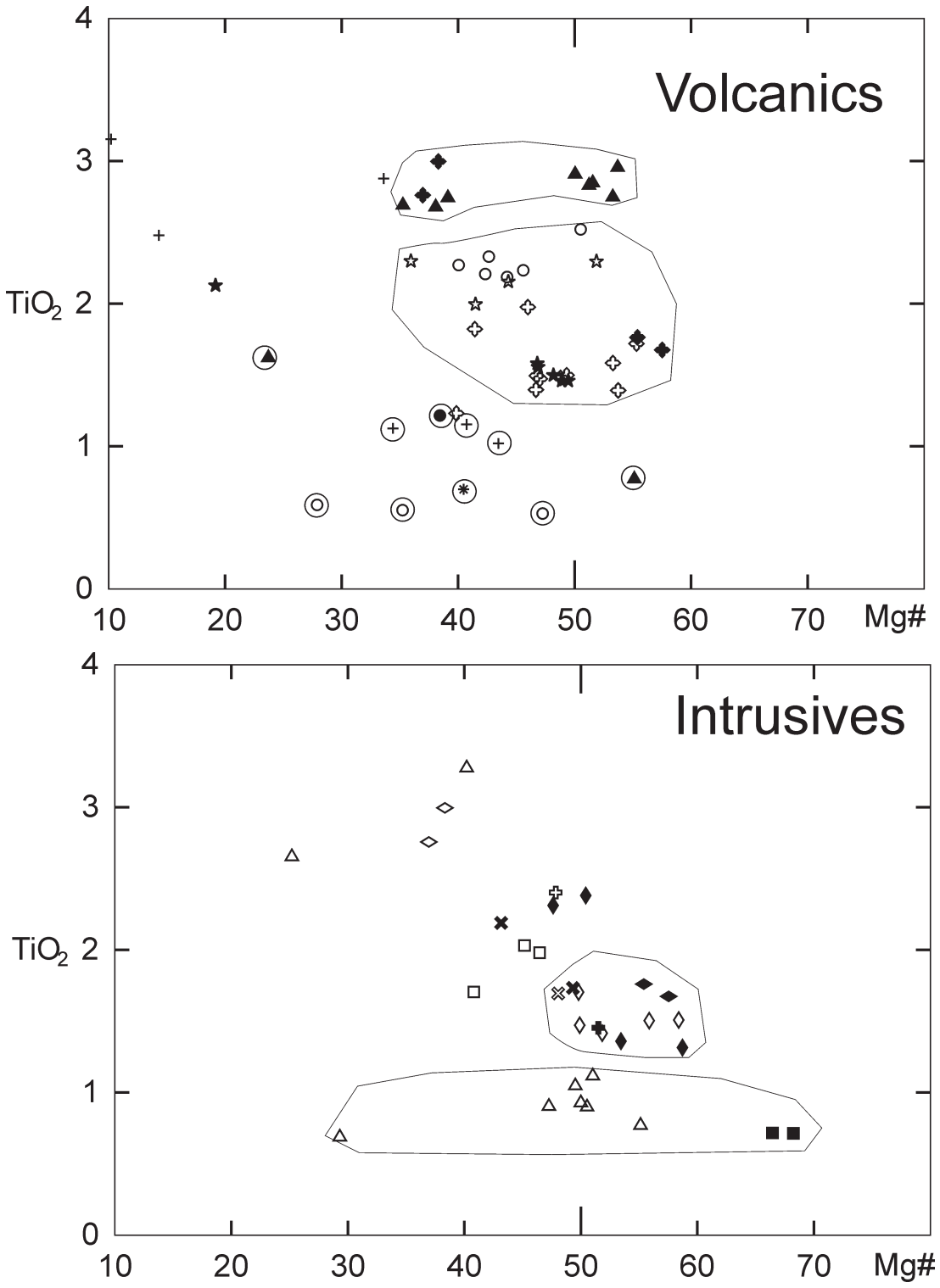

Figure 8. TiO_2 vs Mg#. Symbols as in Fig. 3

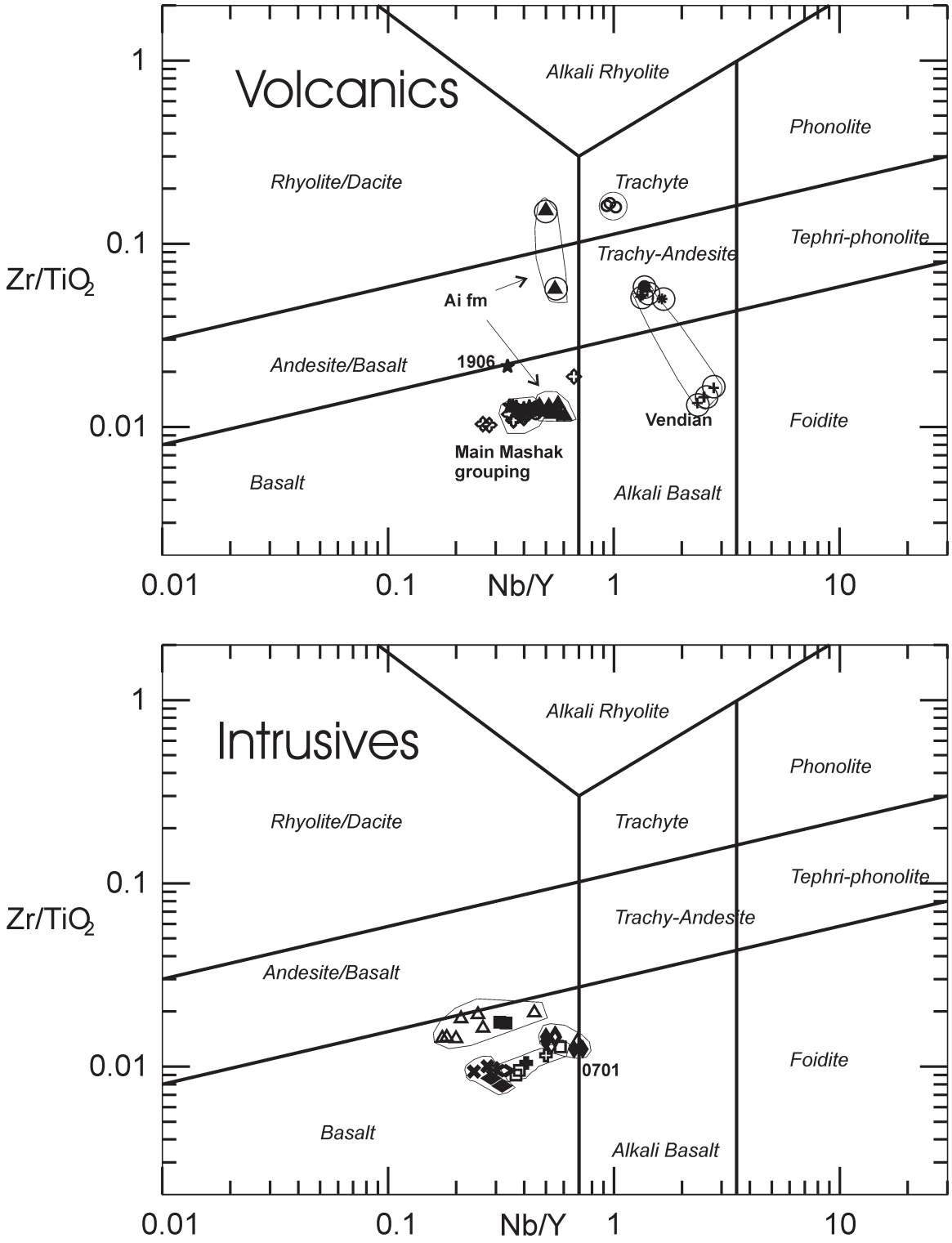

Figure 9. Zr/TiO_2 vs Nb/Y classification diagram of Winchester and Floyd (1977) as revised by Pearce (1996). Symbols as in Fig. 3

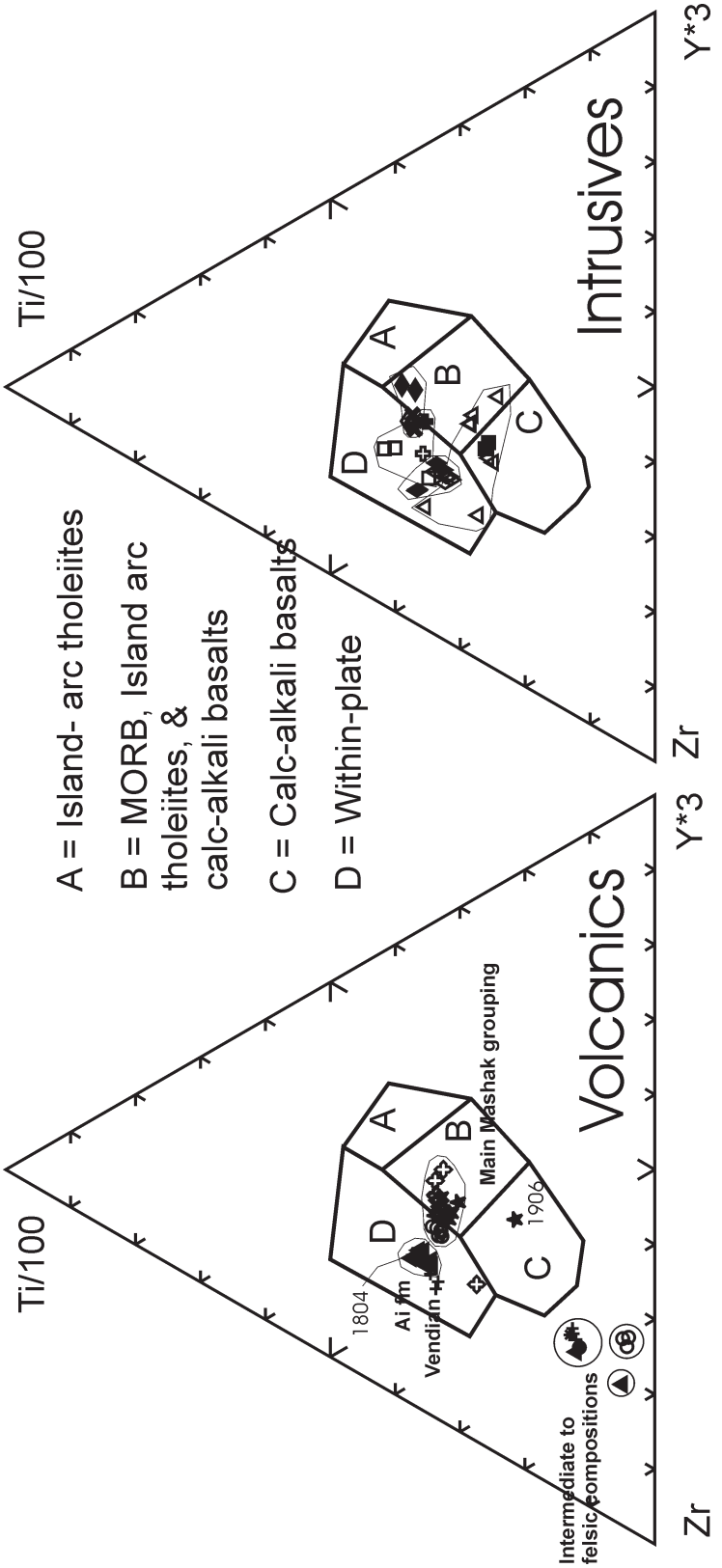

Figure 10. Zr vs Ti/100 vs Y*3 ternary classification diagram after Pearce and Cann (1973). Symbols as in Fig. 3

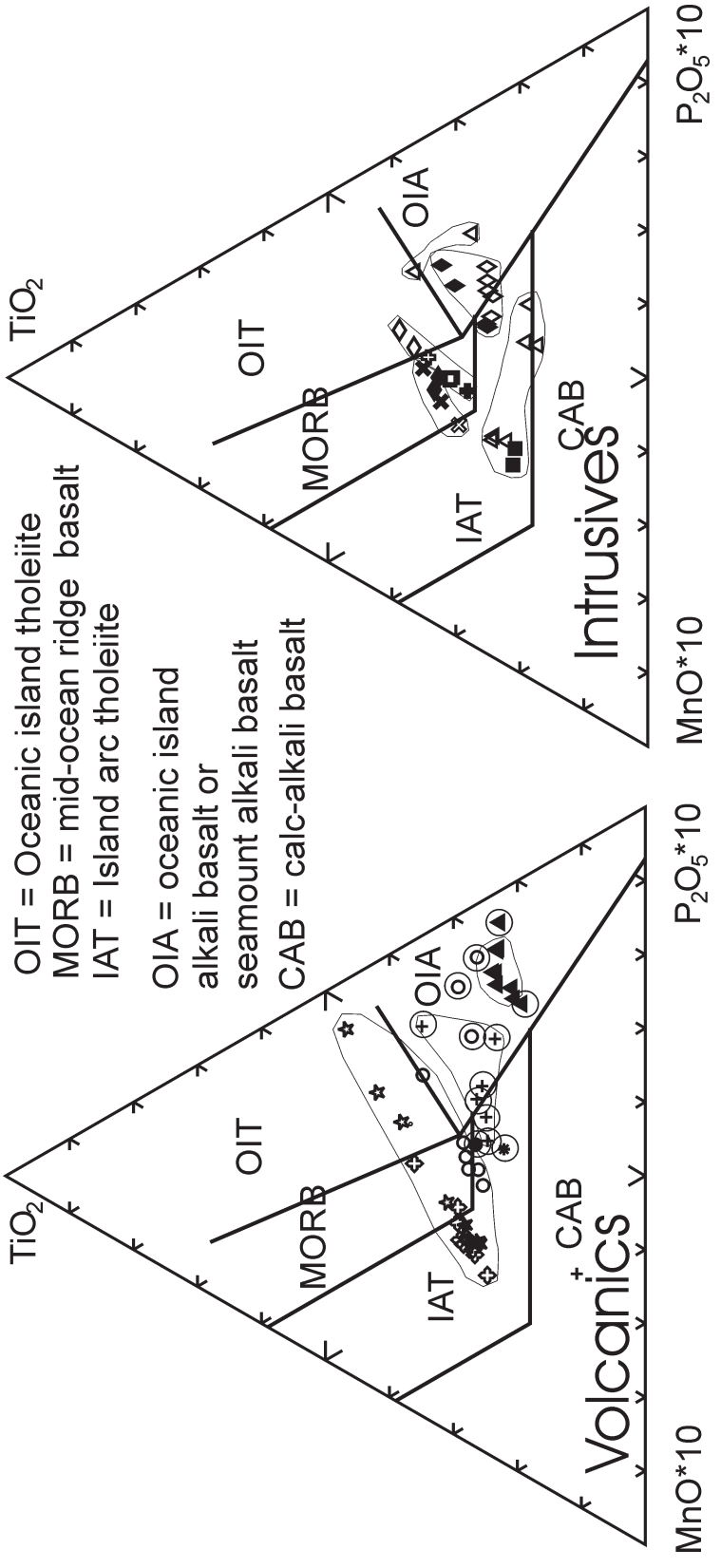

Figure 11. MnO*10 vs TiO_2 vs P_2O_5*10 ternary classification diagram after Mullen (1983). Symbols as in Fig. 3

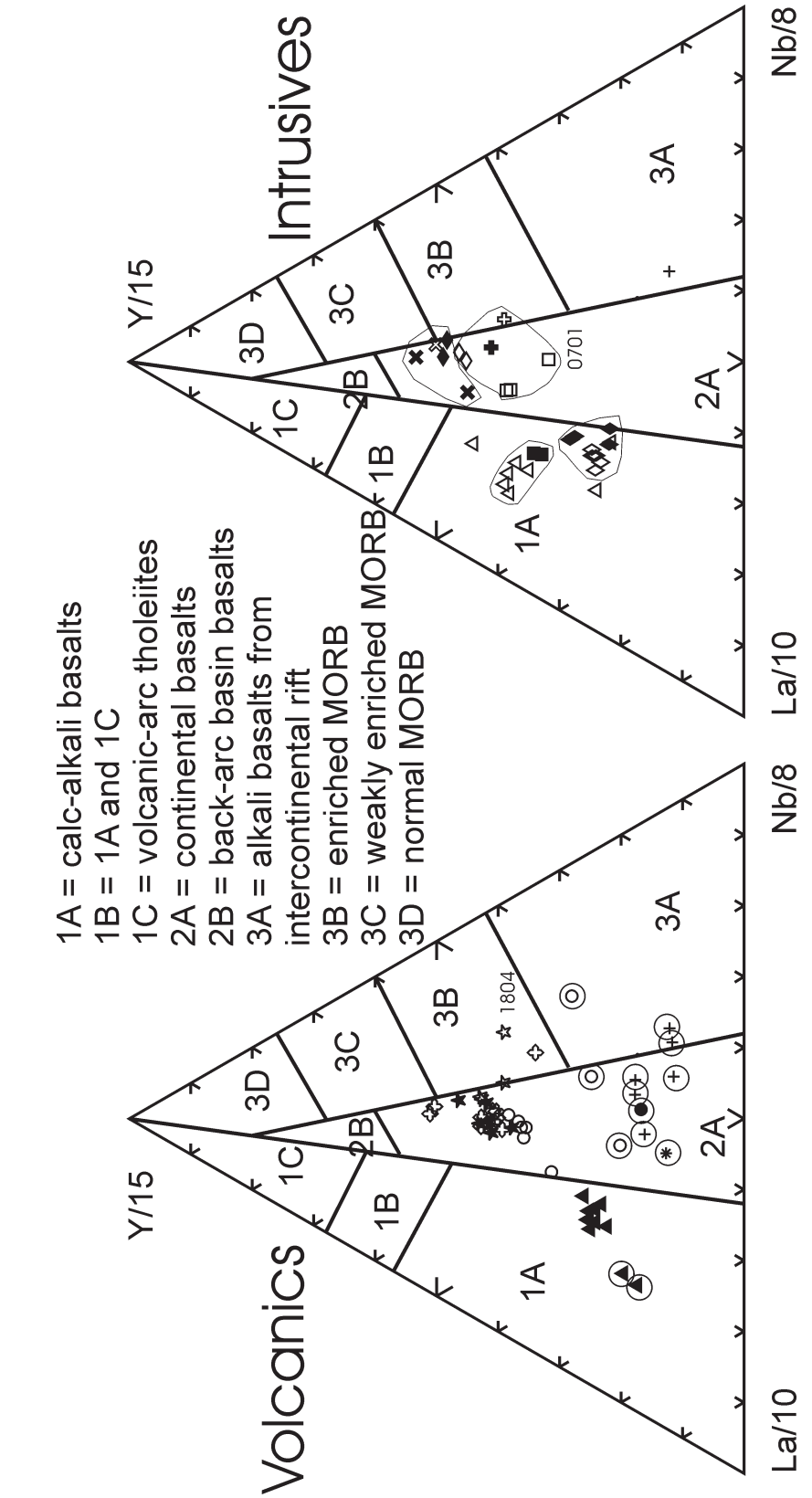

Figure 12. La vs Y vs Nb ternary classification diagram after Cabanis and Lecolle (1989). Symbols as in Fig. 3

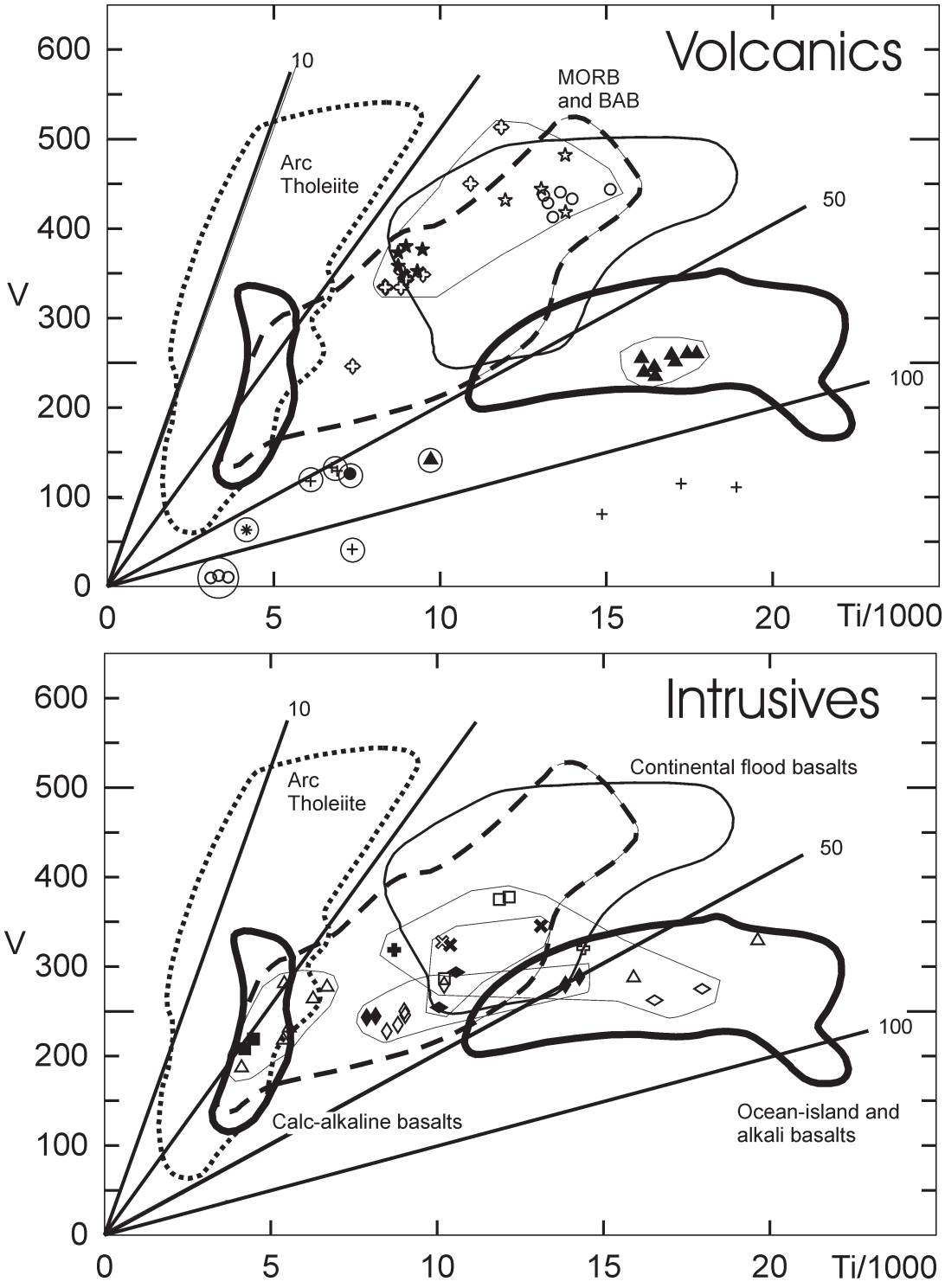

Figure 13. Ti vs V after Shervais (1982). Symbols as in Fig. 3. IAT is island arc tholeiite, MORB is mid-ocean ridge basalt, BAB is back arc basin basalt

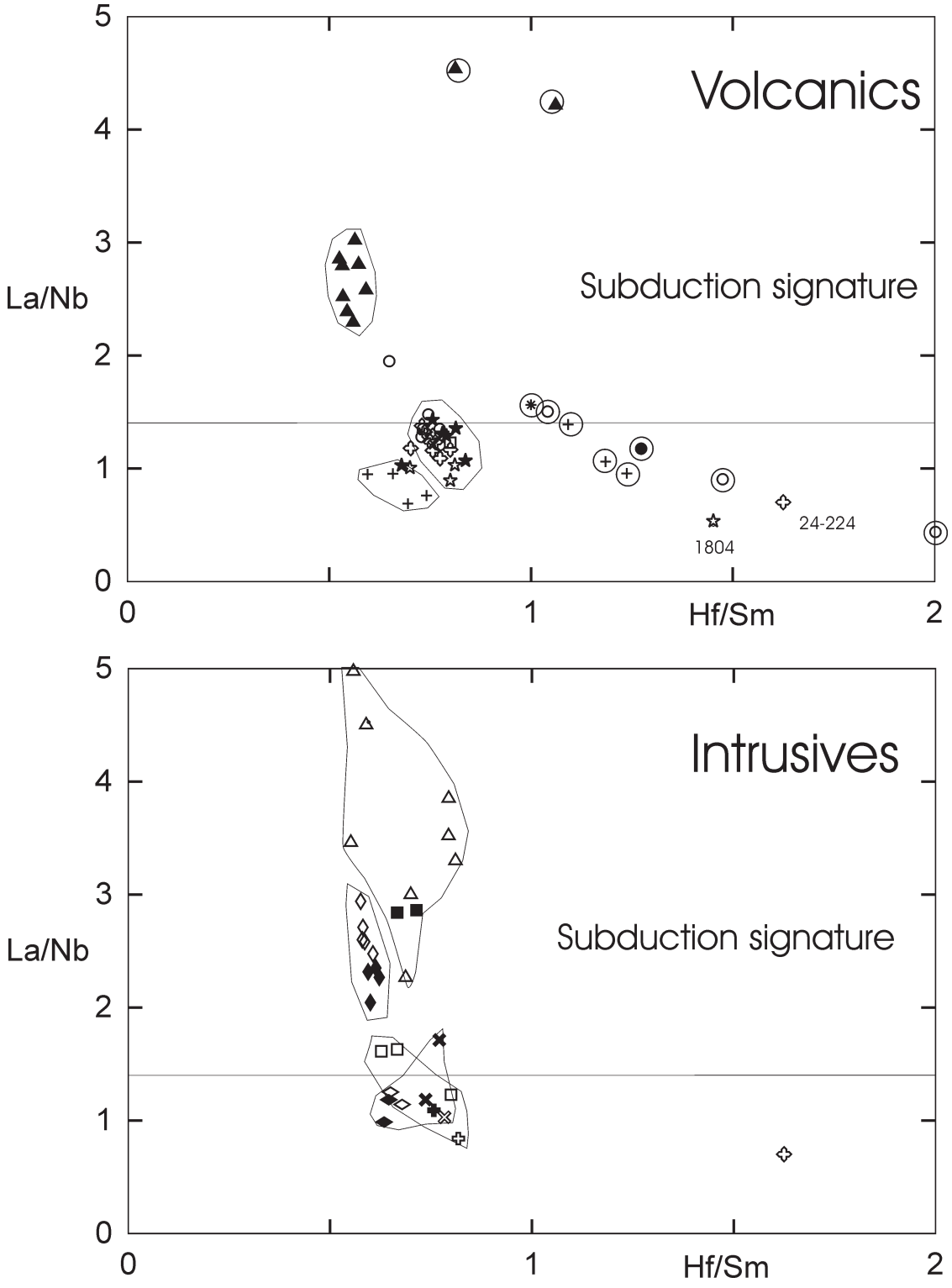

Figure 14. La/Nb ratio for each suite, useful for identifying subduction signature (after Condie, 2003). Symbols as in Fig. 3

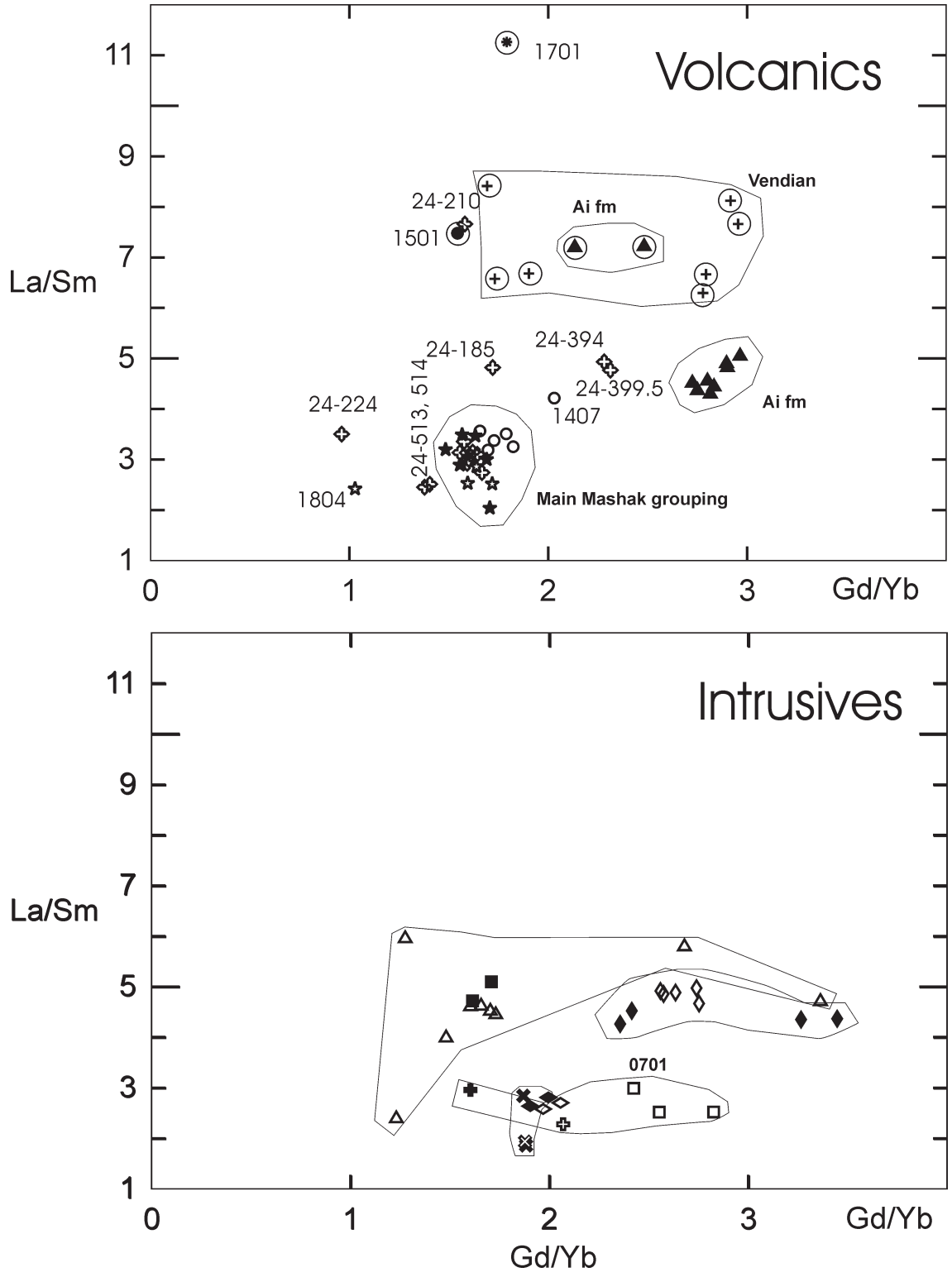

Figure 15. Gd/Yb, versus La/Sm. Ratios used to compare the slope of the heavy rare elements against the slope of the light rare earth elements. Symbols as in Fig. 3

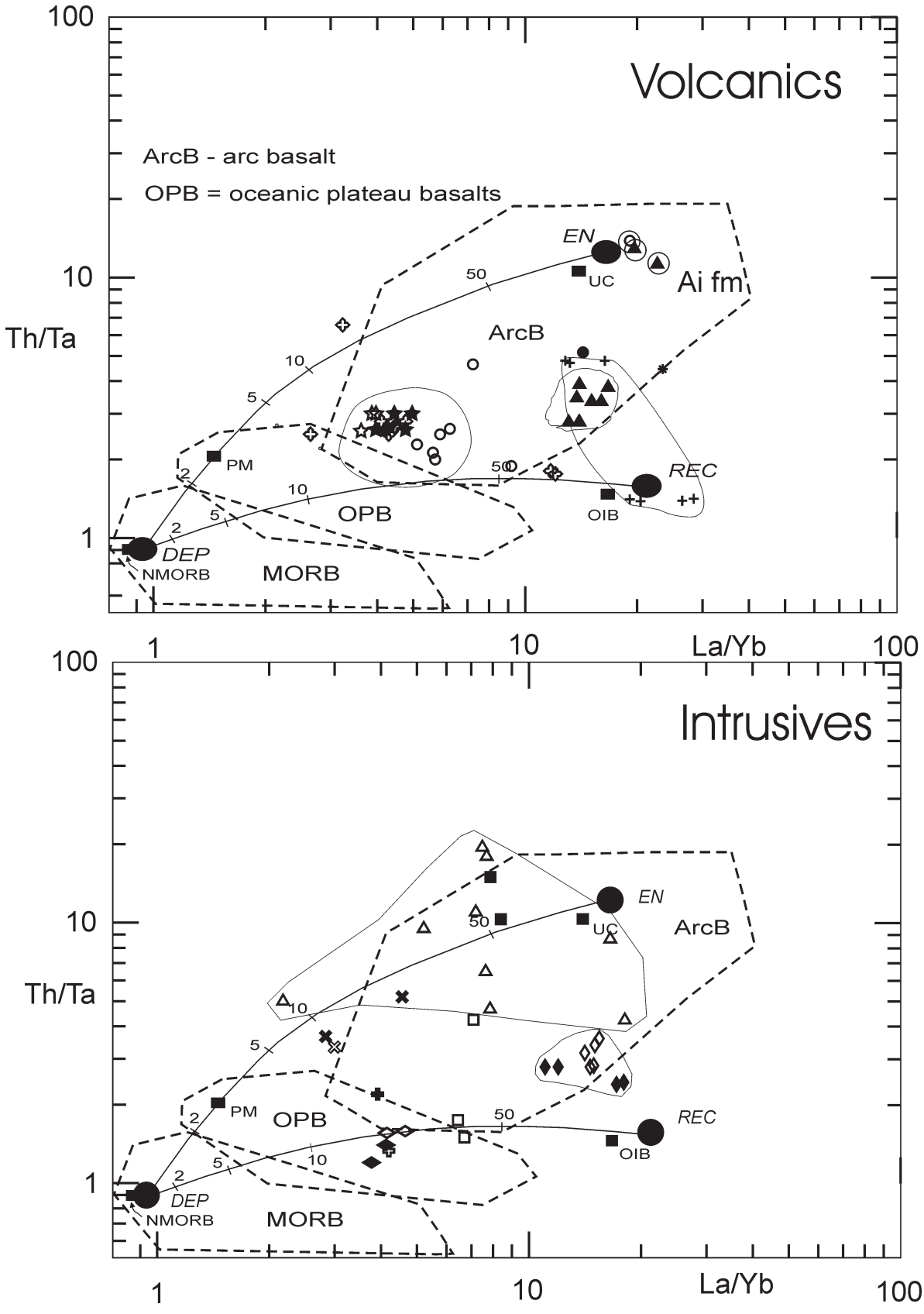

Figure 16. Log Th/Ta vs log La/Yb. After Condie, 1997, 2003 and Tomlinson and Condie (2001). DEP (depleted), REC (recycled), EN (Enriched). OIB is ocean island basalt, PM is primitive mantle, UC is upper crust. NMORB is normal mid-ocean ridge basalt. OPB is ocean plateau basalts, MORB is mid-ocean ridge basalt, ArcB is arc basalt. Symbols as in Fig. 3

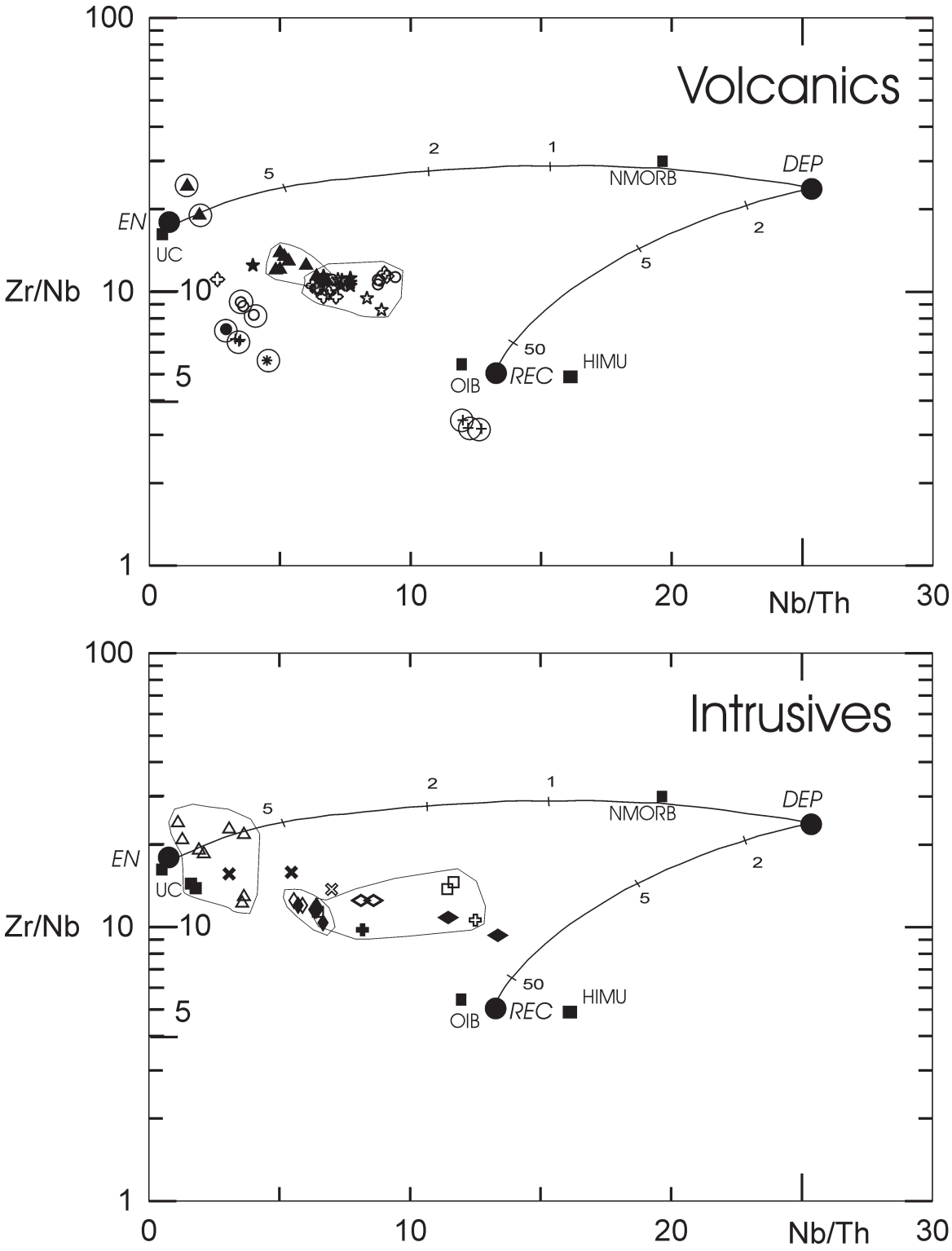

Figure 17. Log Zr/Nb vs Nb/Th after Condie (2003). Symbols as in Fig. 3 and labels as in Fig. 16. HIMU is high ?

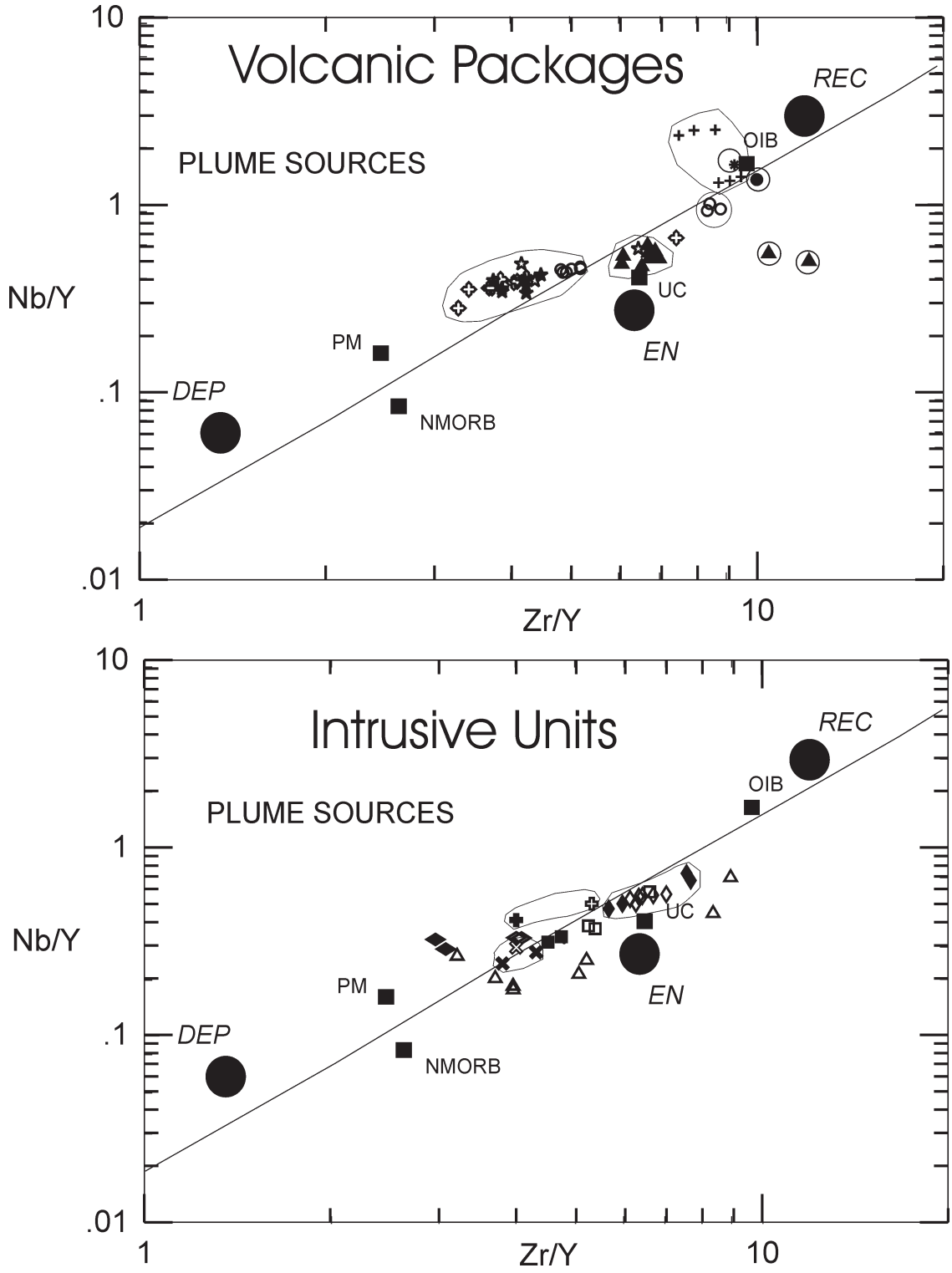

Figure 18. Log Nb/Y vs log Zr/Y (after Fitton et al., 1997 as modified by Condie, 2003). Symbols as in Fig. 3 and labels as in Fig. 16

GEOCHRONOLOGY

A U–Pb baddeleyite age was obtained for the Bakal dyke (site 7) (Fig. 20, Table 6). Two baddeleyite fractions, which are only slightly discordant, yield a precise age of 1385,3±1,4 Ma. This confirms a previously determined, but less precise Rb–Sr age of 1360±35 Ma (Ellmies et al., 2000). This age is broadly similar to Berdyaush dates and slightly older than the most recent estimates for the age of the Mashak formation (see earlier discussion).

DISCUSSION

Comparison of felsic and mafic units of interpreted bimodal suites

The Ai formation has a bimodal composition (c. f. mafic samples from site 5 and felsic samples from site 6 in Fig. 4). On REE diagrams (Fig. 5) and multi-element diagrams (Fig. 6) the patterns are parallel suggesting that the two mafic and felsic groups are related, and that they probably derived by different degrees of differentiation of the same source magma.

For the middle Riphean units however, there is a difference between mafic and felsic units, as noted previously by Karsten et al. (1997). This is most clearly seen for site 14 (e.g. Fig. 6a) where three felsic samples have numerous elemental anomalies (e.g. strongly negative Ti, P and Sr) that are not present (apart from a minor negative Sr anomaly) in the mafic samples. At the same time we know that both felsic and mafic magmatism is very similar in age. Therefore, the origin of felsic component is probably due to crustal melting under the influence of ascending basaltic magma (e.g. Bryan, 2002).

We next consider the age relationship with the Berdyaush pluton and a dyke which crosscuts this pluton. The nepheline syenite phase of the Berdyaush pluton yields a 1368.4±6.2 Ma age, and the crosscutting dyke (site 9) geochemically matches the Bakal dyke dated herein as 1385,3±1,4 Ma. So, if this geochemical match (between sites 9 and dated site 7) is significant, then both the Berdyaush pluton and its crosscutting dyke would belong to the Mashak event and indeed the felsic magmatism may precede some of the mafic magmatism, as can be observed in other bimodal or dominately felsic magmatic suites (e.g. Bryan, 2002).

The Vendian suites (sites 15, 16 and 17) are all broadly felsic (Fig. 4) and are geochemically distinct from the upper Riphean and lower Vendian dykes. However, until precise ages are obtained for these younger suites, comparison of felsic Vendian volcanism with mafic intrusives remains uncertain.

Correlating intrusive and volcanic magmatism based on geochemical fingerprints

In the previous section we noted correlations between intrusive and extrusive suites based on geochemical fingerprinting. In addition a precise 1385 Ma U–Pb age allowed correlation of dyke 7 with the Mashak Igneous Event. These correlations and new geochronology allow the recognition of 5 distinct magmatic events in the region (Table 7): Also these events can be classified in terms of tectonic setting based on various classification diagrams (Figs. 10–14) and mantle sources (Figs. 16–18). The latter include estimates of deep mantle sources: Depleted, Recycled, and Enriched, and the significance of these diagrams is further evaluated in the discussion section.

Event 1: The oldest magmatic suite is represented by the volcanic rocks of the lower Riphean Ai formation (sites 5 and 6). Sills (sites 10–13) are very similar geochemically (Tables 4 & 5), i.e. in terms of high LOI, REE slope, multi-element diagrams, and the various trace element classification and mantle source diagrams. These sills cut the Satka formation, which is lower Riphean in age, but overlie the Ai formation and are therefore at least slightly younger. Pending geochronology, we tentatively conclude that the sills cutting the Satka formation are also lower Riphean in age, but (on stratigraphic grounds) must be at least slightly younger than the Ai formation volcanics.

Event 2: The next magmatic group is represented by middle Riphean volcanic and intrusive rocks. These include the volcanic units (sites 14, 19, 24) and also the dyke from site 7 (dated herein as 1385 Ma). Other dykes cutting lower Riphean and middle Riphean units and which are compositionally similar (Tables 4 & 5), most importantly in REE slope, multi-element diagrams, and various trace element and mantle source diagrams) include sites 9, 20, 21, and 25. We correlate these units into the middle Riphean "Mashak igneous event" (Ronkin et al., 2005).

Event 3: The next magmatic suite includes dykes cutting the basement rocks in Radashny quarry (sites 1–4). These *have* a strong compositional similarity (Table 5) with the high-Mg basalt cutting the Bakal formation (site 8). On this basis we define a separate event with an age of Lower Riphean or younger (sites 1–4 and 8).

Event 4: The fourth *group* is defined by intrusions cutting upper Riphean units.

Event 5: The fifth and probably youngest geochemical grouping identifies the magmatic suite of the Arsha formation (site 19). It is Vendian in age and consists of mostly felsic and intermediate rocks. These have trace element *signatures* distinct from event 4; for this reason we consider the two events to be separate. However, if events 4 and 5 were determined to be coeval, then the difference between mainly felsic (event 4) and mafic (event 5) compositions, could be a consequence of different coeval sources. If the felsic rocks are generated by melting of continental crust caused by mafic magmatism, then the composition of the felsic suite need not have geochemical similarity with the mafic rocks (Bryan et al., 2002). The absolute ages of events 4 and 5 remain to be determined.

Table 6

U–Pb isotopic data for Main (diabase) Dyke, Central Quarry of Bakal

Sample Fraction	Analysis no.	Description	Weight (μg)	U (ppm)	Th/U	Pb* (pg)	Pb_C (pg)	$^{206}Pb/^{204}Pb$	$^{206}Pb/^{238}U$ (± 2σ)	$^{207}Pb/^{235}U$ (± 2σ)	$^{207}Pb/^{206}Pb$ (± 2σ)	$^{206}Pb/^{238}U$ (± 2σ) Age (Ma)	$^{207}Pb/^{235}U$ (± 2σ) Age (Ma)	$^{207}Pb/^{206}Pb$ (± 2σ) Age (Ma)	Disc. (%)	Corr. Coeff.
EQ03–07–01																
Bd–1	MAH4083	Dk brn prismatic blade	0.57	779	0.04	99.2	0.9	7283	0.23654 (0.00070)	2.8723 (0.0094)	0.08807 (0.00014)	1368.7 (3.7)	1374.7 (2.5)	1384.0 (3.0)	1.2	0.8784
Bd–2a	MAH4084	Pale-med brn long blade	0.33	489	0.04	36.3	0.7	3427	0.23793 (0.00062)	2.8907 (0.0104)	0.08812 (0.00019)	1375.9 (3.2)	1379.5 (2.7)	1385.0 (4.1)	0.7	0.8135
Bd–2b	MAH5017b	Pale-med brn long blade	0.27	664	0.04	40.3	1.2	2405	0.23814 (0.00086)	2.8949 (0.0137)	0.08816 (0.00028)	1377.0 (4.5)	1380.6 (3.6)	1386.1 (6.1)	0.7	0.7376
Bd–3a	MAH5018	Dk brn blade tip	0.14	1324	0.03	41.7	2.2	1325	0.23840 (0.00054)	2.8976 (0.0077)	0.08815 (0.00011)	1378.3 (2.8)	1381.3 (2.0)	1385.8 (2.5)	0.6	0.9209

Notes:

All analyzed fractions represent fresh, high-quality, least magnetic single baddeleyite grains (non-magnetic at full Frantz field).

Abbreviations: Dk = dark; brn = brown; med = medium.

Pb* is total amount (in picograms) of radiogenic Pb.

Pb_C is total measured common Pb (in picograms) assuming the isotopic composition of laboratory blank: 206/204 — 18.221; 207/204 — 15.612; 208/204 — 39.360 (errors of 2%).

Pb/U atomic ratios are corrected for spike, fractionation, blank, and, where necessary, initial common Pb; $^{206}Pb/^{204}Pb$ is corrected for spike and fractionation.

Th/U is model value calculated from radiogenic $^{208}Pb/^{206}Pb$ ratio and $^{207}Pb/^{206}Pb$ age assuming concordance.

Disc. (%) - per cent discordance for the given $^{207}Pb/^{206}Pb$ age.

Uranium decay constants are from Jaffey et al. (1971).

Table 7

Magmatic groupings based on new geochemistry and geochronology presented in this paper

MAGMATIC GROUPINGS FROM THIS PAPER	VOLCANIC ROCKS	INTRUSIVE ROCKS	TECTONIC SETTING	MANTLE SOURCES
Event 1: Lower Riphean (ca. 1650 Ma)	Mafic: Ai formation (site 5), Felsic: Ai formation (site 6)	Mafic: Sills cutting Satka formation (sites 10–13)	Within Plate with alkaline affinities; subduction signature (neg Ta–Nb anomaly; strong control by lithosphere?	Strong EN & REC Not plume (strong control by lithosphere?
Event 2: Middle Riphean (1380 Ma Mashak igneous event)	Mafic and Felsic: Mashak and related volcanics (sites 14, 19, 24)	Mafic: Dated dyke site (7), and other dykes cutting lower Riphean and middle Riphean units and which are compositionally similar (9, 20, 21, and 25)	Within plate (could also be back arc basin; no subduction signature	DEP with substantial contribution of EN and REC; Plume
Event 3: Lower Riphean (Bakal formation) or younger (≤1650 Ma)		Dykes cutting basement in Radashny quarry (sites 1–4), high MgO basalt dyke (site 8).	Calc-alkaline- Island arc thol.. strong subduction signature	Subequal DEP & EN (substantial lithospheric contribution?). Not plume
Event 4: Upper Riphean or younger (ca. <700 Ma)		Mafic: sites 22, 23, 26 and 27	Within plate (no subduction signature)	DEP with minor REC and EN contribution; Plume?
Event 5: Vendian (ca. 650–600 Ma)	Mafic and Felsic: Arsha formation (site 15–17)		Within plate (based on basaltic samples)	Mainly REC; Plume

Geodynamic Context (Tectonic Setting, mantle sources)

Lower Riphean (Event 1 in Table 7): There are conglomerates at the base of the Ai formation, overlying the Archean-Paleoproterozoic crystalline complex with angular unconformity and suggest a probable rift relationship for the corresponding event. The Ai formation with its associated mafic volcanics is lower Riphean and is no older than about 1650 Ma. The geographic distribution of the magmatic-sedimentary units of the Ai formation is difficult to determine because of limited outcrop. However, the series of lower Riphean units is different in the north than in the south: In the north the Lower Riphean consists of the Ai, Satka and Bakal formations (Fig. 2). In the south it consists correspondingly of Bolsheinzer, Suran and Jusha formations, with some differences of lithology, compared to the first three (Bolsheinzer lacks conglomerates and volcanics in the lower part of the section and contains carbonates in the upper; Jusha is substantionally more terrigenous). Ai formation volcanic rocks are contemporaneous with the formation of a rift-like NNW-trending Kama-Belsk paleorift in the adjacent platform, which has trend oblique to that of the present day Urals (Puchkov, 2002). In particular it is inferred that the Ai formation sits on a shoulder of this aulacogen. Based on the geochemical similarity we consider the sills cutting the Satka formation to also belong to this interpreted rift event (although a slightly later stage). However, it cannot be excluded that the strong similarity is accidental and that the sills were emplaced much later. The geochemistry of both the Ai formation volcanics and the sills is consistent with a within plate setting with slight alkaline affinity. However, presence of a strong Ta–Nb anomaly indicate subduction character, or alternatively, the involvement of lithospheric mantle. Mantle source diagrams favour a combination of Recycled and Enriched sources, and no plume signature is seen.

Event 2: Mashak event: In contrast the 'grain' of the Mashak formation is parallel to the present Urals, and therefore differs from that of Event 1, which is evidence of a changed geodynamic setting between Events 1 and 2. The Mashak formation sediments (including basal conglomerates) and mafic volcanic rocks define a rift setting and have dates of 1370–1380 Ma (see regional setting section). Several dykes (sites 7, 9, 20, 21 and 25) are provisionally correlated with the Mashak

Igneous event. The setting appears to be Within Plate, but could also be back arc basin. There is no subduction signature. The mantle source is dominantly Depleted with a substantial contribution of Enriched and Recycled components. A plume source is indicated.

Event 3: Lower Riphean or younger: This magmatic event consists of the dykes and sills cutting the Radashny quarry, and also the high Mg dyke cutting the Bakal formation. The only age constraint is that this event must be equal to or post lower Riphean. In terms of tectonic setting, an arc setting is strongly suggested by the consistent calc-alkalic signature, and large negative La–Nb anomaly. Various tectonic diagrams support an arc setting, and there is a strong subduction signature. Mantle sources include sub-equal contributions from Depleted and Enriched sources, but a plume signature is not apparent.

Event 4: upper Riphean or younger: An additional magmatic event is represented by intrusives (dykes) which cut upper Riphean units. This composition of this magmatism is distinct from the Vendian Arsha formation and thus provisionally represents a separate event. Interestingly this magmatic event has composition similar to the middle Riphean event (Event 2) on many diagrams (as discussed earlier) but clearly is distinct given that its members cut upper Riphean units, and unlike Event 2 have no subduction signature. The setting is within plate and there is not subduction signature. A Depleted source with minor Recycled and Enriched contributions is observed. The presence of a plume is equivocal.

Event 5: Vendian: The felsic volcanics of the Arsha formation are Vendian in age. Their geochemistry suggests a within plate setting, and there is no subduction signature (La/Nb < 1.4). The main mantle source is Recycled, and a plume source is implied.

Summary: The data is consistent with early and mid Riphean rifting events (events 1 and 2). However, it is uncertain whether one or both events led to rifting. Event 3 (during post mid-Riphean) is arc related. Late or post-Riphean magmatism (event 4) also has rift/plume signatures. Finally a Vendian event (which may be the felsic equivalent of event 4) has within plate signatures and may be associated with a final rifting event.

Possible Link with 1380 Ma Large Igneous Province remnant in northern Greenland

Intraplate magmatism of identical age to the Mashak Igneous event, especially to the most precise age estimate of 1385 Ma for the Bakal dyke (Fig. 19) age obtained in this study has also been found in western Laurentia (Hart River sills and Salmon River Arch sills), in northern Greenland (Midsommerso sills and Zig-Zag Dal volcanics), in the Anabar Shield of Siberia (Chieress dykes), in Antarctica (Vestfold Hills dykes), and in the Congo craton (see reviews in Ernst and Buchan, 2001; Ernst et al., 2006). In the Rodinia reconstruction, Baltica was adjacent to northeastern Laurentia at 1265 Ma based on paleomagnetism but also consistent geological correlations between the two (Buchan et al., 2000) (Fig. 20). The position of the Mesoproterozoic Uralian margin of Baltica is shown (Fig. 20) and it is considered that this margin was a long-lived passive margin after an initial Mesoproterozoic or Neoproterozoic breakup (Pease et al., 2006). In this reconstruction, the Midsommerso — Zig-Zag Dal magmatism of northern Greenland (Upton et al., 2005) is close to the potential Mesoproterozoic breakup margin. As one of the variations on the reconstruction we suggest that this margin broke-up at 1380 Ma. Consequently, remnants of this magmatism are present at the southern end of the Southern Urals and at the northern end in northern Greenland. This model would predict additional remnants of 1380 Ma magmatism along this margin. However, its recognition may be complicated by poor exposure of pre-Uralian basement rocks.

CONCLUSIONS

A new geochemical study of magmatic suites along the southeastern margin of the East European craton in the southern Ural Mountains allows characterization of 8 volcanic sites, corresponding to 3 volcanic suites, and 19 intrusive sites (in 11 sills and 8 dykes). Geochemical 'fingerprints' allow correlation of intrusive and volcanic units into at least 5 different magmatic events.

The earliest event includes the lower Riphean (ca. 1650 Ma) Ai formation volcanics, for which geochemistry indicates a within plate slightly alkaline character, but also a strong La/Nb anomaly (and negative Ta–Nb anomaly) suggestive of subduction character and mantle sources are mixtures of Enriched and Recycled components, consistent with involvement of lithospheric and asthenospheric sources. The distribution of volcanic rocks and sediments, including the presence of associated conglomerates supports a rift origin and a link with the Kama-Belsk paleorift. Several sill complexes, including the Kusa sill cutting the Satka formation, represent a discrete intrusive geochemical group which can be matched with the Ai formation although on stratigraphic grounds must be at least slightly younger. This first event has within-plate plus alkaline affinities; subduction signature, interpreted to be imparted by interaction with lithosphere. Mantle components are dominantly Enriched and Recycled, but a plume signature is not recognized.

The second event, the Mashak igneous event consists of Middle Riphean volcanic suites and geochemically correlated dykes. A precise U–Pb baddeleyite age of 1385.3±1.4 Ma is obtained herein for the Bakal quarry dyke. This age provides a precise link to Mashak magmatism and represents the most precise estimate available for the Mashak igneous event. Despite geological and structural evidence for an extensional setting, some geochemistry indicates a subduction component (moderate La–Nb anomaly), although this could also

be obtained from involvement of lithospheric mantle. Other diagrams indicate a MORB or Back-Arc setting. This may further point to involvement of lithospheric mantle. The setting is within plate (but could also be back arc). There is no subduction signature. Mantle sources are Depleted with substantial contributions of Enriched and Recycled sources. Plume source is likely.

The third magmatic event of unknown age comprises dykes and sills cutting pre-Riphean basement and a high Mg sill intruding the lower Riphean Bakal formation. An arc setting is strongly suggested by a consistent calc-alkali signature on a variety of diagrams, and large negative Ta–Nb anomaly. This event shows strong arc signature which matches the strong subduction signature. Sub-equal Depleted and Enriched components were involved in the source, and do not match a plume source.

The fourth event comprises mafic dykes which cut upper Riphean formations and which define a compositional grouping distinct from Arsha volcanics (below), with within-plate character. Geochemically, this event is similar to the much older ca. 1380 Ma Mashak (event 3), although it lacks a subduction signature. The age difference rules out a link with event 3 and reaffirms that similar geochemical fingerprints can sometimes be generated by more than one event**.** The mantle source is dominated by a Recycled component, and a plume is implied.

The fifth event comprises felsic volcanics of the Arsha formation of Vendian age. Geochemistry suggests a within plate setting (no subduction signature). The mantle source is Depleted with minor Recycled and Enriched components, and plume involvement is equivocal.

To summarize, the first two events represent early Riphean and middle Riphean rifting events. Event 3 could suggest a calc-alkaline arc. The renewed rifting of events 4 and 5 took place possibly in the Upper Riphean and certainly in the Vendian.

It is possible that the subduction signature (high La/Nb) of the observed events reflects lithospheric or crustal contamination, which was strongest in the Lower Riphean (event 1, and event 3?), weaker in the middle Riphean (event 2) and absent in the younger upper Riphean and Vendian units (events 4 and 5).

Most magmatism is mafic, but felsic rocks are also present. In the Ai formation mafic and felsic suites are

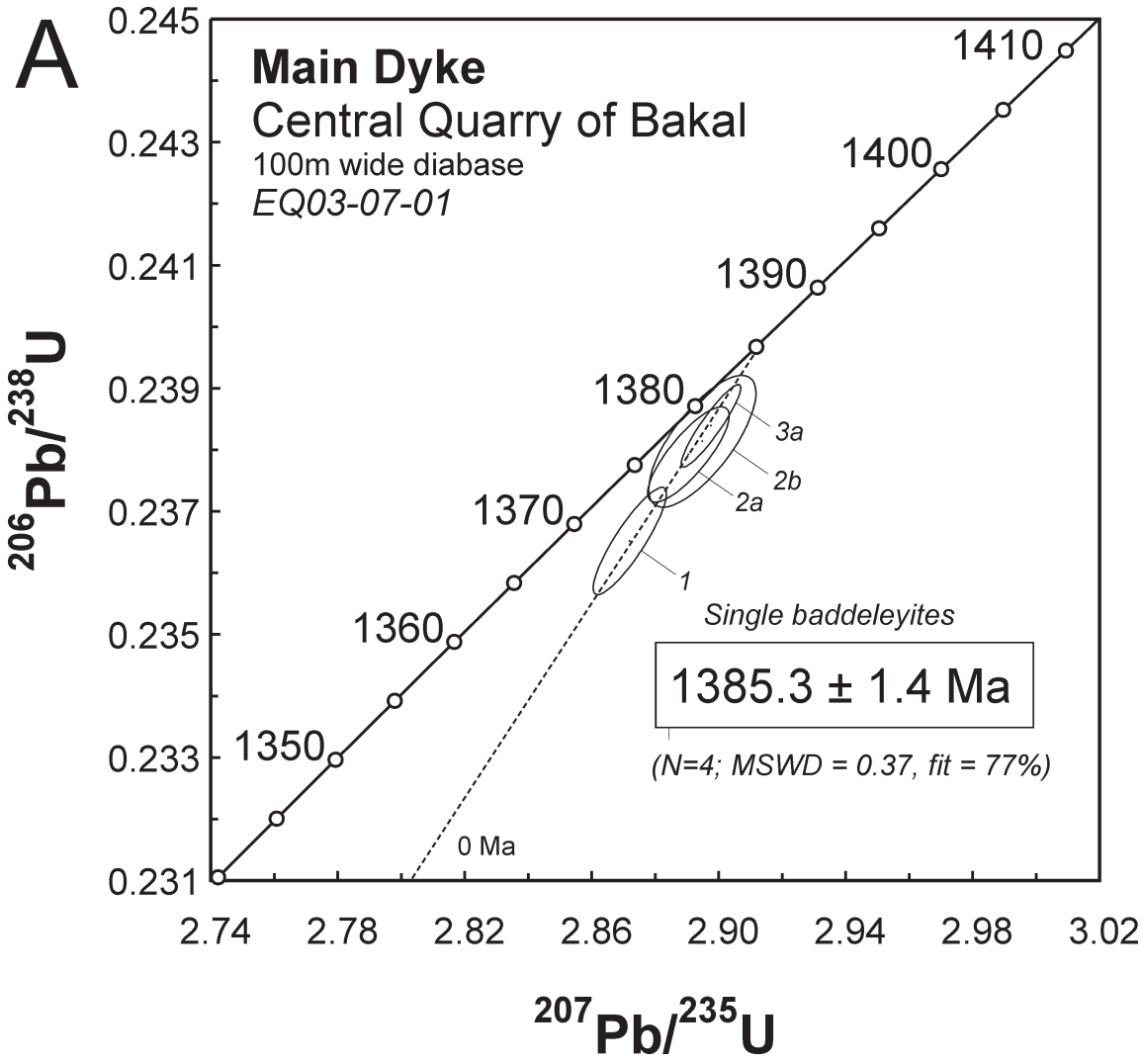

Figure 19. Geochronology of Bakal dyke (see the explanations in the text)

cogenetic, while in the Mashak formation, the mafic and felsic rocks have distinct geochemical patterns. The felsic rocks may represent melting of continental crust by the basaltic component of the event. The Vendian (felsic) volcanics have distinct chemistry from upper Riphean – lower Vendian (or younger) dykes, but age control is very poor, and they could be coeval. It is worth mentioning that the stage of rift volcanism and intrusive activity in the Kvarkush anticlinorium of the Urals, situated to the north of the Bashkirian meganticlinorium, encompasses both the Upper Riphean and Vendian (Petrov et al., 2005).

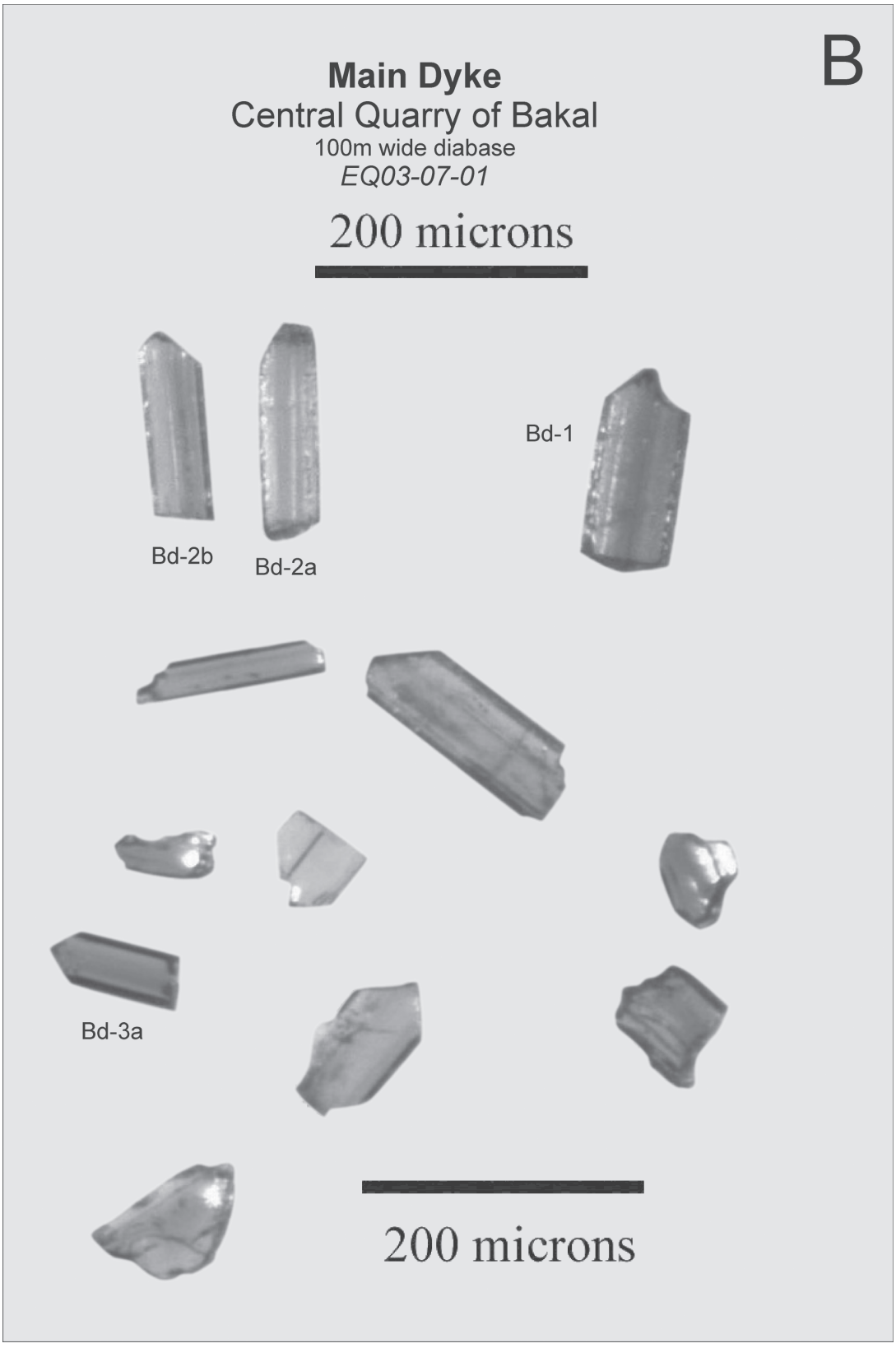

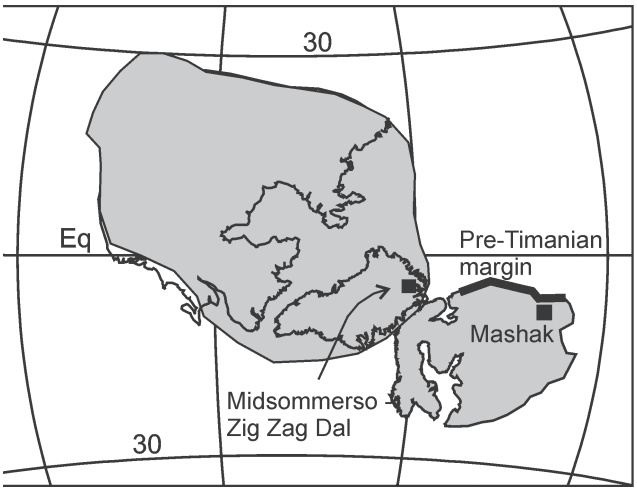

Figure 20. Reconstruction of Baltica and Laurentia at 1267 Ma (after Buchan et al., 2000). Location of pre-Timanian margin inferred from distribution of "Timanian age complexes" from Fig. 1 in Pease et al. (2006)

It is proposed that the Mashak event and the Midsommerso — Zig-Zag Dal event of Greenland are part of the same event which caused rifting along the north eastern margin of Baltica at 1380 Ma. The conjugate margin could be any of the other blocks with 1380 Ma events such as: Siberia, or Antarctica (Ernst and Buchan, 2001).

ACKNOWLEDGEMENTS

The material was collected during the field excursion in 2003, organized and sponsored by IGSP 440 «Rodinia». The authors also gratefully acknowledge financial support from BHP–Billiton company for the U–Pb geochronology done by MH at the University of Toronto laboratory, the Swedish National Science Research Council, the Swedish Royal Academy of Sciences, the Earth Sciences Department of Russian Academy of Sciences, Program 10 "Central Asian Mobile Belt: geodynamics and stages of the Earth's crust formation". IGPET 2000 was used for plotting geochemical data.

REFERENCES:

Alekseyev, A.A. **1984.** Riphean-Vendian magmatism of the western slopes of the Southern Urals. M. Nauka, 136 p (in Russian).

Becker, H., Jochum, K., Carlson, R. **2000.** Trace element fractionation during dehydration of eclogites from high-pressure terranes and the implications for element fluxes in subduction zones. Chemical Geology, 163: 65–99.

Buchan, K.L., Mertanen, S., Park, R.G., Pesonen, L.J., Elming, S.-Å., Abrahamsen, N., Bylund, G. **2000.** Comparing the drift of Laurentia and Baltica in the Proterozoic: the importance of key paleomagnetic poles. Tectonophysics, 319: 167–198.

Bryan, S.E., Riley, T.R., Jerram, D.A., Leat, P.T., Stephens, C.J. **2002.** Silicic volcanism: an under-valued component of large igneous provinces and volcanic rifted margins In: Menzies, M.A., Klemperer, S.L., Ebinger, C.J., Baker J. (eds.) Magmatic Rifted Margins. Geological Society of America Special Paper 362: 99–120.

Cabanis, B., Lecolle, M. **1989.** Le diagramme La/10–Y/15–Nb/8: un outil pour la discrimination des series volcaniques et la mise en evidence des processus de mélange et/ou de contamination crustale. Comptes Rendus de l'Academie des Sciences, Series II, v. 309: 2023–2029.

Condie, K.C. **1997.** Sources of Proterozoic mafic dyke swarms: constraints from Th/Ta and La/Yb ratios. Precambrian Research, v. 81: 3–14.

Condie K.C. **2001.** Mantle Plumes and Their Record in Earth History. Cambridge Univ. Press, Oxford, U.K., 306 p.

Condie, K.C. **2003.** Incompatible element ratios in oceanic basalts and komatiites: Tracking deep mantle sources and continental growth rates with time. Geochemistry, Geophysics, Geosystems. v. 4, no. 1, 1005, doi: 10.1029/2002GC000333.

Ellmies R., Glodny J., Krupenin M. **2000.** A metallogenic model for the sediment-hosted deposits of the Proterozoic Bashkir basin // Geological Survey and mineral deposits of Russia at the verge of the XX century. V. 2. Mineral reserves of Russia. Mat. of the All-Russian Meeting of geologists St-Petersburg, VSEGEI: 6–7(in Russian).

Ernst, R.E., Wingate, M.T.D., Buchan, K.L., Li, Z.X. **(in prep).** Global Record of Large Igneous Provinces (LIPs) during the life cycle (1600–700 Ma) of the proposed supercontinent Rodinia Precambrian Research (Special issue on Rodinia).

Fitton, J.G., Saunders, A.D., Norry, M.J., Hardarson, B.S., Taylor, R.N. **1997.** Thermal and chemical structure of the Iceland plume. Earth Planet. Sci. Lett. 153: 197–208.

Garan M.I. **1969.** The Lower and Middle Precambrian. Geology of USSR. Permian, Sverdlovsk, Chelyabinsk and Kurgan oblast. V. 12, part 1 (1). W, Nedra: 64–149 (in Russian).

Glasmacher, U.A., Bauer, W., Giese, U., Reynolds, P., Kober, B., Puchkov, V., Stroink, L., Alekseyev, A., Willner, A.P. **2001.** The metamorphic complex of Beloretzk, SW Urals, Russia — a terrane with a polyphase Meso- to Neoproterozoic thermo-dynamic evolution. Precambrian Research, 110: 185–213.

Gorozhanin V.M. **1995.** The Rb–Sr isotopic method in solving problems of geology of the Southern Urals. Autoreferate of thesis of candidate of geol.-min. sci. Ekaterinburg, 23 p. (in Russian).

Gradstein F.M., Ogg J.G., Smith A., Bleeker W, Lourens L.J. **2004.** A new geologic Time Scale, with special reference to Precambrian and Neogene/ Episodes, V. 27, No 2: 83–100.

Grachev A.F. **1977.** Rift zones of the Earth. Leningrad, Nedra. 247 p. (in Russian).

Hart, S.R. **1988.** Heterogeneous mantle domains: signatures, genesis and mixing chronologies. Earth. Planet. Sci. Lett. 90: 273–296.

Hart, S.R., Hauri, E.H., Oschmann, L.A., Whitehead, J.A. **1992.** Mantle plumes and entrainment: isotopic evidence. Science 256: 517–520.

Herzberg, C. **1995.** Generation of plume magmas through time: An experimental approach. Chemical Geology 126: 1–16.

Irvine, T.N., Baragar, W.R.A. **1971.** A guide to the chemical classification of the common volcanic rocks. Can. J. Earth Sci. 8: 523–548.

***Karsten K.A., Ivanov K.S., Maslov A,V., et al.* 1997.** The nature of Mashak volcano-sedimentary formation of Bashkirian meganticlinorium: new geochemical data. In: Riphean of the Northern Eurasia. Geology. General problems of stratigraphy. Ekaterinburg, IGG Uralian Branch of RAS: 155–165 (in Russian).

***Keller, B.M. and Chumakov, N.M. (ed.)* 1983.** The Riphean Stratotype: Stratigraphy and Geochronology. Nauka, Moscow. 183 p. (in Russian).

***Kozlov, V.I. (Ed.)* 2002.** The geologic map of the Russian Federation and adjoining territory of Kazakhstan Republic . Scale 1:1 000 000 (new series). Sheet No 40 (41). Ufa, St. Petersburg, VSEGEI (in Russian).

***Kozlov, V.I., Krasnobaev, A.A., Larionov, N.N., Maslov, A.V., Sergeeva, N.D., Ronkin, Yu.L., Bibkova, E.V.* 1989.** The Lower Riphean of the southern Urals. M., Nauka. 208 p (in Russian).

***Krasnobaev A.A.* 1986.** Zircon as an indicator of geological processes. M., Nauka. 146 p (in Russian).

***Krasnobaev, A.A. Bibikova, E.V, Ronkin, Yu.L, et al.* 1992.** Izv. Ross. Akad Nauk.Ser.Geol. No. 6: 25–40 (in Russian).

***Krupenin, M.T.* 2004.** The Middle Riphean time on the western slope of the southern Urals: Mineragenic and geodynamic implications. Doklady Earth Sciences 399A (9): 1189–1191 (in Russian).

***LeBas, M.J, LeMaitre, R.W., Streckeisen, A., Zanettin, B.* 1986.** A chemical classification of volcanic rocks based on the total alkali silica diagram. Journal of Petrology 27: 745–750.

***Lennykh V.I., Petrov V.I.* 1974.** New data on the magmatism and metamorphism of the western slope of the Southern Urals in connection with the history of its tectonic development. In: Tectonics and magmatism of the Southern Urals. M., Nauka: 129–140 (in Russian).

***Lennykh V.I., Pankov Yu.D., Petrov V.I.* 1978.** Petrology and metamorphism of a migmatite complex . Petrology and iron deposits of a migmatite complex. Sverdlovsk, Uralian Sci. Centre: 129–140 (in Russian).

***Mocek, B.* 2001.** Geochemical evidence for arc-type volcanism in the Aegean Sea: the blueschist unit of Siphnos. Cyclades (Geece). Lithos 57: 262–289.

***Mullen, E.D.* 1983.** $MnO/TiO_2/P2O_5$: a minor element discriminant for basaltic rocks of oceanic environments and its implications for petrogenesis. Earth Planet. Sci. Lett 62: 53–62.

***Parnachev V.P.* 1981.** The volcanic complexes and tectonic regime of the western slope of the Southern Urals in the Late Precambrian. The ancient volcanism of the Urals. Sverdlovsk, Uralian Sci. Centre: 18–30 (in Russian).

***Parnachev V.P., Rotar A.F., Rotar Z.M.* 1986.** The Middle Riphean volcano-sedimantary association of the Bashkirian anticlinorium. Sverdlovsk, Uralian Sci. Centre. 103 p (in Russian).

***Parnachev V.P, Kozlov V.I.* 1979.** New data on the specific features of the Vendian volcanism of the Southern Urals (as an example, the Arsha formation of the Tirlyan area). Sverdlovsk, IGG Uralian Branch of Russian Ac. Sci.: 66–70 (in Russian).

***Pearce, J.A. Cann, J.R.* 1973.** Tectonic setting of basic volcanic rocks determined using trace element analyses. Earth and Planetary Science Letters 19: 290–300.

***Pearce, J.A.* 1996.** A user's guide to basalt discrimination diagrams. In: Wyman, D.A. (ed.) Trace Element Geochemistry of Volcanic Rocks: Applications for Massive Sulphide Exploration. Geological Association of Canada, Short Course Notes 12: 879–113.

***Pease, V., Daly, J.S., Elming, S.-Å., Kumpulainen, R., Moczydlowska, M., Puchkov, V., Roberts, D., Saintot, A., Stephenson, R.* 2006.** Baltica in the Cryogenian, 850–630 Ma. Precambrian Res. (in prep).

***Petrov G.A., Maslov A.V., Ronkin Yu.L., Krupenin M.T.* 2005.** New data on geochemistry and age of Pre-Paleozoic magmatic complexes of the Kvarkush-Kamennogorsk Megantiklinorium (Middle Urals) // Ezhegodnik–2004, IG of the Uralian Branch of RAS: 274–283.

***Polat, A., Hofmann, A., Munker, C., Regelous, M., Apple, P.* 2003.** Contrasting geochemical patterns in the 3.7–3.8 Ga pillow basalt cores and rims, Isua Greenstone Belt, southwest Greenland: Implications for postmagmatic alteration processes. Geochimica et Cosmochimica Acta, 67: 441–457.

***Puchkov, V.N.* 1988.** The place of intraplate events in the history of foldbelts. In: Intraplate Events in the Earth's Crust. M., Nauka: 167–175 (in Russian).

***Puchkov, V.N.* 2000.** Paleogeodynamics of the central and southern Urals. Ufa, Dauria, 145 p. (in Russian).

***Puchkov, V.* 2002.** Paleozoic evolution of the East European continental margin involved in the Uralide orogeny. In: Mountain Building in the Uralides: Pangea to the Present. Geophysical Monograph 132, American Geophysical Union: 9–31.

***Ronkin, Yu. L., Maslov, A.V, Matukov, D.I., Lepikhina, O.P., Popova, O., Yu.* 2005.** The Mashak riftogenic event: of the Riphean type region (southern Urals): new isotopic-geochronological framework. In: Structure, geodynamics and mineralogenic processes in lithosphere. Syktyvkar, Geoprint: 305–307. (in Russian)

***Rollinson, H.* 1993.** Using geochemical data: evaluation, presentation, interpretation. Longman, UK, 352 p.

***Rudnick, R.* 1995.** Making continental crust. Nature 378: 571–578.

***Scarrow, J.H., Hetzel, R., Gorozhanin. V.M., Dinn, M., Glodny, J., Gerdes, A., Ayala, C. and Montero, P.* 2002.** Four decades of geochronological work in the southern and middle Urals: a review. In: Brown, D., Juhlin, C., Puchkov, V. (eds.). 2002. Mountain Building in the Uralides: Pangea to the Present. American Geophysical Union. Geophysical Monograph 132: 233–256.

***Semikhatov M.A., Shurkin K.A., Aksenov E.M.et al.* 1991.** The new stratigraphic scale of the Precambrian in the USSR . Izvestia of the Ac. Sci. USSR, ser. geol, No 4: 3–13 (in Russian).

***Shervais, J.W.* 1982.** Ti–V plots and the petrogenesis of modern and ophiolitic lavas. Earth and Planetary Science Letters 59: 101–118.

***Sun, S.S. and McDonough, W.F.* 1989.** Chemical and isotopic systematics of oceanic basalts. Implications for mantle composition and process. Geological Society of London, Special Publication 42: 313–345

***Thompson, R.N., Morision, M.A., Dickin, A.P., Hendry, G.L.* 1983.** Continental flood basalts — arachnids rule OK? In Hawkesworth, C.J.,and Norry, M.J. (eds.) Continental Basalts and Mantle Xenoliths. Nantwich, UK. Shiva Press.

***Upton, B.G.J., Rämö, O.T., Heaman, L.M., Blichert-Toft, J., Kalsbeek, F., Barry, T.L., Jepsen, H.F.* 2005.** The Mesoproterozoic Zig-Zag Dal basalts and associated intrusions of eastern North Greenland: mantle plume-lithosphere interaction. Contrib. Mineral. Petrol. 149: 40–56.

***Winchester, J.A., Floyd, P.A.* 1977.** Geochemical discrimination of different magma series and their differentiation products using immobile elements. Chemical Geology, 20: 325–343.

***Yamayev F.A., and Shvetsov P.N.* 1973.** The Beletur Volcano in the Yamantau anticlinorium. Magmatism and endogenic metallogeny of the western slope of the Southern Urals. Ufa: 105–110 (in Russian).